

**Mechanical properties  
of tree roots for soil  
reinforcement models**

Promotor:           prof. ir. U.D. Perdok  
                          Hoogleraar in de bodemtechnologie

Co-promotor:       dr.ir. A.J. Koolen  
                          Universitair hoofddocent,  
                          Departement Agrotechnologie en voedingswetenschappen

**Samenstelling**

promotiecommissie:  prof. dr.ir. G.P.A. Bot (Wageningen Universiteit)  
                          prof. dr. N. van Breemen (Wageningen Universiteit)  
                          prof. dr.ir. G.M.J. Mohren (Wageningen Universiteit)  
                          prof. dr. I. Wästerlund (Sveriges Lantbruksuniversitet, Zweden)

NW08201, 2920

**Mechanical properties  
of tree roots for soil  
reinforcement models**

**Peter Cofie**

**Proefschrift**

ter verkrijging van de graad van doctor  
op gezag van de rector magnificus  
van Wageningen Universiteit,  
prof. dr.ir. L. Speelman,  
in het openbaar te verdedigen  
op maandag 8 januari 2001  
des namiddags te vier uur in de Aula.

WU 1602013

The research described in this dissertation was carried out at the Department of Agrotechnology and Food Sciences of Wageningen University.

CIP-Gegevens Koninklijke Bibliotheek, Den Haag

Cofie, P.

Mechanical properties of tree roots for soil reinforcement models.

Dissertation Wageningen University - With ref. - With summaries in English and Dutch.

ISBN 90-5808-333-0

#### Keywords

Shear strength, tensile strength, beech, larch, PLAXIS, interface properties, geotextiles, bearing capacity, FEM (finite element method)

To my mother Mary Acquah

## ACKNOWLEDGMENT

I am indebted to Prof.Ir. U.D. Perdok (Promotor) and Dr.Ir. A.J. Koolen (Co-promotor) for their support and guidance from the beginning of this thesis till its completion. I am also to indebted to the Soil Technology Group, Department Agrotechnology and Food Sciences, Wageningen University, who sponsored this study.

I will seize this opportunity to also express my sincerest gratitude to my partner Corrie Vrijhoef for her encouragement and support in the course of preparing the thesis. Special thanks to Mr. B.W. Peelen who also helped me in the collection of roots samples from State forest 'Speulder and Sprielderbos' in Garderen.

Many thanks to Dr. M.A. Aliu and Mr. Mahama Seidu who agreed to be my local supervisors in Ghana. The following persons also deserve my acknowledgment: Albert Boers, Mr. Steve Duku (MSc), Oil Palm Research Centre, Kusi, Ghana, Dr. V.K. Agyemang, Forestry Research Institute of Ghana, Kumasi, Ghana, Mr. D.K.O Appiakubi, Mr. Robert Quansah and Mr. Emmanuel Amoah.

Last but not the least, my gratitude to all co-workers in the Soil Technology Group who directly or indirectly assisted to bring this thesis to a successful and timely completion.

## ABSTRACT

Cofie, P., 2000. Mechanical properties of tree roots for soil reinforcement models. Doctoral thesis, Wageningen University, Wageningen, The Netherlands.

Evidence from forestry has shown that part of the forest floor bearing capacity is delivered by tree roots. The beneficial effect however varies and diminishes with increasing number of vehicle passes. Roots potential for reinforcing the soil is known to depend among others on root mechanical properties, distribution, morphology, etc. Rooting intensity and root patterns of forest trees are complicated, but some information is available. The objectives of this study are therefore as follows: (1) addressing the occurrence of field traffic on forest soils, (2) identifying root mechanical properties that play a role in soil reinforcement, (3) measuring root stress-strain relationships, root failure stress and strain and root behaviour under repeated loading and (4) simulating root reinforcement effect using a FEM (Finite Element Method) code capable of accounting for root properties in reinforcement simulations.

The repeated loading experiments included repeated loading of tree roots to different loading levels and loading with different loading rates or elongation rates. These studies revealed that tree roots possess stiffness and failure strengths. They show elastic as well as plastic behaviour. They also show fatigue phenomena in repeated loading. Available FEM codes were studied with respect to their capability in dealing with soil reinforcement by roots. PLAXIS which is a commercially available FEM code was used due to its ability to calculate stresses, strains and failure states of soil mechanical problems. It can also cope with unsaturated reinforced soil. The finite element calculations conducted with PLAXIS are intended for soils loaded by forestry vehicles. These involved situations with and without reinforcement by tree roots. The reinforcement effects are, among others, decrease of wheel rut depth and rolling resistance, decrease of damage to soil structure by the wheel load and as a negative effect, physiological damage to the tree root system. The magnitude of these effects depends on a number of parameters: stiffness and strength of the tree roots, soil mechanical properties like cohesion, angle of internal friction, compression index, preconsolidation stress, depth of a hard sublayer (if present), distance between vehicle and tree, rooting patterns, adhesive and frictional properties of the soil-root interface, wheel load and contact surface. The presented simulation results, which are based on realistic input data, show the sensitivity of the reinforcement effect to the listed variables.

**Keywords:** shear strength, tensile strength, beech, larch, PLAXIS, interface properties, geotextiles, bearing capacity, FEM (Finite Element Method).

## STELLINGEN

1. Number of loading cycles before root failure depend on the percentage stress level.  
- this thesis.
2. Spread of stress-strain values of pairs of root pieces that were neighbours are closer to each other than that exhibited by random pieces from their corresponding diameter classes.  
- this thesis.
3. Only relatively small numbers of people directly depend on forests for their livelihood, but vast numbers are concerned about their use and condition.  
- Mather, A.S., 1990. Global forest resources, Belhaven Press, London, 341 pp.
4. The extent to which a soil will be compacted during field operations depends on the type of field traffic as well as on the prevailing soil conditions.  
- Van den Akker, J.J.H., and A.L.M. van Wijk, 1987. *A model to predict subsoil compaction due to field traffic*. In: G. Monnier and M.J. Goss (eds), *Soil compaction and regeneration*, Balkema, Rotterdam, 69-84.
5. As cultivatable land resources are limited, increased agricultural production can only be attained through increased yields per unit area of land and improved preservation of already produced commodities.  
- Hall, C.W., 1973. *Principles of agricultural mechanization*. In: M.L. Esmay and C.W. Hall (eds), *Agricultural mechanization in developing countries*, Shin-Norinsha Co., LTD, Tokyo, Japan, 1-15.
6. Stilstand is achteruitgang.
7. Een goede leefbaarheid is gebruiken wat de natuur ons biedt.

---

Stellingen behorend bij het proefschrift

**Mechanical properties of tree roots for soil reinforcement models**

Peter Cofie

Wageningen, 8 januari 2001



# CONTENTS

<b>1</b>	<b>GENERAL INTRODUCTION.....</b>	<b>1</b>
1.1	BACKGROUND.....	1
1.2	PROBLEM FORMULATION.....	1
1.3	OBJECTIVES.....	3
1.4	LAYOUT OF THE THESIS.....	3
<b>2</b>	<b>ROOTS.....</b>	<b>5</b>
2.1	INTRODUCTION.....	5
2.2	THE PHYSIOLOGY AND MORPHOLOGY OF ROOTS.....	5
2.2.1	Root initiation.....	5
2.2.2	Root growth.....	8
2.2.2.1	Introduction: basic root systems.....	8
2.2.2.2	Classification of individual roots.....	10
2.2.2.3	Patterns and distribution of roots.....	10
2.3	INFLUENCE OF ROOT SURFACE STRUCTURES.....	16
2.4	ROOT STUDY METHODS.....	19
<b>3</b>	<b>PROPERTIES OF ROOT STRENGTH.....</b>	<b>21</b>
3.1	INTRODUCTION.....	21
3.2	MEASURED VALUES OF ROOTS MECHANICAL PROPERTIES.....	21
3.2.1	Tensile strength and Young's modulus of elasticity.....	21
3.2.2	Shear strength.....	26
<b>4</b>	<b>MEASURING ROOTS MECHANICAL PROPERTIES.....</b>	<b>31</b>
4.1	INTRODUCTION.....	31
4.2	MATERIALS AND METHODS.....	37
4.2.1	The testing machine.....	37
4.2.2	Clamping procedure.....	38
4.2.3	Collection, preparation and storage of root samples.....	39
4.2.4	Experimental scheme.....	40
4.2.4.1	General.....	40
4.2.4.2	Experiment 1: effect of beech and larch root pairs.....	40
4.2.4.3	Experiment 2: effect of elongation rate (speed effect) on stress-strain relationships of beech roots.....	40
4.2.4.4	Experiment 3: failure stresses and strains and behaviour of thick beech roots under cyclic loading.....	41
4.3	RESULTS.....	41
4.3.1	Experiment 1: effect of beech and larch root pairs.....	41
4.3.2	Experiment 2: effect of elongation rate (speed effect) on stress-strain relationships of beech roots.....	44
4.3.3	Experiment 3: failure stresses and strains and behaviour of thick beech roots under cyclic loading.....	46
4.4	DISCUSSIONS.....	55
4.5	CONCLUSIONS.....	58

<b>5</b>	<b>SOIL REINFORCEMENT BY ROOTS</b>	<b>59</b>
5.1	INTRODUCTION: FIBRE REINFORCEMENT	59
5.1.1	Composite materials	59
5.1.2	Failure	63
5.1.3	Soil reinforced by geotextiles	65
	5.1.3.1 Introduction	65
	5.1.3.2 Soil-geotextile interface properties	72
	5.1.3.3 Modelling soil reinforced by geotextiles	79
5.2	MODELLING SOIL-ROOT REINFORCEMENT	85
5.2.1	Soil-root models	85
5.2.2	Shear zone	95
5.3	SOIL-ROOT AND VEHICLE MECHANICS	98
	PLAXIS: finite element code	105
5.4	SIMULATING REINFORCEMENT EFFECTS OF TREE ROOTS IN A SOIL-WHEEL SYSTEM	109
5.4.1	Introduction	109
5.4.2	Methods	116
	5.4.2.1 Reference case	116
	5.4.2.2 Other cases	118
5.4.3	Results	120
	5.4.3.1 Reference case	120
	5.4.3.2 Other cases	124
5.4.4	Discussion	128
5.4.5	Conclusions	129
<b>6</b>	<b>GENERAL DISCUSSION AND CONCLUSIONS</b>	<b>131</b>
	Further studies	135
	<b>REFERENCES</b>	<b>137</b>
	<b>SUMMARY</b>	<b>153</b>
	<b>APPENDIX I</b>	<b>155</b>
	Definition of biological terms	155
	<b>APPENDIX II</b>	<b>157</b>
	Symbols	157
	<b>APPENDIX III</b>	<b>162</b>
	Soil parameters	162
	<b>SAMENVATTING</b>	<b>163</b>
	<b>CURRICULUM VITAE</b>	<b>165</b>

# **1 GENERAL INTRODUCTION**

## **1.1 BACKGROUND**

Soil mechanics in relation to plant growth has developed significantly, as can be seen from numerous textbooks (Gill and Van den Berg, 1967; Koolen and Kuipers, 1983; McKyes, 1985; Larson et al., 1989; Soane and Van Ouwerkerk, 1994). Strength of soil with a vegetation depends among other things on the vegetation roots (Waldron, 1977; Waldron and Dakessian, 1981; Waldron and Dakessian, 1982; Wu et al., 1979; Wu et al., 1988; Willatt et al., 1990; Abe and Ziemer, 1991; Terwilliger and Waldron, 1991). However, knowledge of soil reinforcement by roots is very limited and needs further attention (Wästerlund, 1990). The Soil Technology Group of Wageningen University has been involved in forestry since 1980 (Beekman, 1987; Koolen, 1989; Heij and Koolen, 1993; Koolen, 1994; Makarova et al., 1998). An earlier work done by Liu (1994) on soil reinforcement by tree roots was mainly focussed on the development of experimental techniques for measuring failure stresses and strains, and stress-strain relationships of thin tree roots. It showed that in repeated loading, thin tree roots exhibit permanent strain that increases with the number of loading cycles and that roots can show fatigue failure.

## **1.2 PROBLEM FORMULATION**

The threat of soil structure deterioration/compaction in forest soils is on the rise due to increase in mechanized timber harvesting with large forestry machinery. Tree roots in forest soils are however known to contribute to the bearing capacity of soil and hence tending to reduce soil deformation. In order to take full advantage of this, it should be possible to predict the reinforcement effect by roots. Until now, soil-vehicle mechanics does not account for this effect, which depends on the mechanical properties of the soil itself, the mechanical properties of the root material, soil-root interface properties, the morphology of the root system and loading characteristics. In relation to dense and dry soil, roots have a great resilience. So, the benefit from roots is expected to be higher in weak soils than in strong soils. The overall mechanical properties of a root are determined by the mechanical properties of the different root components such as bark, sap wood, and core wood. These properties vary with season and root age. The shearing resistance of

soil-root interfaces depends on the "true" soil material-root surface angle of friction and adhesion, on the relative softness of the outer part of the root and the soil material and the normal stress on the interface. Important root system factors include root patterns, root thickness, root hairs, etc. Significant loading characteristics include the stress level in the soil, loading duration, and the number of load repetitions. In the case of repeated loading the length of the time intervals between successive loading events and residual stresses/strains during these dwell times must be considered. A mechanistic approach to arrive at the desired prediction will include quantification of the above factors, and to incorporate these factors into an adequate prediction model. The complex nature of the stress and strain distribution in the loaded soil-root system will require the use of FEM (Finite Element Methods). Only this advanced calculation procedure will be capable to handle the complexities involved. Literature currently available on loaded soil-root systems is very limited. Knowledge of fibre reinforcement mechanics will therefore be important to better understand root reinforcement. Studies have however shown that elongation rate (test speed) does affect the magnitude of mechanical properties of fibres (Morton and Hearle, 1976; Lopes, 1996). Effect of elongation rate on mechanical properties of tree roots has not been studied. In cyclic loading experiments, relative loading  $\sigma_{\max}/\sigma_f$  ( $\sigma_{\max}$  and  $\sigma_f$  are maximum stress and failure stress respectively) in a single loading are not accurately determined due to wide scatter of  $\sigma_f$  measuring values. It is expected that  $\sigma_f$  measurement of a piece of root that was adjacent to the piece that has been subjected to cyclic loading will provide a good estimate. Among the scientific questions that will be investigated in this thesis are the following:

- (1) are failure stresses of a pair of adjacent root pieces closer to each other than those from the diameter class to which they belong?
- (2) does elongation rate affect stress-strain relationship of roots?
- (3) does the diameter of a thick root affect its stress-strain relationship?

The emphasis of this thesis will be on the measurement and analysis of mechanical properties of roots (single as well as repeated loading of root experiments will be carried out) and the use of FEM to study roots contribution to increase in soil bearing capacity.

### 1.3 OBJECTIVES

The main aims of this thesis are as follows:

- (1) addressing the occurrence of field traffic on forest soils
- (2) identifying root mechanical properties that play a role in soil reinforcement
- (3) measurements of root stress-strain relationships, root failure stresses and strains, and root behaviour under repeated loading
- (4) simulating the root reinforcement effect using finite element code known as PLAXIS.

Results from the above studies will be significant with respect to forestry and other types of land use under permanent vegetation such as grassland, slopes, roadsides and dikes.

### 1.4 LAYOUT OF THE THESIS

Chapter 2 deals with those aspects of tree roots which more or less are relevant to assist in examining the role of roots in soil stabilizing and/or contribution to increase in soil strength. This includes reviews on physiology and morphology of tree roots, root growth patterns and distribution, and influence of root surface structures on the soil. Definitions of some biological terms used in the thesis can be found in appendix I. Measurements of roots mechanical properties are reviewed in chapter 3, emphases are placed on tensile and shear stress experiments. Chapter 4 covers the experimental section and focuses on finding an appropriate clamping procedure for roots to minimize slippage and promote failure further away from clamp jaws, measurement of failure stresses and strains, measurement and comparison of stress-strain relationships of neighbouring root parts to those of their diameter classes, fatigue behaviour of thick roots using reliable percentage stress level, and studying the effects of speed on measured values of root strength. Chapter 5 contains information on composite materials, soil reinforced by geotextiles, soil-geotextile modelling techniques, interface properties, and soil-root reinforcement models, etc. and simulation of root reinforcement effects in the soil-wheel system. Chapter 6 presents general discussions and conclusions resulting from the thesis. Symbols used in the thesis are compiled in appendix II. In appendix III soil parameters derived from Mawcook gravel-sandy loam and Ste-Rosalie clay are listed.

## **2            ROOTS**

### **2.1           INTRODUCTION**

Environmental damages caused by the usage of field machinery (especially heavy and large ones) are often clearly noticeable during/after mechanized forestry operations. During such operations damage is caused to remaining trees, regrowth, surface covering, and most importantly, the soil. Disturbances caused to the forest floor may consist of soil compaction, displacement and puddling, and is aggravated by the usage of heavier machinery. These disturbances may be manifested as ruts (Heij and Koolen, 1993) and occur as a result of inability of the soil section under the wheel to support the exerted vertical pressure. The extent of deformation caused is usually associated with: (1) vehicle properties, e.g., type of vehicle, wheel dimensions, inflation pressure, wheel load, contact pressure, etc., (2) number of wheel passes and (3) prevailing soil conditions (Pollock et al., 1986; Van den Akker and van Wijk, 1987). Several methods ranging from practical to theoretical approaches that tend to estimate the magnitude of the deformation have been proposed. Presence of roots acting as reinforcement members and fallen leaves as cushions (i.e., between the wheel and the soil) are however known to reduce the magnitude of deformation caused to the soil (Waldron, 1977; Waldron and Dakessian, 1981; Waldron and Dakessian, 1982; Wu et al., 1988; Wästerlund, 1990; Willatt and Sulistyaningsih, 1990; Ess et al., 1988).

In this chapter an attempt has been made to present a brief discussion on those aspects of roots or root systems, such as physiology and morphology, growth patterns and distribution, association with microorganisms, etc., which are relevant in revealing the role played by roots in stabilizing and/or contributing to increase soil strength. Definitions of some of the biological terms used in this chapter can be found in appendix I.

### **2.2           THE PHYSIOLOGY AND MORPHOLOGY OF ROOTS**

#### **2.2.1        Root initiation**

In terms of well-being of the plant, roots are equally as important as the other main structures such as shoots or leaves. However, in comparison to these structures, little

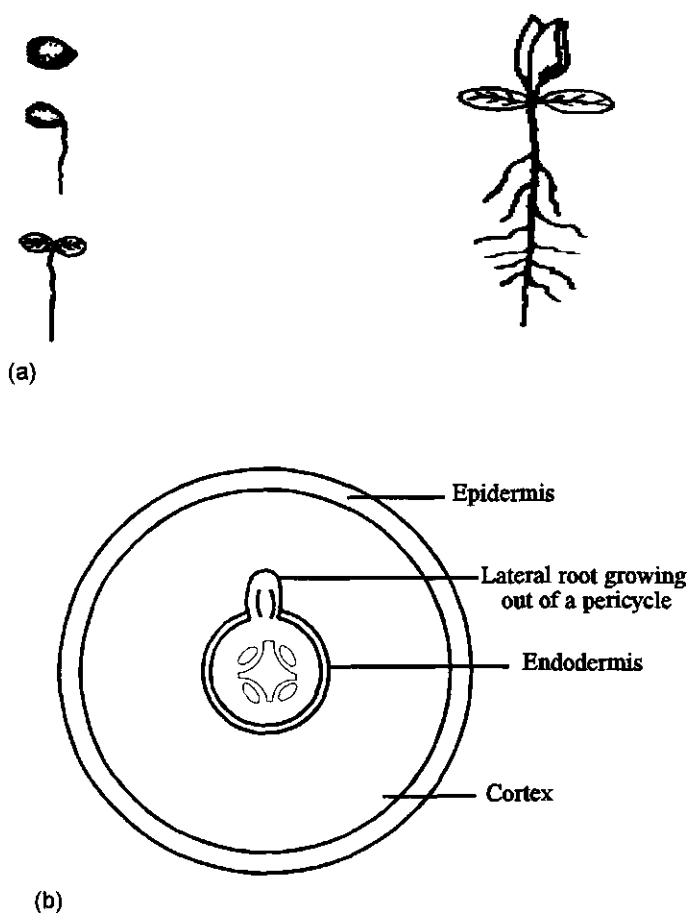


Figure 2.1 Root initiation: (a) root arising from the initial radicle of a seedling and (b) development of lateral roots.

Source: Adapted from Berrie et al. (1987)

attention has been paid to the study of roots. Partly, this is attributed to extensive root branching behaviour, variable forms, and labourious study methods that are involved. But as Russell (1977) puts it, the performance of root systems seemed of minor interests. In situations where root studies were conducted, seedlings or small trees were mostly used.

According to Craul (1993), a healthy tree will have a well-developed root system, whilst a sickly tree will have a limited root system. This rule of thumb may provide a clue as to the reason why in agriculture interest is preferably focussed on the creation of soil conditions favourable for plant growth (e.g., ploughing, seedbed preparation, irrigation, fertilizer application) rather than extensive study of plant roots.

Roots develop from a root primordium. Two basic ways in which these occur can be cited: (1) root primordia arising from the initial radicle of a seedling, giving rise to lateral root primordia (figure 2.1 (a)) and (2) root primordia arising endogenously in the stem tissues (figure 2.1 (b)), giving rise to an extensive adventitious root system. In general, the prerequisites for root initiation appear to be the availability of parenchyma cells which may be stimulated into cell division, and also provide part of the stimulus for new root formation. Environmental factors which influence root initiation include temperature, aeration, pH of the medium, water availability and light.

A developing root in its primary growth consists of four main portions: (1) root cap, (2) meristematic region, (3) region of elongation and (4) region of differentiation and maturation (see figure 2.2).

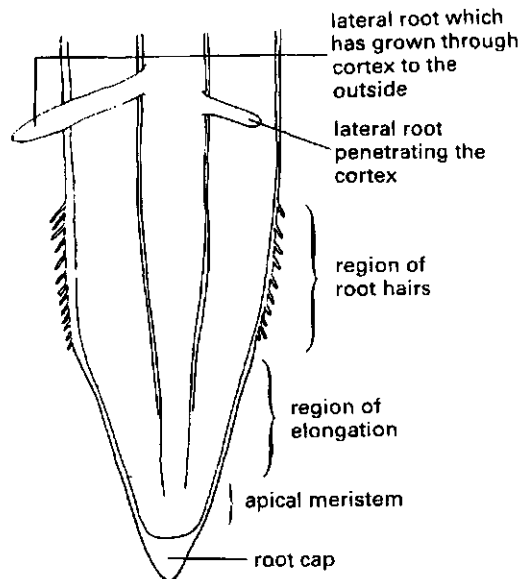


Figure 2.2 Tip of a developing root.

Source: Berrie et al. (1987)



The root cap is commonly regarded as a structure that protects the root meristem and assists the root in the penetration of the soil during its growth. The latter function is suggested by the mucilaginous consistency of the walls of the outermost root cap cells. Existence of friction between the soil and roots during growth causes the root cap to wear away. In most roots, cells are however added to the root cap about the same rate to compensate for this wear. In maize, a rate of about 10,000 cells a day have been estimated by Berrie et al. (1987). The root cap can easily be seen in aerial roots such as *Rhizophora* spp., Red Mangroves, *Pandanus* spp. Behind the root cap is the meristematic region mainly characterized by cell differentiation and absorption. Next to this region is the elongation region in which existing cells undergo elongation. These cells tend to be thin walled and are active in absorption of water and nutrients. The fourth region, is the region of differentiation and maturation. This region is characterized by the formation of root hairs arising from the root epidermis and in some cases, from the cortex.

## **2.2.2 Root growth**

### **2.2.2.1 Introduction: basic root systems**

Generally, root systems are classified into two main groups. Those characteristic of: (1) monocotyledonous plants (monocots) and (2) dicotyledonous plants (dicots), (Bell, 1991; Haper et al., 1991). In monocots, the first root (i.e., tap root) usually lives a relatively short time and the root system is then further formed by adventitious roots arising on the shoot. This kind of root system is usually referred to as the fibrous root system. Common examples of plants with fibrous root systems are cereals and grasses (Russell, 1977). In dicots plants, the entire root system is usually subtended by a single tap root. Major roots of dicots plants are usually massive structures, sometimes showing annual growth rings in cross-section and developing a thick bark (Bell, 1991). Comparing fibrous and tap root systems, the former branches less (Berrie et al., 1987), penetrates less deeply in the soil, but binds the superficial layers of the soil more firmly than the latter (Esau, 1977). Other methods of root systems classification have been based on the growth behaviour and functions (Schneemann, 1988), as well as shape (Lichtenegger and Kutschera-Mitter, 1991). Root systems at any time, may consist of a mixture of individual roots of different kinds and ages (Atkinson, 1983). Examples of root systems of some common forest trees are as shown in figure 2.3. Brief summaries of root systems of desert trees have been

presented by Fitter (1991); Rundell and Nobel (1991).

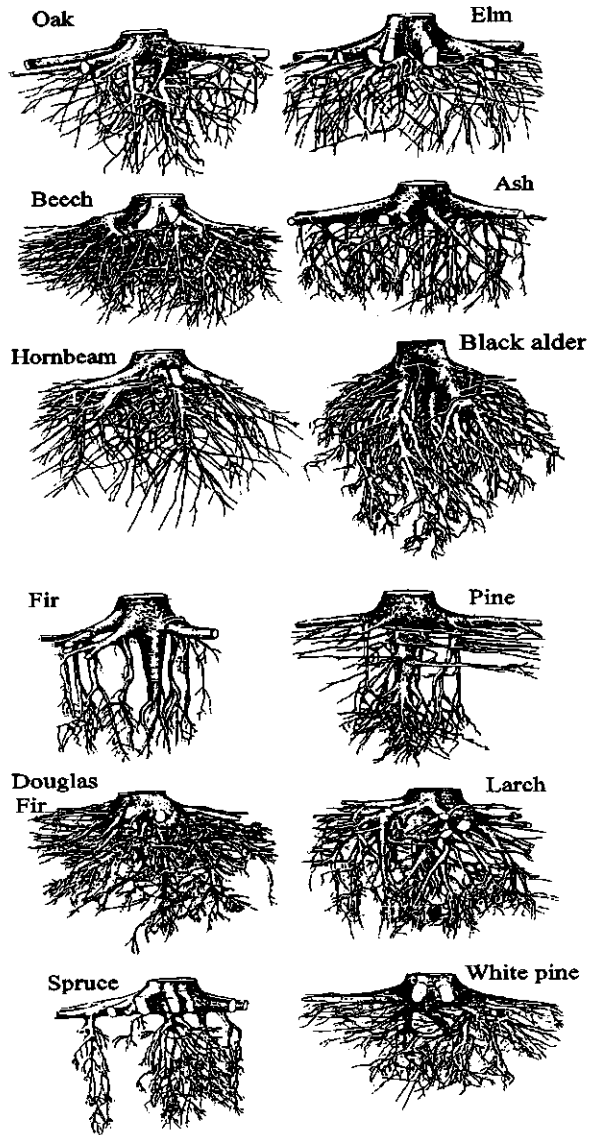


Figure 2.3 Root systems of common forest trees.

Source: Köstler et al. (1968)

#### **2.2.2.2 Classification of individual roots**

Various ways of classifications of individual roots have been documented. In terms of distribution, Kolesnikov (1971) divided them into vertical and horizontal roots, whilst according to length and thickness, he grouped them into skeletal and fibrous roots. Horizontal roots are considered as those growing more or less parallel to the soil surface (at a depth of about 30 to 100 cm), whereas vertical roots grow vertically downwards into the soil. Skeletal roots, on the other hand, are considered to be long and thick (i.e., from several centimetres to several metres long and diameter can be up to several centimetres). In terms of diameter, Gliński and Lipiec (1990) classified roots into 6 main groups: very fine (< 0.5 mm), fine (0.5 to 2 mm), small (2 to 5 mm), medium (5 to 10 mm), large (10 to 20 mm) and very large (> 20 mm).

Most fine roots are found within the surface 1 m of the medium textured soils, with the majority of fine, non-woody roots in the upper 15 cm of soil. Craul (1993) attributed this to genetic control and proximity of favourable growth conditions of the surface soil. According to Wästerlund (1989), roughly about 70% of roots in thinning stands (i.e., roots of both tree and ground vegetation) are found in the humus layer. Some of the important characteristic features of individual roots are surface texture, colour and diameter (Fitter, 1991). Young roots may be unpigmented or tinged with pink or orange, however, they attain one of the various shades of brown when older. In addition to root hairs the following structures may be seen on the root surface away from its apex: nodules in association with bacteria, mycorrhiza in association with fungi (discussed in section 2.3) and root buds capable of developing into new complete shoot systems.

#### **2.2.2.3 Patterns and distribution of roots**

Root distribution and growth patterns are seen to be exceedingly diverse both in the same species (e.g., under different environmental conditions) and different species (e.g., under the same environmental conditions), with some exhibiting changing architecture as they develop. Roots of neighbouring trees interlock often forming a kind of root net in the soil. This usually leads to the uprooting of surrounding tree(s) when one of the trees with its roots in the root-net is uprooted (Coultts, 1983). In general, rooting patterns of forest trees exhibit superficial root systems (frequently lacking a taproot) whilst smaller trees show

deeper and fewer wide-spreading root systems (Schneemann, 1988). Architecture of root systems is noted to depend on a number of variables. These include: extent of elongation, branching angle, mortality of axes and apices, size, topology (i.e., distribution of branches within the root system) and link lengths (distance between branching points) (Haper et al.,

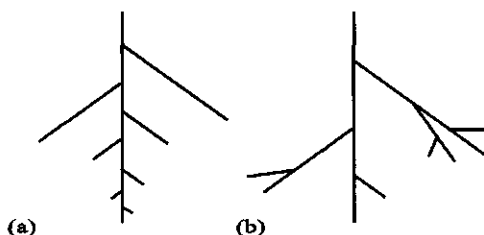


Figure 2.4 Distribution of root branches within the root system:  
(a) herringbone and (b) dichotomous.

Source: Fitter (1991)

1991; Fitter, 1991). Fitter divided the topology of root systems into two extremes groups: herringbone and dichotomous pattern (figure 2.4).

Within the last two decades, computer modelling or simulation is commonly used as non-destructive method in studying root growth, patterns and distribution. Hettiaratchi and Ferguson (1973) presented a theoretical model which seeks to throw light on the growth of roots. Their model consists of four main steps: (1) when the axial elongation of the root tip is arrested by the inability of the root cap to penetrate the soil ahead of it, the elongation zone of the root located just behind the meristem enlarges radially outwards, (2) this radial enlargement causes a reduction in penetration resistance at the root cap, (3) the root then extends longitudinally until the root cap is once again in a zone of soil where it is unable to penetrate and (4) the cycle repeats again. Rose (1983), on the other hand, used an analytical model to represent root growth. Assumptions made in her model include: (1) roots are undamaged and healthy, (2) laterals emerge strictly acropetally, (3) rates of extension and branching of each class of root members are uniform throughout the root (ie there is no spatial variation) and (4) no aging of roots. Though some of her assumptions seem unrealistic, the model can be used to estimate total length of root members, and total number of root members in the root system. Similar growth models

have been presented by Jones et al. (1991).

Deans and Ford (1983) demonstrated the use of the method of path reconstruction to simulate root patterns and distribution in the root system. A test of the model conducted with inputs from a root system of a 16-year-old Sitka spruce tree produced results that bore close resemblance to the actual (i.e., excavated) root system of the plant (figure 2.5 (a) and (b)).

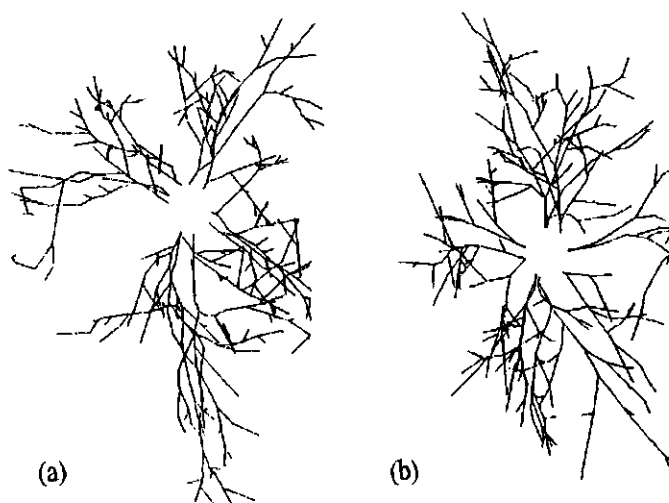


Figure 2.5 Plan views of (a) excavated and (b) simulated root systems of 16 year old Sitka spruce tree.

Source: Dean and Ford (1983)

Attempts have been made by a number of authors to relate root parameters such as number, diameter and orientation to the size of the stem or crown diameter. For example, Kuiper and Coutts (1992) reported that highly significant positive correlations exist between stem diameter at a height of 1.3 m and root biomass. This was also portrayed in root geometry model presented by Wu et al. (1988). Relation between stem diameter and root geometry was represented by figure 2.6 and equations 2.01 to 2.03. In this model, the main lateral root was assumed to start radially from the stem and from there on follows

a random walk process.

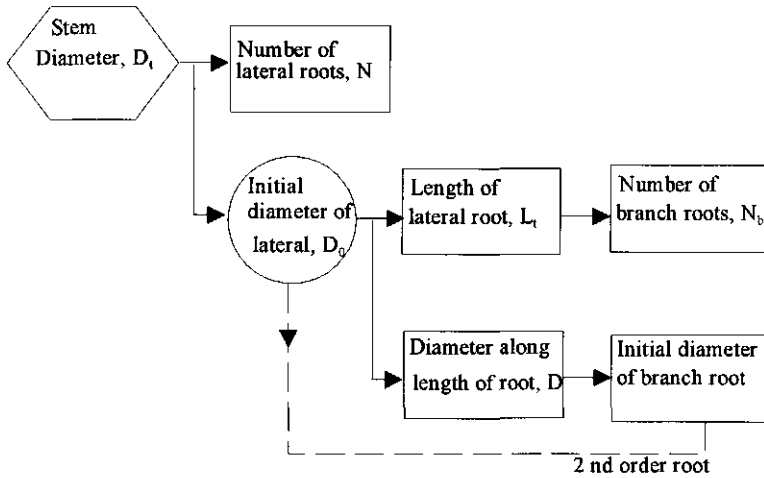


Figure 2.6 Root geometry model.

Source: Wu et al. (1988)

$N$	$= 3.35 + 0.15 D_t$	2.01
$D_0$	$= 1.33 + 0.39 D_t$	2.02
$L_t$	$= 89.44 D_0$	2.03

where  $N$ ,  $D_0$ ,  $L_t$ ,  $D_t$  equal the number of laterals formed on stem, mean of the initial diameter of the lateral, total length of a root and stem diameter respectively.

Van Noordwijk et al. (1996) reported two parameter descriptive models that describe root length density as a function of depth and horizontal distance from the plant. Distribution of castor plants has been studied by Smith et al. (1991). According to Löhmanns et al. (1991), vertical distribution of fine roots is one of the most important characteristics that show connection between the stand and the soil. Work done by Watson (1993) indicated, that the rate of new root elongation in temperate climates is smaller than that in subtropical climates. The former was given as 300 - 600 mm/year, whilst the latter was given as 600-1100 mm/year (his comparison was based on roots under climates of

northern United States (i.e., temperate) and Florida (i.e., subtropic)). Growth rates (mm/day) of some root species are as presented in table 2.1.

Table 2.1 Growth rates of some root species.

Root species	Growth rate (mm/day)	Source
Grass	12	Gliński and Lipiec (1990)
Pine	2.5	Gliński and Lipiec (1990)
Maize	60	Russell (1961)
Apple	3 - 9	Russell (1961)
Oak	8.2*	Watson (1993)

\*Growth rate of oak was given as 3000 mm/year in Florida. 1 year = 365 days

Basic differences in root pattern and distribution have been attributed to plants genetic constitutions. This is depicted by numerous papers (e.g., Troughton and Whittington, 1968; Pearson, 1974; Van Noordwijk, 1989; Waisel and Eshel, 1991) that have been written on the subject. Van Noordwijk (1989) pointed out, that different species of tree roots grown under the same circumstances may develop root systems which differ in total weight or length, orientation (geotropy), total depth, as well as branching patterns.

Table 2.2 Probe pressure at which root elongation ceases.

Plant	Texture	Bulk density (g / cc)	Measure of resistance	Critical probe pressure, q, (bar)
Pea and barley	Sand	1.40 - 1.65	Constant rate probe	12
Cotton	Fine sandy loam	1.55 - 1.85	Constant rate probe	34
Pea	Sandy loam	1.10 - 1.70	Constant rate probe	33
Pea and wheat	Loam	1.50 - 1.70	Constant rate probe	36
Corn	Clay	0.90 - 1.30	Constant rate probe	8

Source: Greacen et al. (1969)

Though plant's genetic constitutions play significant roles in the attainment of final rooting patterns, physical and chemical environment of the root is equally significant in most field situations (Pearson, 1974). Pearson argued, that mechanical impedance by compacted soil layers, for example, can turn a normally deep-rooted plant into a very shallow-rooted one. Earlier experiments conducted by Taylor and Ratliff (1969) on root elongation rates of cotton and peanuts confirmed, that the elongation rate of root decreases as soil strength increases. Greacen et al. (1969) constructed a table of values of probe pressure at which root elongation ceased in a range of soils (table 2.2).

Effect of root zone temperature on the morphology and distribution of tree roots has been examined by Nielsen (1974). Nielsen (1974) indicated, that in cooler temperatures roots usually become whiter, thicker (i.e., diameter) and branch less than at warmer temperatures. Also in cold periods, cell maturation is usually delayed, whilst elongation is favoured. With respect to the effect of soil aeration, three main factors have been identified: oxygen content in the soil air, carbon dioxide content in the soil air and content of by-products of anaerobic decomposition, such as hydrogen sulphide, methane, etc. High carbon dioxide ( $\text{CO}_2$ ) and low oxygen ( $\text{O}_2$ ) concentrations in the soil have been found to be detrimental to roots development and growth. According to Russell (1961),  $\text{CO}_2$  concentration of about 9% to 10% can be tolerated by roots only for short periods. For optimum growth, concentration of under 1% is expected. With regards to oxygen, a minimum concentration of 5% has been quoted for root growth (i.e., below which growth ceases).

Availability of carbohydrates for translocation to the roots for growth appear to be proportional to those not immediately needed by the aerial parts of the plant (Russell, 1961). Thus, it can be readily deduced that any factor which allows carbohydrate production to go on but discourages aerial growth in the plant will tend to encourage active root growth. For example, in corn crops and fruits, it has been found that when seed or fruits are ripening, root growth does not take place, since at that period the aerial parts are drawing heavily on the available carbohydrate supplies. Within perennial species matured plants may have root forms which are different from the youthful plants. This change of form has been attributed to aging.



## 2.3

## INFLUENCE OF ROOT SURFACE STRUCTURES

In this section attempts will be made to briefly discuss the common structures that are found on root surfaces, such as root hairs, nodulus, mucilage and root association with rhizobium and fungi (mycorrhiza). These root structures or associations are of paramount importance because they do not only enhance the absorption of water and nutrients by roots, but also contribute immensely towards the improvement of frictional properties between the root and the soil.

Removal of water from the soil by roots shrinks the soil, allowing other soil particles to come into contact and eventually become cemented (Koolen and Kuipers, 1983; Craul, 1993). Micro-organisms are attracted in great numbers and diversity to roots producing exudates, mucilages, etc., in addition to what is produced by the roots themselves. Recent studies show, that contact between growing roots and the soil matrix is established largely by mucigel and secretions that are found on the root surfaces (Russell, 1977). Whilst mucilages enhance the formation of bridges between soil particles and the root surface, root secretions flocculate colloids and cement soil aggregates (Gliński and Lipiec, 1990). Sloughing of root epidermal cells by friction between the roots surface and soil particles, as well as cyclic death of fine roots and sometimes the entire root systems contributes enormously to the amount of organic matter which causes cementation of the soil.

Root hairs are considered as important component of the root system. They do not only enhance anchorage of roots, they also increase the absorbing surface of the root system. Hofer (1991) described them as having cylindrical straight forms with dome-shaped tips often forming right angles with the root surfaces. Formation of root hairs is much influenced by the environment. In a favourable environment root hairs frequently emerge from the epidermal cells in the zone of cell extension within 5-10 mm of the apex. They develop acropetally (i.e., progressively towards the root apex) and their emergence appears to follow a retardation in the elongation of the parental epidermal cells (Russell, 1977). Depending on the species, lengths and diameters of individual root hairs range from 80 to 1500  $\mu\text{m}$  and 5 to 20  $\mu\text{m}$  respectively (Hofer, 1991). According to Kolesnikov (1971), the absorbing surface of a root system may be increased by a factor of 2 to 10 by the presence of root hairs. His studies that were conducted on one-year-old anis apple seedling showed as many as 17 million root hairs with a total length of about 3 km. In a

matured root system of winter rye, more than  $10^{10}$  root hairs have been estimated (Russell, 1977). Root hairs, however, have short lives, collapsing and being worn away after a few days or weeks (Schneemann, 1988; Hofer, 1991).

Associations of rhizobium and specific fungi with root systems of forest trees have adequately been documented. Root association with rhizobium often leads to the development of root nodule. The rhizobium bacteria invade the root mostly through the root hairs and in multiplying form an infection thread which further develops into nodules. Some authors argued that root nodules are modified lateral roots, but developmental studies do not support this concept (Esau, 1977). Fungi that form mutually beneficial relationships (symbiotic association) with plant roots are known as mycorrhizae. Two principal forms of mycorrhizae have been identified. These are (1) ectomycorrhizae and (2) endomycorrhizae (Bowen and Rovira, 1991; Esau, 1977; Craul, 1993; Foth, 1990). With ectomycorrhizae roots, the fungi envelop on the entire root surface forming a sheath but penetrate only the outer cell layers of the root cell walls. In such roots the development of root hairs may be depressed, and the volumes of apical meristem and root cap may as well be reduced. These roots are mostly short, branched and appear swollen (figure 2.7).

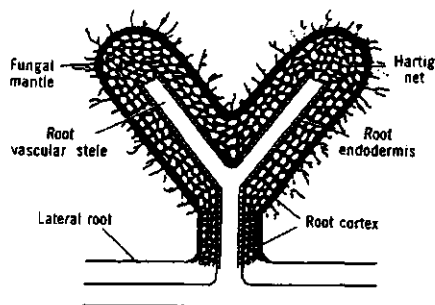


Figure 2.7 Anatomy of ectomycorrhizae root.

Source: Foth (1990)

Unlike ectomycorrhizae roots, the cells of endomycorrhizae roots are deeply penetrated by the fungi. This therefore makes the presence of the fungi difficult to determine visually. Endomycorrhizae roots are normally similar to uninfected roots in form but are darker in colour. Mycorrhizae associations with roots are known to occur under conditions of low or lack of balance in the availability of nitrogen, phosphorous, potassium, and

calcium. Light and substances exuded by roots are said to enhance their initiations. From the roots the fungus presumably receives sugars, amino acids, etc., whilst in return the following benefits may be derived by the root: (1) increase in amount of absorbing surface in contact with the soil, (2) increase in diameter and branching, (3) longer life (ectomycorrhizae infection prolongs the life of the roots) and (4) increased drought and heat resistance.

## 2.4

## ROOT STUDY METHODS

Work done by Böhm (1979) provided a good basis and insight into root studies. He pointed out, that a unique classification of the existing root-study methods on a systematic basis is impossible because several methods, different in principle may have certain features which are similar. He documented the following root-study methods: excavation methods, monolith methods, auger methods, profile methods, glass wall methods, container methods and indirect methods. In his book, (i.e., root study methods) detailed discussions of each of these methods were presented.

Hamazah et al. (1983) reported of the use of soil-block technique for estimating fine roots (roots of less than or equal to 5 mm in diameter) formation in forest ecosystems. Soil-block technique is considered more environmentally friendly than other methods used for similar purpose, since with this technique soil removed during root studies can be returned to its original location in the soil profile without much physical disturbance. Other advantages of this method over soil coring method include: (1) less labour and (2) can be used in a system where there are no significant changes in the standing root biomass throughout the year. Bragg et al. (1983) compared four different methods that are used to measure root distribution: mini-rhizotrons installed vertically, mini-rhizotrons installed at an angle of 45°, core-break root counts (i.e., counting the number of living roots per unit area on horizontal soil surfaces at different depths) and direct measurement of lengths of roots washed from soil cores. Between 30 cm below the soil surface and maximum rooting depth, it was found, that mini-rhizotrons installed at 45° gave better estimates of root distribution than the other methods. However, a number of conditions need to be satisfied to ensure good estimates (Vos and Groenwold, 1983). These include the following: (1) roots should not evade the interfacial area, (2) roots should not proliferate preferentially at the interface and (3) soil properties in the interfacial area should not be different from the rest of the soil. The use of autoradiographic technique for studying spatial distribution, density and length of roots has been documented by Fusseder (1983). With this method, autoradiograms obtained from serial soil sections were used to reconstruct spatial distribution of roots, as well as for calculating root length and density. The main advantage of this technique over other methods is that only living roots or root parts of the plant under investigation are considered. Summary of root study methods including their disadvantages and significance presented by Harper et al. (1991) is as shown in table 2.3.

Table 2.3 Root study methods for structure and distribution of root systems.

Root study method	Type of data obtained	Disadvantages
Excavation of whole plant system	Information on whole root system structure of individual plants.	Limited data about precise distribution of roots. No data concerning the interaction between roots of neighbouring plants.
Profile wall	Information on vertical and horizontal distribution of roots.	Only part of root system studied. No data on structure.
Pinboard	As in profile wall, with additional data about root length.	Data limited to 'slice' of the root system. Roots have to be separated from the soil.
Coring (soil samples taken using auger)	Information about length/weight in soil samples taken from various areas.	No insight into structure or neighbouring effects. Roots must be separated from soil.
Isotopes	Information about the inter-penetration of the root systems of neighbours.	No information on structure parameters.
Solution containing radioactive element (usually P or S) injected into plant or into soil around plant.		
Resin embedding.	Precise spatial distribution of roots in the soil.	Time consuming. Requires special equipment.
Rhizotrons	Changes in lengths and numbers of roots over time.	Expensive to build.
Mesh bags	Growth of root system into 'rootless' soil.	Data limited to net changes in growth over time. Roots must be separated from the soil.
Soil cores taken from field and bags filled with soil free from roots put in place.		
Dyeing	Changes in root length over time	Method works well only with porous media. Need to separate roots from the soil to obtain the data.
Different coloured dyes applied sequentially to soil.		
Parts of root system which are of different colours indicate amount of growth made.		

Source: Harper et al. (1991)

### **3**

## **PROPERTIES OF ROOT STRENGTH**

### **3.1**

## **INTRODUCTION**

The importance of mechanical properties of roots in soil-root reinforcement studies have been highlighted by many authors: Makarova et al. (1998); Liu (1994); Liu et al. (1994); Blackwell et al. (1990); Commandeur and Pyles (1991); Terwilliger and Waldron (1991); Wu et al. (1988); Wästerlund (1986); Waldron and Dakessian (1982); Waldron and Dakessian (1981); Waldron (1977), etc. Until recently, needed root mechanical properties for use in analysing soil-root systems were assumed or extrapolated from studies that were not always applicable to these systems. With these systems, the likelihood of producing results that significantly deviate from actual situation (ie., where roots are involved) seems highly probably. Investigations on root mechanical properties have mainly been focussed on the study of tensile strength, Young's modulus of elasticity, and shear strength because of the paramount roles they play in soil-root reinforced systems. Recent studies on mechanism of soil nailing have however indicated, that with regards to soil-reinforcement interaction, pull out strength and bending force of the reinforcement must be studied as well. Other mechanical properties which have also featured in discussions involving continual contribution of roots to improvement in soil strength and stability are creep, fatigue failure and Poisson's ratio. Few measurements on root strength properties have been reported (Wästerlund, 1989), therefore in the succeeding sections, discussion on measured data of root mechanical properties will be centred on: (1) tensile and (2) shear properties.

### **3.2**

## **MEASURED VALUES OF ROOT MECHANICAL PROPERTIES**

#### **3.2.1**

### **Tensile strength and Young's modulus of elasticity**

Generally, single roots of grass species are known to be weaker than that of trees species. On the average, axial strengths of the former have been found to be 3-10 MPa whilst that for the latter have been estimated to range from 10-70 MPa (Gliński and Lipiec, 1990). Tests conducted on individual roots of tree species put the estimates of tensile strengths of Sitka spruce, Western hemlock and Red huckleberry to be 17-52 MPa, 14-61 MPa and

15-23 MPa respectively. Wästerlund (1986) found tensile strength of Douglas-fir roots to range between 20 and 50 MPa for the cross section area inside the bark. Studies conducted on conifer tree roots indicated a tensile strength between 10-60 MPa.

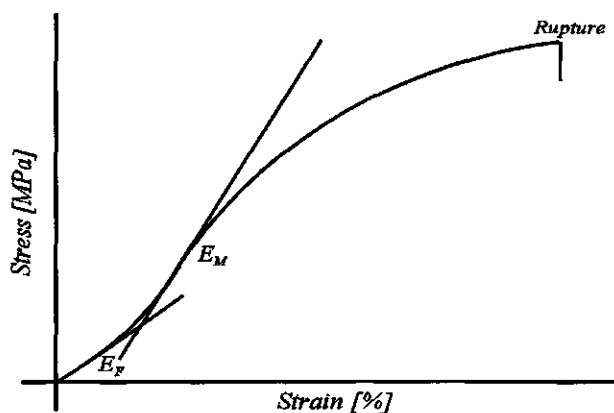
Both tensile strength and modulus of elasticity of roots of 20-year-old Douglas-fir (diameter ranged between 0.25 - 2.00 cm) have been studied by Commandeur and Pyles (1991). Roots used in their experiments were collected below the humus layer (down to a depth of about 30 cm) and were generally straight and free from major imperfections. Before testing, the roots were packed in a mixture of moist moss, humus and mineral soil, sealed in plastic bags, and stored in a refrigerator (at 10° to prevent desiccation and maintain freshness) for a duration of two weeks. Load cell and a linear variable differential transformer were used for measuring the tensile force and elongation of the gauged section of the roots respectively. Gauge length varied between 13.5 and 18 cm, whilst the distance between the grips was kept at 7.9 cm more than the gauge length. This was done to avoid the influence of end effects on the determination of the modulus of elasticity. Roots were debarked at their ends to ensure a firm grip of the clamps. Young's modulus of elasticity,  $E$ , was defined as the proportionality between stress and strain (equation 3.01).

$$E = \frac{\Delta Stress}{\Delta Strain} \quad 3.01$$

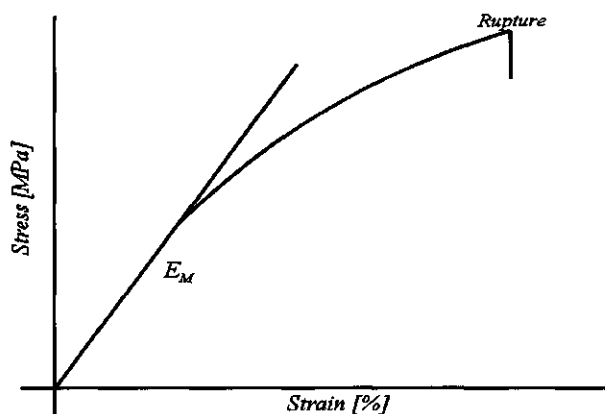
where,  $\Delta Stress$  and  $\Delta Strain$  = change in stress and strain respectively.

Basically, two different types of curves evolved from the experiments conducted by Commandeur and Pyles (1991): (1) sigmoid type of behaviour (figure 3.1 (a)) and (2) hyperbolic type of behaviour (figure 3.1 (b)). Behaviour of the sigmoid curve was attributed to straightening up of tortuous roots in the first portion, and then producing a hyperbolic curve in the second portion after the roots have straightened. From the first straight line segment, Young's modulus of elasticity was termed as form modulus,  $E_F$ , whilst in the second portion it was termed as material modulus,  $E_M$  (see figure 3.1). Average material modulus of intact root (i.e., with barks) was found to be at least 2.5 times as large as the form modulus (i.e.,  $E_M = 604$  MPa,  $E_F = 240$  MPa), whilst average tensile strength was found to be 17 MPa.

In a related study, Waldron and Dakessian (1981) measured modulus of elasticity,  $E$  and maximum tensile strength,  $\sigma_{\max}$  of pine and barley roots using an Instron model 1130 tensile tester with a cross head speed of  $2.5 \text{ mm min}^{-1}$ .



(a)



(b)

Figure 3.1 Stress versus strain for root displaying: (a) sigmoid and (b) hyperbolic behaviours.

Source: Commandeur and Pyles (1991)



Pine roots exhibited two linear parts: first part extending from 3 to 5% strain; second part extending from 5 to 6% strain to failure. Generally, ultimate tensile strength and modulus of elasticity of roots decreased with increasing root diameter and their relationships were given according to equations 3.02 and 3.03.

$$E = aD^b \quad 3.02$$

$$\sigma_{max} = cD^f \quad 3.03$$

where  $D$  = diameter of root (cm) and  $a$ ,  $b$ ,  $c$  and  $f$  are constants for the root species (see table 3.1).  $E$  and  $\sigma_{max}$  were measured in  $g\ cm^{-2}$ .

Table 3.1 Root constants for barley and pine.

Type of root	a	b	c	f
Barley	$8.32 * 10^3$	-1.210	$7.85 * 10^3$	- 0.944
Pine	$5.88 * 10^5$	-0.389	$6.89 * 10^4$	- 0.116

Source: Waldron and Dakessian (1981)

Tensile strengths of beech and larch roots were found by Liu (1994a) to be  $24 \pm 1.58$  MPa and  $18.45 \pm 2.25$  MPa respectively. Roots used in his experiments were taken from old beech and larch stands about 3 m away from the parent trees, and within a depth of 0-30 cm of the soil surface. Root diameter ranged between 0.8 - 6.0 mm. Liu's calculation of the Young's Modulus of elasticity followed similar procedure as reported by Commandeur and Pyles (1991). Modulus of elasticity of the first linear portion of the curve was called initial modulus of elasticity, whilst that for the second portion was referred to as final modulus of elasticity. The former for beech and larch roots were found to be  $527 \pm 49.87$  MPa and  $293 \pm 61.42$  MPa respectively, whilst the latter were found to be  $61.95 \pm 9.9$  MPa and  $53.88 \pm 7.6$  MPa respectively.

In a companion paper, Liu (1994b) presented a report on the time-dependent characteristic of root strength under cyclic loading (ie. repeated loading). Similar roots (i.e., beech and larch, diameter = 0.8 - 6.0 mm) were used. Elastic as well as plastic strains were observed during each loading cycle. When the test included non-zero dwell times at the force

reversal points, during which root length was fixed, root stress appeared to change during the dwell times. This change was a relaxation for the upper reversal points and a strength recovery (stress increase) for the lower reversal points. In this report he indicated that beech roots exhibited more stable characteristic on dynamic load than larch roots. Beech roots generally failed after 10-15 cycle loads whilst larch roots failed after 6-8 cycle loads.

Tensile properties (i.e., loading to failure and cyclic loading) of beech and larch roots have also been studied by Makarova et al. (1998). In their experiments, axial stress-strain relationships of the aforementioned roots were measured. Modulus of elasticity in this case was termed as an overall modulus of stiffness. Values for the first 10 cycles for beech and larch roots ranged between 162-763 MPa and 123-461 MPa respectively. During loading to failure, thin roots lost up to 60% of their water content and showed failure strains up to 16%. Results from this study showed that incremental plastic strains decreases with increase in number of cycles.

In his earlier research conducted with roots (diameter = 4-10 mm) of Sitka spruce, Coutts (1983) confirmed that, in fact, roots under tension follow a curve with a linear relationship between stress and strain up to the elastic limit before undergoing plastic deformation. Roots taken from a distance of about 80 cm away from the base of the stem were used for his experiments. He presented data on tensile strength of some tree roots. Among these, are those found in table 3.2.

Table 3.2 Tensile strength of tree roots.

Species	Proportionality limit		Failure	
	Stress (kPa)	Strain (%)	Stress (kPa)	Strain (%)
<i>Picea sitchensis</i>	15000	3	35000	13
<i>Pinus ponderosa</i>	4300	4	9000	20
<i>Populus deltoides</i>	8900	3	26600	12
<i>Populus yunnanensis</i>	12900	4	41000	18
<i>Salix matsudana</i>	12900	3	41000	18
<i>Salix purpurea</i>	15800	2	45300	18

Source: Coutts (1983)

### 3.2.2 Shear strength

Shear strength of the root is often calculated as the difference between shear strength of root permeated soil and the corresponding volume corrected root-free shear strength of the soil (see Terwillinger and Waldron, 1991; Waldron and Dakessian, 1982; Waldron and Dakessian, 1981). This is stated in equation 3.04. Often, this is estimated from soil-root in-situ shear test, soil-root in-situ pullout tests or simulation conducted from soil-root interaction models.

$$\Delta S_a = S_r - S_{(fallow)} \quad 3.04$$

where,

$\Delta S_a$  = absolute increase in soil's shear strength by roots

$S_r$  = shear strength of rooted soil

$S_{(fallow)}$  = shear strength of root free soil.

According to Waldron (1977), a direct shear device in which a prism of soil is sheared along a plane perpendicular to the axis of the prism, is particularly well suited to study the effect of plant roots on soil shearing resistance. To measure the contribution of roots, such as alfalfa (1 year old), barley and yellow pine (6 months) to soil shear strength, he conducted direct shear tests on 25-cm diameter root-permeated soil columns at shear depths of 15, 30 and 45 cm. Displacement rate of  $2.74 \text{ mm min}^{-1}$  was used. Before testing, matric potential of the shear plane of the samples were brought as close as possible to zero by adding water approximately 2 cm deep on the soil surface. This was done to ensure a steady flow through the column immediately sheared. Graphs of shearing resistance against horizontal shear displacement showed a rapid rise of shear stress with displacement to a maximum and then declined to a rather constant value. This behaviour of the graphs was more pronounced in barley and pine than alfalfa. Increase in soil shear resistance was observed in all the soil samples containing roots, with alfalfa registering the highest shear resistance. Absolute strength increase due to alfalfa at this depth (i.e., 30 cm) was  $100 \text{ g/cm}^2$ , whilst that of barley and pine were  $23 \text{ g/cm}^2$  and  $10 \text{ g/cm}^2$  respectively. From other studies Waldron (1977) quoted the shear strength of the root of European alder (*Alnus glutinosa-L*) at 20 cm depth to be  $83.7 \text{ g/cm}^2$ .

Waldron and Dakessian (1982) studied shear strength increase due to the presence of a number of young root species ranging from 3 to 52 months old. Among these plant species were hardinggrass (*Phalaris tuberosa-L*), Wimmera 62 ryegrass (*Lolium rigidum-L*), Palestine orchardgrass (*Dactylis glomerata-L*), Blando brome (*Bromus mollis-L*), greenleaf sudangrass (*Sorghum bicolor sudanense-L*), Anza wheat (*Triticum oestivum-L*), and barley (*Hordeum vulgare-L*). Cylindrical samples of rooted and root-free soil materials were each sheared along a predetermined plane perpendicular to a cylinder axis. The samples were prepared by packing soil materials into containers of 0.61 m in length made from two sections of 0.25 m diameter tubular concrete form taped together with a 3 mm thick spacer at the joint. When samples were to be tested, the tape and spacer were removed and the soil column sheared at the plane of the joint at a horizontal displacement speed of 2.7 mm/min. At shear displacement and soil cohesion of 25 mm and 2.0 kPa respectively, estimated values of roots contribution to soil shear strength,  $\Delta S_u$ , are as shown in table 3.3. These  $\Delta S_u$  values however showed a decrease of about 10% with increase in soil depth from 0.30 m to 0.45 m.

Table 3.3 Increase in the soil's shear strength ( $\Delta S_u$ ) for soil depths of 0.30 m and 0.45 m.

Root types	$\Delta S_u$ for soil depth of 0.30 m (kPa)	$\Delta S_u$ for soil depth of 0.45 m (kPa)
Hardinggrass	10.6	9.4
Ryegrass	9.8	7.7
Orchardgrass	9.5	6.2
Oak	9.4	5.1
Bromegrass	6.4	3.6

Source: Waldron and Dakessian (1982)

Terwilliger and Waldron (1991) used a direct shear device that had been specially designed to measure shear strength of large (0.25 m diameter by 0.61 m) root permeated soil samples. They used soil samples extracted under three vegetation types: chaparral, prescription-burned chaparral, and grassland. Shear strength of the rooted soil  $S_r$  in their tests was determined to be the maximum shearing force  $S_{Fmax}$  exhibited during horizontal

displacement per cross-sectional area of soil being sheared. This is as given by the equation 3.05 below.

$$S_r = \frac{S_{Fmax}}{A} \quad 3.05$$

where,  $A$  = cross-sectional area of the soil sample.

In the above experiments, root-free-soil samples were produced by decaying roots from extracted soil samples using hydrogen peroxide ( $H_2O_2$ ). This was accomplished by treating the tops of those samples with 1 ml of 30%  $H_2O_2$  on two consecutive days and covering them with metal slab to prevent frothing or other significant movement of soil particles. The samples were then stored for one month at 30° C on a stand slightly above a pool of water in a covered container. In order to gather enough trials necessary to simulate natural field conditions, a rapid horizontal displacement rate of 2.74 mm min<sup>-1</sup> was used. Load applied to the shear plane of each shear test was the weight of the soil above the area being sheared. In this studies, soil's strength was found to increase significantly by the presence of all the vegetation types (paired t-tests;  $P < 0.00001$  for grassland and burned chaparral;  $P \leq 0.0003$  for unburned chaparral). Mean values and coefficient of variation (c.v) of  $S_r$  and  $S_{(fallow)}$  found for the three vegetation types are as presented in table 3.4.

Table 3.4 Shear strength values for three different vegetation types.

Vegetation type	$S_r$ (kPa)		$S_{(fallow)}$ (kPa)		$\Delta S_r$ (kPa)	
	Mean	c.v	Mean	c.v	Mean	Max.
Unburned chaparral	2.5	0.4	2.1	0.3	0.4	3.0
Burned chaparral	2.6	0.3	2.0	0.3	0.6	2.7
Grassland	2.8	0.3	2.2	0.3	0.6	2.4

Source: Terwilliger and Waldron (1991)

Measuring the in-situ shear strength of soil-root ball interface, Smith (1986) used an apparatus which has been designed to apply a maximum torque of 50 kNm. This apparatus

was an adaptation of a torsional shear test. It consisted of a torque bar, equalizing bar, winch, load cell and various wire ropes, shackles, slings and blocks. The theoretical principle underlying the use of his apparatus was that, if the shear strength of the interface at failure is assumed to be uniform across the shear failure, then the torque developed can be estimated by equation 3.06.

$$S_r = \frac{3T}{2 \pi R^3} \quad 3.06$$

where,

- $S_r$  = shear strength on the failure surface
- $T$  = torque
- $R$  = radius of failure surface.

Comparatively very little field studies have been done on the pull-out resistances of roots. Pull-out resistances of single roots of field pea (*Pisum sativum-L*) is quoted to be 100 g/cm<sup>2</sup> root surface in the absence of root hairs and 300 g/cm<sup>2</sup> to 600 g/cm<sup>2</sup> where root hairs were present. These values were found in a compacted clay loam with a bulk density of 1.7 g/cm<sup>3</sup> and matric potential of -0.3 bar.

In general many confounding factors make it difficult for the true magnitude of roots contribution to increase in the soil shear strength to be determined. These are not only soil factors (some of which are discussed in section 2.3), but may include factors which directly or indirectly affect the measurement of root tensile properties and/or soil-root in-situ shear strength. Measurement of root tensile properties may be affected by:

- (1) rate of elongation used
- (2) season
- (3) clamping
- (4) root preparation before measurement.

On the other hand, factors affecting the measurement of soil-root in-situ shear strength may include: (1) testing equipment used, (2) scheme of root placement in the soil and (3) level of soil compaction.

## 4 MEASURING ROOTS MECHANICAL PROPERTIES

### 4.1 INTRODUCTION

Stress versus strain relationships of tree roots have been studied by only a few number of researchers. They include Liu (1994), Makarova et al. (1998), Commandeur and Pyles (1991) and Coutts (1983). These studies showed that a tree root under tension follows a curve with a more or less a linear relationship between stress and strain up to the elastic limit, undergoes plastic deformation, before failure occurs. Failure strains ranging between 10-20% have been reported.

In addition to the above characteristics, plant roots are reported to exhibit features of fatigue that are known in material testing. Repeated or cyclic loading of tree roots in forest floors are caused mainly by the action(s) of wind or forestry vehicles, or both. Wind action may directly affect anchorage or tree stability and has been studied by Henwood (1973), Coutts (1983), Coutts (1986), Blackwell et al. (1990), O'Sullivan and Ritchie (1993). From these studies, reductions in peak overturning moments with repeated loading were observed. Roots in the top layers of forest soils are subjected to repeated loading when a forestry vehicle passes through the same track or repeatedly travels in the same track as it often occurs during forestry operations. The roots acting as reinforcements tend to reduce rut formation induced on the soil by vehicles. However, in contrast to other soil reinforcement materials such as boulders and rocks, the reinforcement effect provided by roots is not durable and diminishes with increasing number of vehicle passes. Figure 4.1 shows idealized axial force-elongation relations of roots which may occur when a root-soil system is loaded by one or more vehicle passes: figure 4.1 (a) idealizes the case in which one wheel (or track) forms a permanent rut, figure 4.1 (b) applies to the case in which some immediate rut recovery occurs behind a wheel because of the resilience of many and/or thick roots, figure 4.1 (c) presents idealized root forces and elongations that occur when rut depth increases due to repeated passes and figure 4.1 (d) shows root forces and lengthening/shortening for the case that wheel passes are repeated and root forces have turned to zero between successive wheel passes.

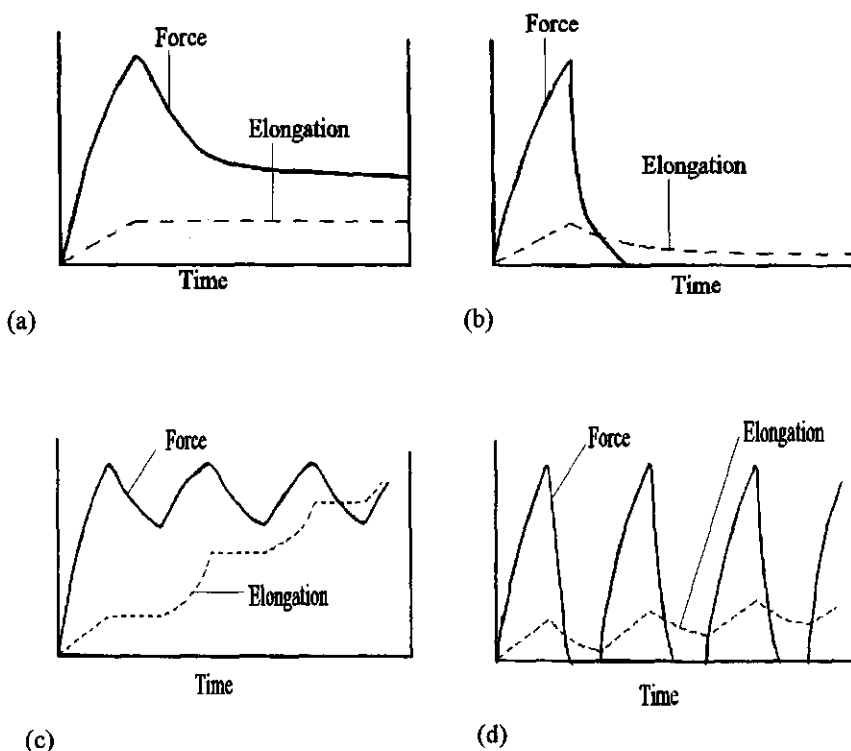


Figure 4.1 Idealized axial force-elongation relations of roots loaded by vehicle wheels or tracks.

Beech (*Fagus sylvatica* - L) and larch (*Larix decidua* - L) roots under action of cyclic loading have been studied by Liu (1994) using uniaxial tensile tests. In these experiments, loading was cyclic between a chosen lower and an upper boundary force being much lower than the failure force. Elastic as well as plastic strains were observed during each loading cycle. When the test included non-zero dwell times at the force reversal points during which root length was fixed, root stress appeared to change during the dwell times. This change was a relaxation for the upper reversal points and a strength recovery for the lower reversal points.



One of the problems that is commonly encountered in uniaxial tensile experiments, but which has attracted very little investigation is clamping of the test specimen. In most publications, the way in which clamping was achieved during testing is not adequately documented. Improper clamping may cause slippage or breakage of the test specimen (i.e., at or near the clamp) or both. These partly lead to registration of incorrect testing results. Selection of appropriate clamping or gripping device and procedure is therefore considered essential in the measurement of root mechanical properties. Generally, clamping devices work on the principle of two jaws being drawn together by a screw. An example is the drill press device shown in figure 4.2.

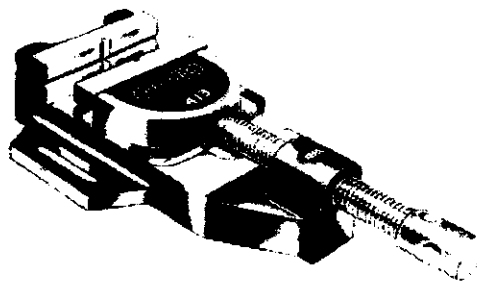


Figure 4.2 Drill press device.

Source: Pettit (1984)

Among the important functions of gripping devices is their ability to transmit loads from the heads of testing machines to the test specimen and will be achieved if the load is transmitted axially to the specimen. This implies that: (1) centres of action of the grips must be in alignment at the beginning and during the progress of a test, (2) no bending, or twisting be introduced by action or failure of the grips and (3) the device should be adequately designed to carry loads and should not be loosened during testing. Slippage in clamps may be reduced when those parts of the clamp jaws which come into direct contact with the test specimen are serrated. This will promote friction within the grips, thus, ensuring good grips of the specimen. Fast drying glue may also be applied when necessary (see Chang et al., 1996; Liu, 1994). In situations where soft specimens are to be clamped, indentation on the specimen can be avoided by using clamps with jaws made from soft material (e.g., aluminium, copper, lead) or liners.

Failure of test specimen close to the jaws of the clamping device may be prevented if the jaws of the clamping device are blinded or chamfered as illustrated in figure 4.3 and/or optimum clamping force is applied. Optimum clamping force can be found through series of test trials.

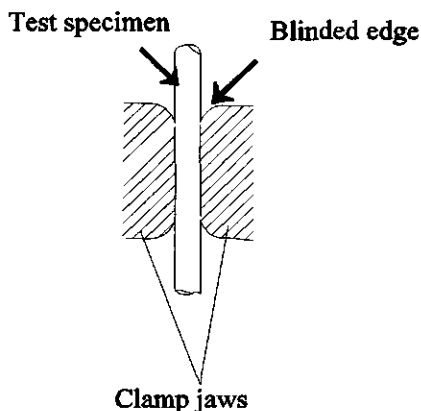
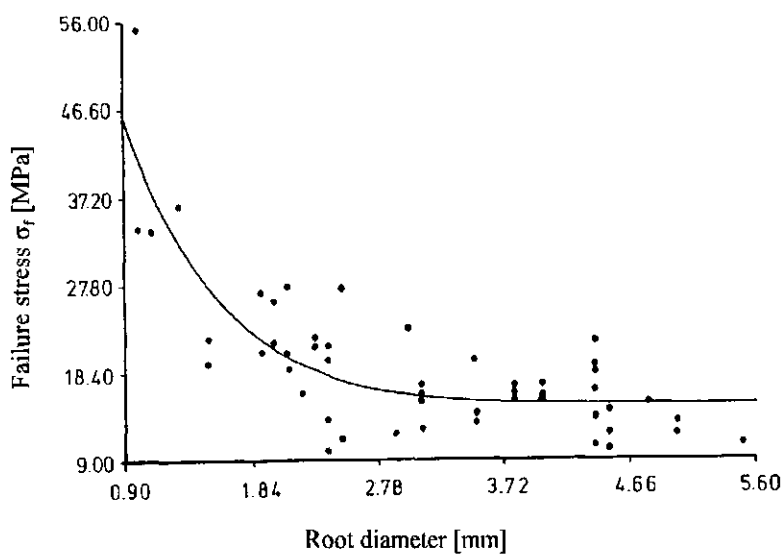
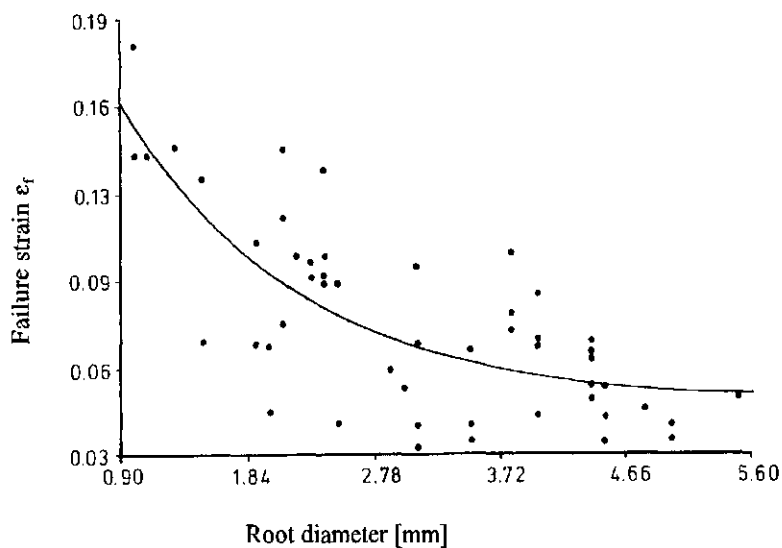


Figure 4.3 Illustrating rounded clamp jaw edges.

Our earlier studies on beech and larch roots (see Makarova et al., 1998) showed that failure stresses and strains of fine roots relate very well to the roots diameter (figure 4.4). Values of moduli of elasticity estimated in these experiments referred to the entire ranges of observed strain and was termed as overall stiffness modulus. Relationships between the stiffness moduli on cyclic loading ( $E_{li}$ ) and unloading ( $E_{ui}$ ) and the maximum stress ( $\sigma_{max}$ ) were given by equations 4.01 and 4.02 respectively.  $E_{li}$  was found to be relatively low whilst incremental plastic strain was found to be relatively high for the first loading cycle. The latter was also found to decrease with increasing root diameter.



(a)



(b)

Figure 4.4 Measured relationship between root diameter and (a) failure stress and (b) failure strain.

Source: Makarova et al. (1998)

$$\Delta \varepsilon_{ei} = \frac{\sigma_{\max}}{E_{li}} - \Delta \varepsilon_{pi} \quad 4.01$$

$$E_{ui} = \frac{\sigma_{\max}}{\Delta \varepsilon_{ei}} \quad 4.02$$

where,

$\Delta \varepsilon_{ei}$  = elastic part of incremental strain respectively in cycle i

$\Delta \varepsilon_{pi}$  = plastic part of incremental strain in cycle i.

Published reports on roots cyclic loading experiments have shown that upper reversal stresses used in these experiments are taken far below the estimated failure stresses. Effects of cyclic loading with upper reversal stresses close to the estimated failure stress and with non-zero dwell times have not yet been investigated. These results may depend on elongation rate or test speed. Studies have shown that elongation rates do influence the magnitude of mechanical properties of fibres. Morton and Hearle (1976) reported of an increase in tensile strength of fibres of about 6% to 9% for each tenfold increase in the elongation rate. Similar findings have been reported by Lopes (1996). Effects of elongation rate on mechanical properties of roots are still not known. Our earlier root studies (Makarova et al., 1998) revealed, that in cyclic loading experiments, the relative loading,  $\sigma_{\max}/\sigma_f$ , in which  $\sigma_{\max}$  and  $\sigma_f$  are maximum stress and failure stress (in a single loading) cannot be accurately determined. This was mainly due to the fact that failure stresses ( $\sigma_f$ ) of the same pieces of roots, that have been subjected to cyclic loading, cannot be measured. It can neither be estimated accurately because of wide scatter of  $\sigma_f$  measuring values. It is expected that an adjacent piece of the same root (i.e., on the same root length) will provide a good estimate. Hence, this study will mainly be centred on: (1) finding an appropriate clamping procedure for roots to minimize slippage and promote failure of roots further away from the clamp jaws, (2) comparing the spread of stress-strain relationships of root pairs to that of their corresponding diameter classes, (3) studying the effect of test speed (rate of elongation) on measured stress-strain relationship, (4) measurement of failure stresses, failure strains and (5) fatigue behaviour of thick roots using a reliable percentage of stress level. Influence of percentage stress levels and diameter on stiffness modulus and plastic strain increment will also be studied.

## 4.2 MATERIALS AND METHODS

### 4.2.1 The testing machine

Failure and cyclic loading experiments of roots (diameter ranging between 2-12 mm) were carried out with a computer-controlled Zwick 1455 Universal Material Testing Machine. These experiments consisted of force-elongation measurements.

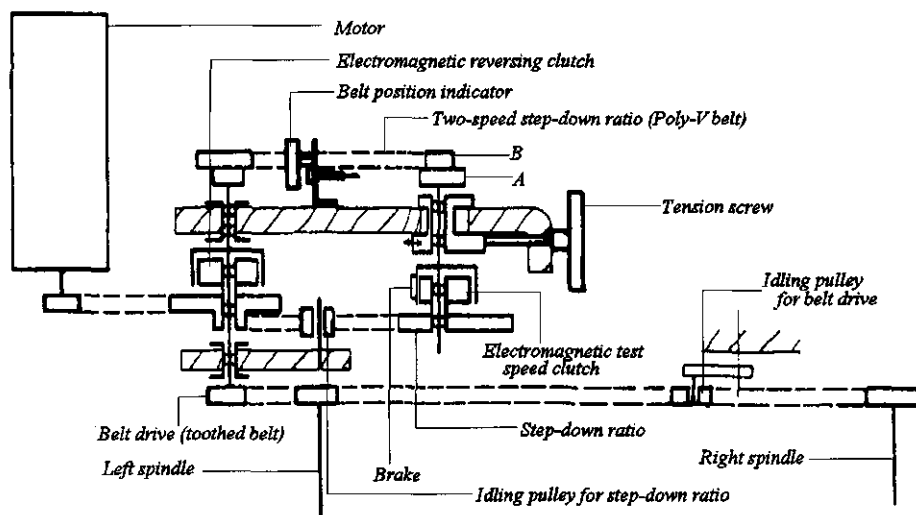


Figure 4.5 Zwick Universal Testing Machine: DC variable speed drive.

The Zwick machine uses a stiff strain-gauge type force transducer and a mechanical drive which produced constant linear speeds. Its two-speed step-down mechanism permits matching of speed and test force in a ratio of 1:2. Speeds which are attainable with ratios A and B (see figure 4.5) and their corresponding maximum test forces permissible are presented in table 4.1. Test parameters such as elongation rates (test speeds), return speeds, test directions, etc., are preselected on the Materials Testing Computer. Slippage and failure of roots during testing were monitored on the material testing computer connected to the Zwick machine. Testing was immediately stopped and results discarded when slip occurred. Measured values of force-elongation were later converted into stress-strain values by dividing the force and elongation values by initial cross-sectional area and length of the root respectively.

Table 4.1. Test speeds and force permitted by the Zwick Universal Testing Machine.

Ratio	Test speed (mm/min)	Max. test force (kN)	Max. return speed (mm/min)
A	0.5 - 1000	10	2000
B	0.2 - 500	20	2000

#### 4.2.2 Clamping procedure

Clamping of the root samples was done by introducing two wooden blocks, one on each side of the root within the jaws of the clamping device used on the testing machine (figure 4.6). Suitable hardness of the wood blocks was selected by considering woods of different hardness: soft; medium; and hard. Each wooden block was provided with a groove that had a semi-circular cross section. The blocks were positioned in such a way that the grooves formed a cylindrical hole, hence clamping the root sample within its cylinder walls. Matching groove size and magnitude of clamping force was developed by experience.

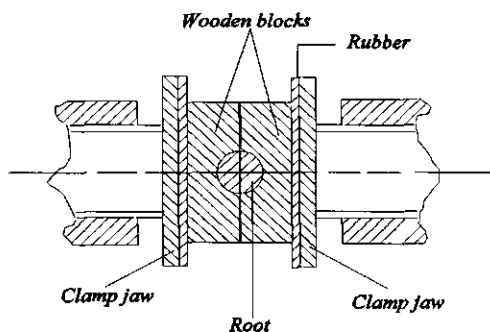


Figure 4.6 Method of clamping.

#### 4.2.3 Collection, preparation and storage of root samples

Roots for the experiments were collected from old beech (*Fagus sylvatica* - L) and larch (*Larix decidua* - L) stands in the months of November 1997 and 1998 from the State forest 'Speulder and Sprielderbos' (Garderen) situated on the western slope of the Veluwe. This area is on an elevation of about 35 metres above sea level and was chosen because it constitutes the main sampling sites for most of the research works in the direction of Soils and Forestry carried out in the Wageningen University. Soil and plant data, for example, soil development, soil physical properties and management practices of the forest are therefore well documented and easy to obtain. The soil profile consisted of a greyish A-horizon (0-10 cm), a yellowish B/C-horizon (10-60 cm) and a yellow C-horizon (> 60 cm). The A-horizon is fairly loose and the field capacity tension of the topsoil is approximately 10 cbar (pF 2.0). According to Beekman (1987), this tension seldom decreases below 10 cbar because the soil exhibits high unsaturated conductivity at low tension and is adequately drained. Little evidence of earthworms or other large soil fauna activities has been found within the soil. Soil pH-KCl varies from 3.5-4.5 depending on organic matter content. Water table in this area is relatively deep (>2 m). Roots are therefore concentrated in the topsoil and that part of the soil profile which contains some amount of organic matter.

Beech (*Fagus sylvatica* - L) and larch (*Larix decidua* - L) roots were taken from compartments 106 g and 235 n respectively. The roots were taken between trees at a depth of about 30 cm below the soil surface. Their diameters ranged between 4 and 12 mm. In order to prevent pre-stress effects, none of the roots were pulled, instead they were cut with sharp scissors, put in plastic bags, and loosely sealed. In the laboratory, the roots were thoroughly inspected for possible breakage and peeling and root hairs were carefully dismembered. Suitable samples of a length of about 20 cm were put in different plastic bags, with added free water (to keep water content at a normal level), sealed and stored in a refrigerator at about 5° C. Roots testing begun after few days of collection.

#### **4.2.4 Experimental scheme**

##### **4.2.4.1 General**

Before each experiment began, average root diameter was found by measuring diameters at 10 different positions along the length of the root. Each root sample of length 20 cm was divided into two of 10 cm each which constituted a root pair. Effective lengths (i.e., grip to grip separation) of test samples were always fixed at 50 mm. By visual inspection root samples were positioned as vertical as possible with their axis coinciding with the load cell axis. For each test a pre-load of 1 N and elongation rate of 10 mm/min (unless otherwise stated) were used. In-depth statistical analyses will not be carried out here (see discussions 4.4). Experimental results will however be displayed by means of scatter plots to provide complete pictures of the relationships between root stresses and strains. Further analyses (i.e., when required) of experimental results will be done by using other mathematical procedures which in accordance with the aims of this study will provide more practical and realistic interpretations.

##### **4.2.4.2 Experiment 1: effect of beech and larch root pairs**

Roots were classified into diameter classes. Within a particular diameter class, stress-strain relationships of root pairs were measured. Experimental results were displayed by means of scatter plots. Spread occurring within root pairs was compared to the spread occurring within the corresponding diameter class. Root diameters ranged between 2.0 mm and 5.0 mm.

##### **4.2.4.3 Experiment 2: effect of elongation rate (speed effect) on stress-strain relationships of beech roots**

Using pairs of small beech roots, stress-strain relationship of one member of the pairs was measured at a displacement rate of 10 mm/min, whilst that for the other member was measured at 400 mm/min. Speed effect was estimated as the difference between the stress-strain relationships of root samples measured at 10 mm/min and that measured at 400 mm/min. Root diameters ranged from 2.2 mm to 2.7 mm.



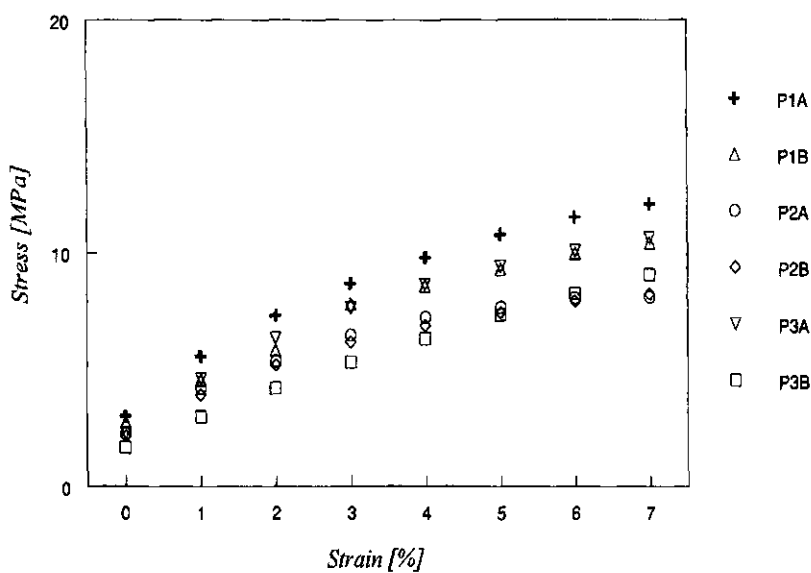
#### **4.2.4.4 Experiment 3: failure stresses and strains and behaviour of thick beech roots under cyclic loading**

Fatigue behaviour of beech roots was measured using pair samples. One member of the pairs was used in measuring failure stress and strain, whilst the other was subjected to cyclic loading. Nominal number of cycles used for the cyclic loading was taken to be 50, but sometimes testing was interrupted due to root failure. For each cyclic loading test, lower reversal stress was kept constant at 1 MPa, whilst upper reversal stress was taken as either 25%, 50%, 75%, or 90% of the failure stress measured earlier. Root diameter ranged between 4-12 mm. Overall stiffness moduli and plastic strain increments for the various loading cycles were estimated from the experimental curves.

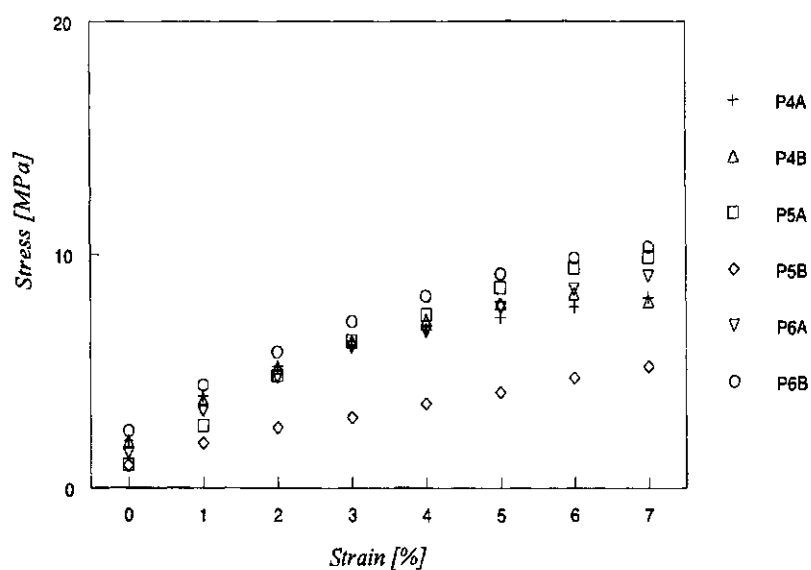
### **4.3 RESULTS**

#### **4.3.1 Experiment 1: effect of beech and larch root pairs**

Roots used in this experiment were beech (*Fagus sylvatica* - L) and larch (*Larix decidua* - L). Root pairs and pair members were differentiated by adopting the following system of identification: root filenames showing the pair number and a letter "A" or "B" to differentiate between pair members. Implying that roots P1A and P1B originally came from the same root piece of about 20 cm long, but which was later divided into 10 cm each for experimentation. Other root pairs were P2A and P2B; P3A and P3B; P4A and P4B; P5A and P5A; P6A and P6B. Stress-strain relationships of both members of the root pairs were measured at 10 mm/min. Scatter plots of the stress-strain relationships of larch and beech roots are shown in figures 4.7 and 4.8 respectively.

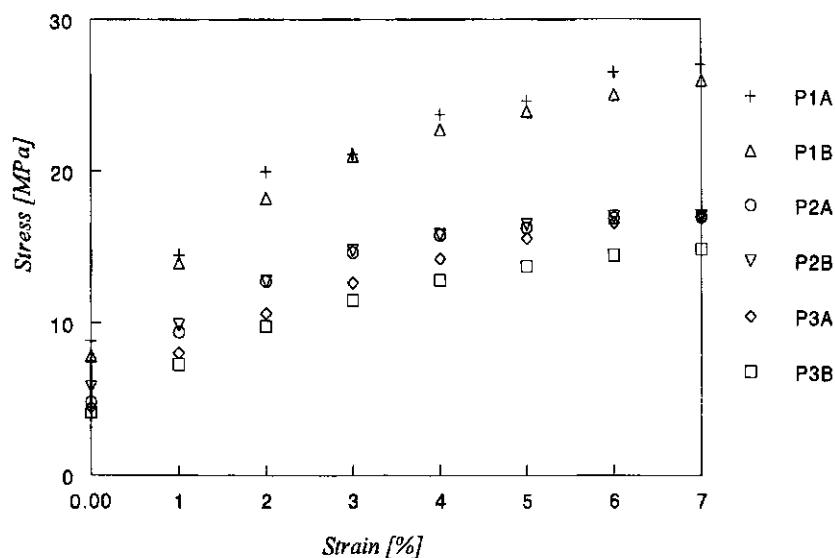


(a)

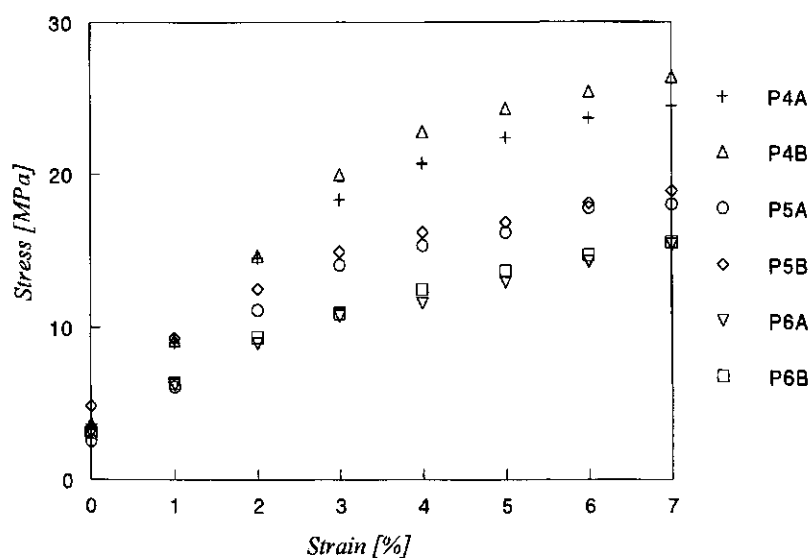


(b)

Figure 4.7 Stress-strain relationships of larch root pairs in diameter ranges: (a) 3.0-3.9 mm and (b) 4.0-4.9 mm.



(a)

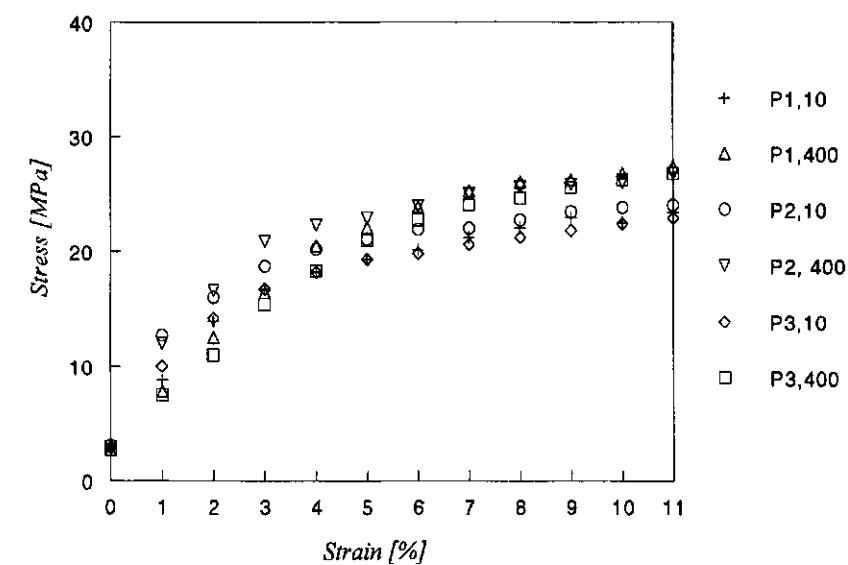


(b)

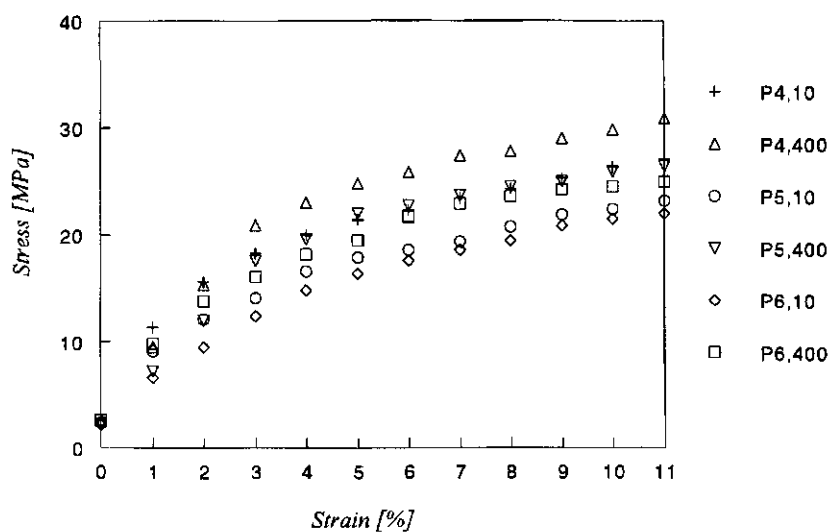
Figure 4.8 Stress-strain relationships of beech root pairs in diameter ranges:  
(a) 2.0-2.9 mm and (b) 3.0-3.9 mm.

#### **4.3.2 Experiment 2: effect of elongation rate (speed effect) on stress-strain relationships of beech roots**

Using beech root pairs, stress-strain relationship of one pair member was measured at an elongation rate of 10 mm/min, while the other pair member was measured at 400 mm/min. In order to distinguish between root pairs and pair members a system of identification was adopted where root filenames consisted of two parts: first part showing the pair number and the second part showing the magnitude of the elongation rate used. Implying that roots with filenames P1,10 and P1,400 constitute a pair with the stress-strain relationship of the former being measured at 10 mm/min whilst that of the latter was measured at 400 mm/min. Other root pairs were P2,10 and P2,400; P3,10 and P3,400; P4,10 and P4,400; P5,10 and P5,400; P6,10 and P6,400. Scatter plots showing the effect of elongation rate on measured stress-strain values of beech root pairs are as shown in figure 4.9.



(a)



(b)

Figure 4.9 Effect of elongation rate on stress-strain relationship of beech root with diameter ranging from: (a) 2.2 mm-2.4 mm and (b) 2.5 mm-2.7 mm.

### 4.3.3 Experiment 3: failure stresses and strains and behaviour of thick beech roots under cyclic loading

Scatter plots of failure stresses versus diameter and failure strains versus diameter are as shown in figures 4.10 and 4.11 respectively.

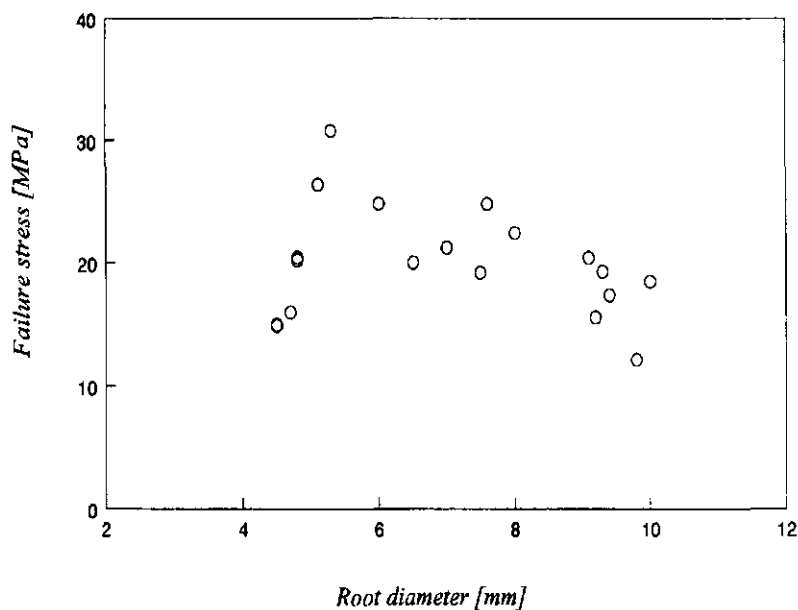


Figure 4.10 Measured relationship between failure stress and diameter of beech roots harvested in November.

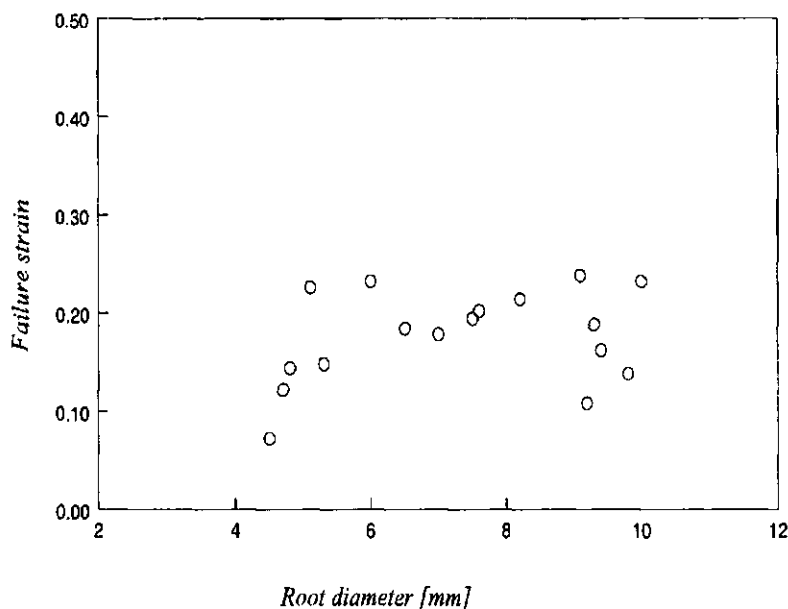


Figure 4.11 Measured relationship between failure strain and diameter of beech roots harvested in November.

Cyclic loading of beech roots showed two main characteristics during the first loading cycle. These characteristics were identified as hyperbolic (figure 4.12 (a)) and sigmoid (figure 4.12 (b)). Overall stiffness modulus for the first loading cycle of roots exhibiting characteristics shown in figure 4.12 (a) and figure 4.12 (b) were estimated below by equation 4.03 and 4.04 respectively. Stiffness modulus for the second and subsequent cycles were calculated using the definition in equation 4.05. Plastic strain increments for the first loading cycle in the hyperbolic and sigmoid curves were calculated using equations 4.06 and 4.07 respectively.

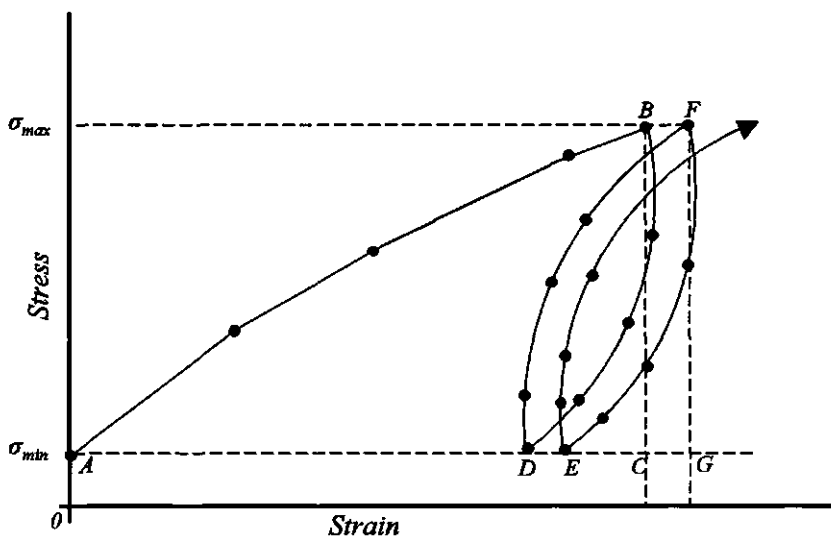
Overall modulus of stiffness for the first hyperbolic loading cycle ( $E_{11h}$ ) =  $BC/AC$  4.03

Overall modulus of stiffness for the first sigmoid loading cycle ( $E_{11s}$ ) =  $BC/A'C$  4.04

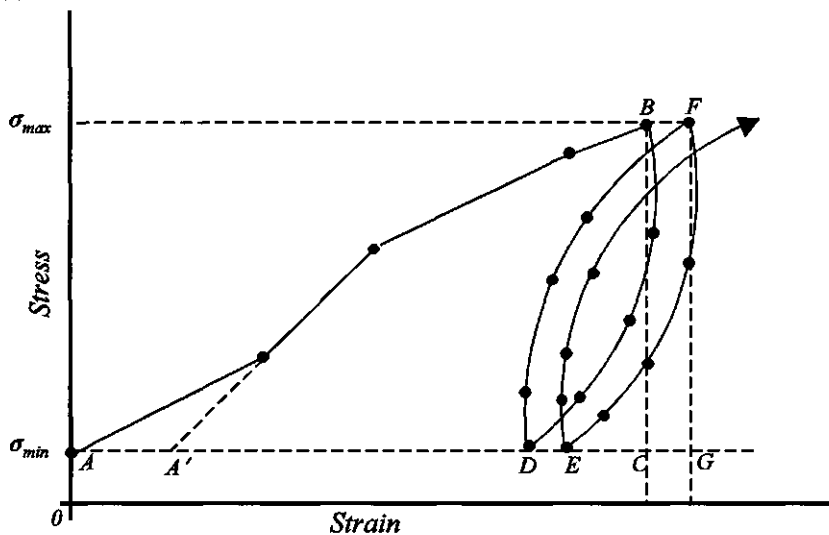
Overall modulus of stiffness for the second loading cycle ( $E_{12}$ ) =  $FG/DG$  4.05

Plastic strain increment for the first hyperbolic loading cycle ( $\Delta\epsilon_{1h}$ ) =  $AD$  4.06

Plastic strain increment for the first sigmoid loading cycle ( $\Delta\epsilon_{1s}$ ) =  $A'D$  4.07



(a)



(b)

Figure 4.12 Characteristic curves of beech roots (diameter = 4-12) on cyclic loading: (a) hyperbolic and (b) sigmoid.



Tables 4.2 and 4.3 show results of stiffness modulus and plastic strain increment respectively for the first ten loading cycles of the experiments.

Table 4.2 Overall modulus of stiffness  $E_{ji}$  of beech roots of diameter  $D$  in the loading cycle  $i$  with an upper reversal stress  $\sigma_{\max}$  and lower reversal stress  $\sigma_{\min}$  of 1 MPa.

D (mm)	$\sigma_{\max}$ (MPa)	$E_{ji}$ (MPa)									
		i=1	2	3	4	5	6	7	8	9	10
4.7	4.0 <sup>a</sup>	382	592	612	655	655	680	655	655	680	680
5.1	6.6 <sup>a</sup>	175	206	216	223	229	235	235	238	238	241
6.0	6.2 <sup>a</sup>	219	449	474	492	502	502	512	522	522	533
6.5	5.0 <sup>a</sup>	599	761	790	790	790	790	822	822	856	856
7.5	4.8 <sup>a</sup>	152	448	481	494	507	507	507	500	513	513
8.0	5.6 <sup>a</sup>	229	653	671	691	691	691	691	691	691	691
7.6	12.4 <sup>b</sup>	247	562	579	591	597	610	619	624	631	624
6.4	10.6 <sup>b</sup>	272	539	558	564	571	585	578	578	585	607
4.8	10.2 <sup>b</sup>	280	539	552	565	573	580	580	580	587	587
7.0	10.6 <sup>b</sup>	228	527	533	539	552	558	571	571	571	571
9.8	6.1 <sup>b</sup>	276	406	406	420	427	434	427	427	427	434
4.5	7.5 <sup>b</sup>	145	265	274	285	285	285	285	285	285	285
9.3	14.6 <sup>c</sup>	149	327	344	353	354	351	353	354	360	366
10.0	13.9 <sup>c</sup>	199	443	459	456	466	483	483	490	494	494
5.3	23.1 <sup>c</sup>	168	361	384	395	396	407	408	411	416	425
4.8	15.2 <sup>c</sup>	142	226	231	233	233	233	233	233	233	240
9.1	15.3 <sup>c</sup>	123	263	280	288	292	295	295	296	301	307
4.5	13.5 <sup>d</sup>	171	323	332	378	339	-	-	-	-	-
9.2	14.0 <sup>d</sup>	181	353	367	371	373	375	377	386	460	460
9.4	15.7 <sup>d</sup>	188	385	404	407	409	-	-	-	-	-
10.3	19.0 <sup>d</sup>	346	714	743	755	769	769	789	-	-	-

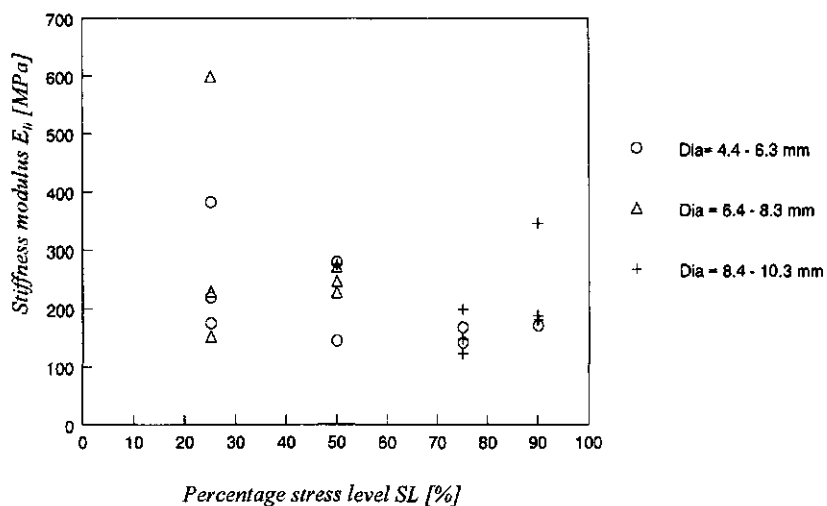
a, b, c, d = 25, 50, 75, 90 percent of failure stress respectively.

Table 4.3 Plastic strain increment  $\Delta\epsilon_{pi}$  of beech roots in cycle  $i$  of cyclic loading to an upper reversal stress  $\sigma_{max}$  and lower reversal stress  $\sigma_{min}$  of 1 MPa.

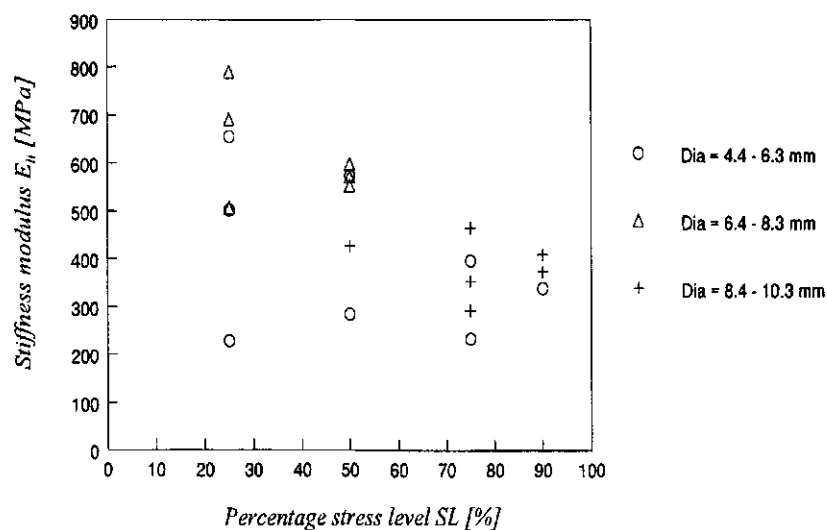
D (mm)	$\sigma_{max}$ (MPa)	$\Delta\epsilon_{pi} * 10^3$									
		i=1	2	3	4	5	6	7	8	9	10
4.7	4.0 <sup>a</sup>	5.6	1.2	0.6	0.4	0.6	0.2	0.2	0.2	0.0	0.0
5.1	6.6 <sup>a</sup>	23.0	1.8	1.4	0.8	1.0	0.4	0.4	0.2	0.2	0.2
6.0	6.2 <sup>a</sup>	14.6	1.0	0.6	0.4	0.2	0.4	0.2	0.2	0.2	0.2
6.5	5.0 <sup>a</sup>	2.4	0.4	0.2	0.2	0.2	0.2	0.2	0.2	0.0	0.0
8.0	5.6 <sup>a</sup>	14.8	0.4	0.40	0.2	0.0	0.2	0.0	0.0	0.0	0.2
7.5	4.8 <sup>a</sup>	23.6	0.8	0.4	0.2	0.2	0.2	0.2	0.2	0.0	0.0
7.6	12.4 <sup>b</sup>	31.0	1.4	0.8	0.6	0.8	0.4	0.4	0.4	0.0	0.0
6.4	10.6 <sup>b</sup>	22.2	1.2	0.8	0.4	0.6	0.2	0.2	0.4	0.2	0.0
4.8	10.2 <sup>b</sup>	25.8	1.0	0.8	0.4	0.4	0.2	0.2	0.2	0.0	0.0
7.0	10.6 <sup>b</sup>	27.0	1.4	0.6	0.6	0.4	0.8	0.2	0.0	0.0	0.0
9.8	6.1 <sup>b</sup>	8.8	0.6	0.8	0.4	0.4	0.2	0.2	0.2	0.2	0.4
4.5	7.5 <sup>b</sup>	27.4	1.4	1.2	0.0	0.0	0.0	0.0	0.0	0.0	0.0
9.3	14.6 <sup>c</sup>	55.6	0.4	2.4	1.6	1.4	1.0	1.0	1.0	0.6	0.4
10.0	13.9 <sup>c</sup>	39.6	2.4	1.4	1.2	1.4	0.6	0.6	0.6	0.2	0.2
5.3	23.1 <sup>c</sup>	76.0	6.4	3.4	2.6	2.0	1.4	1.4	0.12	2.0	1.2
4.8	15.2 <sup>c</sup>	42.6	3.4	2.0	1.4	1.0	1.4	0.8	1.0	1.6	0.6
9.1	15.3 <sup>c</sup>	69.4	5.8	3.4	2.4	1.8	1.8	1.4	1.2	2.2	1.0
4.5	13.5 <sup>d</sup>	40.6	4.0	2.6	1.8	1.6	-	-	-	-	-
9.2	14.0 <sup>d</sup>	40.2	3.3	2.0	1.4	1.2	1.0	1.6	-	-	-
9.4	15.7 <sup>d</sup>	44.8	3.8	2.0	1.4	1.4	-	-	-	-	-
10.3	19.0 <sup>d</sup>	31.4	2.2	1.4	1.0	0.8	0.8	-	-	-	-

a, b, c, d = 25, 50, 75, 90 percent of failure stress respectively.

Considering the first and fifth loading cycles, effects of percentage stress level and root diameter on stiffness modulus and plastic strain increment were studied. The resulting scatter plots are shown in figures 4.13 to 4.15.

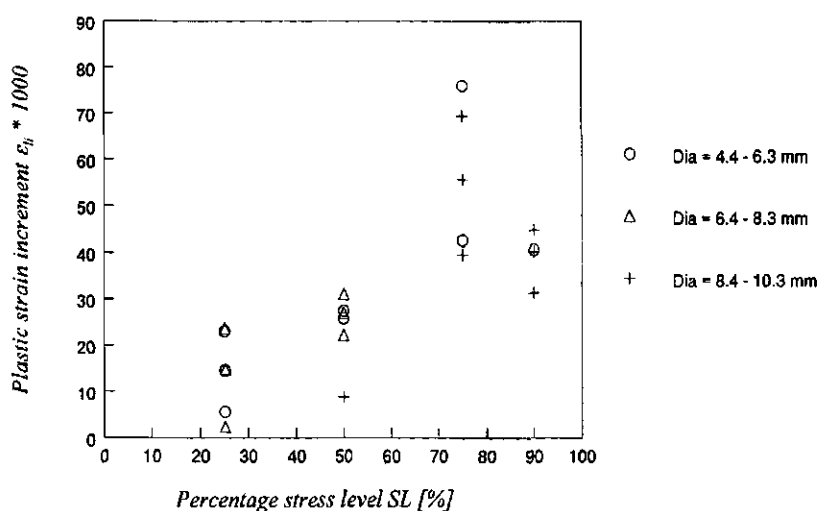


(a)

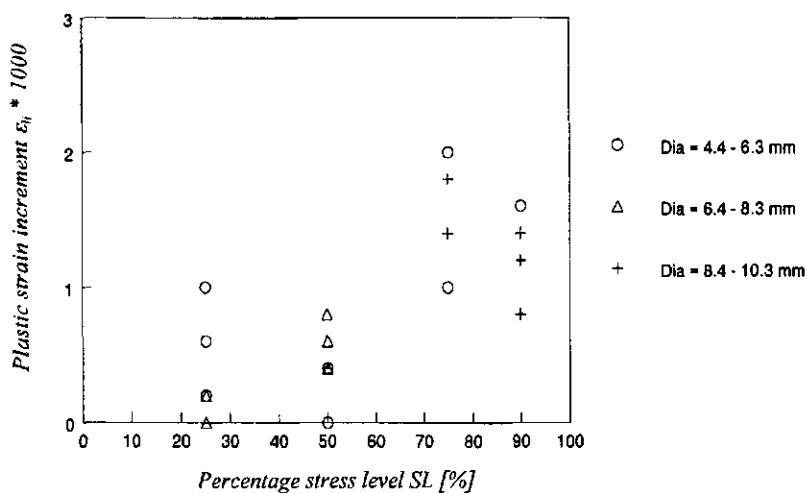


(b)

Figure 4.13 Stiffness modulus  $E_{ii}$  versus percentage stress level SL for: (a) first and (b) fifth loading cycle and for three diameter classes.

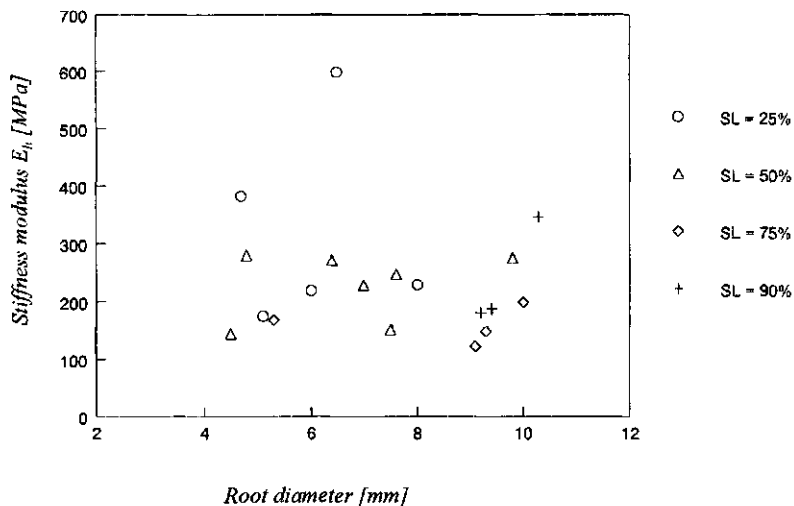


(a)

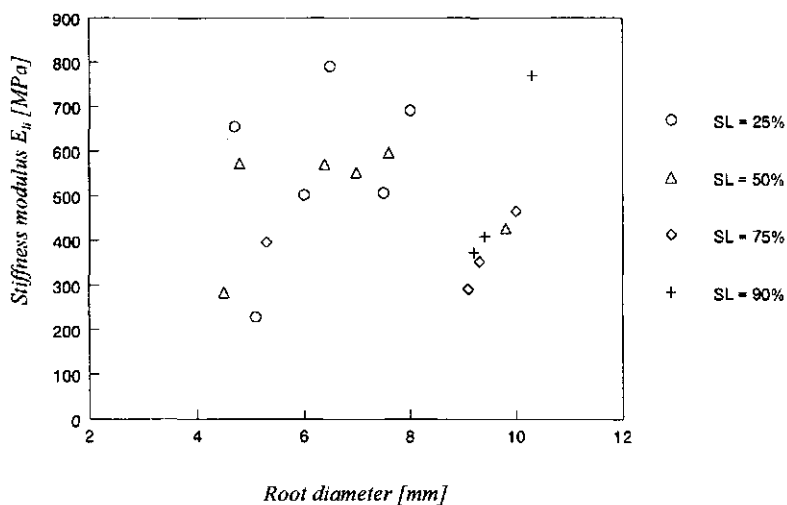


(b)

Figure 4.14 Effect of percentage stress level SL on plastic strain increment  $\epsilon_{li}$  for: (a) first and (b) fifth loading cycle and for three diameter classes.



(a)



(b)

Figure 4.15 Effect of root diameter and stress level SL on stiffness modulus  $E_h$  for: (a) first and (b) fifth loading cycle.

More than 250 single root experiments were conducted in this study. During the experimentation it was found that root slippage within the clamping devices was associated with: (1) moist root bark and (2) exertion of inadequate clamping force. On the other hand, failure of roots within or close to the clamping devices was partly caused by: (1) application of large clamping forces and (2) hard sharp edges of the clamping devices coming into direct contact with the root sample.

After a number of initial trials, appropriate clamping force was developed by experience, and wooden blocks with suitable hardness were found which were used as protections of the root samples against the edges of the clamping device. Introduction of the wooden blocks also contributed to improvement of friction between the root sample and clamping devices. This contributed in minimizing root slippage, and hence enhanced accurate measurements of root stress-strain relationship to be obtained. In some experiments however root slippage did occur and such results were discarded.

Importance of statistics in mechanics is sometimes overestimated. This happens especially when the restrictions imposed by statistical methods and implications involved are not carefully considered. Therefore in mechanics the adoption of other practical mathematical alternative(s) to replace or supplement statistical methods in some instances is very common. Scatter plots of results of the root experiments were made to show the overall pattern between root stress and strain relationships. For further in-depth bivariate statistical considerations it should be hypothesized that stress-strain curves of roots used in this experiments show linear relationships. This was however not the case (scatter plots of stress-strain relationships of tree roots were not completely linear, see illustrations in figure 4.12). In addition to non-linearity of root stress-strain relationships, the objectives of this study also make the performance of in-depth statistical analysis not very attractive, hence, further processing of results was made based on mathematical procedures used by researchers such as Morton and Hearle (1976) and Lopes (1996) in studies similar to this study. With this approach, change in stress values (i.e., caused by an external factor, for example, change in elongation rate) at any particular strain was expressed as a percentage of a reference (initial) stress value.

In general, beech roots in experiment 1, figure 4.8 showed greater strength than larch roots, figure 4.7. Considering the two root diameter classes, the spreads of stress-strain values were also found to be slightly greater in beech roots than in larch roots. Spread of stress-strain values within root pairs was found to occupy a narrow band as compared to their corresponding diameter classes. This therefore makes the usage of stress-strain values within root pairs a better substitute for each other than those found within the diameter classes. Within small roots (diameter less than 5 mm), it was found that increases in their diameters were associated with decrease in strength. This general trend of decreasing strength with increasing diameter of roots is consistent with findings published by Commandeur and Pyles (1991) and Makarova et al. (1998). The characteristics shown by small roots are partly attributed to difference in their composition, for example, cellulose versus lignin. Spread or scatter of root stress-strain values may be associated with a combination of many factors which may include the following:

- (1) changes in diameter along root length
- (2) root tortuosity, that is, twists or bends in roots
- (3) soil conditions
- (4) possible weakened point(s) along root length that was not detected, etc.

From the studies in experiment 2, figure 4.9, it was also found that stress-strain values of roots depend on the magnitude of elongation rate used in their measurement. At any particular strain, stress values of roots tend to increase with increase in the rate of elongation. In general, stress values were estimated to increase between 8 to 20% for an increase in the rate of elongation from 10 mm/min to 400 mm/min. Similar results have been found in fibres by Morton and Hearle (1976), Lopes (1996).

Failure experiments in experiment 3, figure 4.10 and 4.11 conducted with the beech roots (diameter = 4-12 mm) showed, that diameter of roots within this diameter range (i.e., diameter = 4-12 mm) has little or no influence on failure stresses and strains. These results are consistent with the results published by Makarova et al. (1998). However, it was found that failure stresses and strains recorded in the current experiments were relatively higher than those reported by Makarova et al. (1998). This may partly be associated with seasonal changes: roots for the current experiments were collected on the 4th November, whilst that for Makarova et al was collected on the 7th February. This increase in root strength due to seasonal changes may be related to the findings reported by Wästerlund

(1989). In this report he showed, that strength of root bark reaches its maximum in December and then falls to the minimum in June-July.

Cyclic loading of thick beech roots (figure 4.12) showed that failure cycle number depends on the stress level. High failure cycle number was found to correspond to low stress level, whilst low failure cycle number corresponded to high stress level. Curves for the first cyclic loadings showed two main characteristics: (1) hyperbolic and (2) sigmoid. The latter finding is consistent with the report published by Commandeur and Pyles (1991). The first part of the sigmoid curve may be associated with straightening up of tortuous roots, and then producing a hyperbolic curve in the second portion after the roots have been straightened.

From tables 4.2 and 4.3 it is observed that values of overall stiffness modulus increase with increasing number of loading cycles, whilst plastic strain increment decreases with increasing number of loading cycles. Loading cycles chosen for further considerations were the first and fifth loading cycles. These cycles were chosen because the first loading cycle represents the beginning of the experiments whilst some roots failed after the fifth loading cycle. From these studies (see figure 4.13 and figure 4.14) it was found, that stiffness modulus decreases with increasing percentage stress level, whilst plastic strain increment increases with increasing percentage stress level. From these figures it can be seen that effect of percentage stress level, SL, on both the stiffness modulus and plastic strain increment is more pronounced on the first loading cycle than the fifth. Effect of root diameter on stiffness modulus was less obvious or pronounced (see figure 4.15).



Clamping procedure adopted for the root measurements was effective, that is, root slippage was minimized and induced root failure further away from the clamping devices. Test speed (elongation rate) was found to affect stress-strain relationship of roots. Increase of about 8-20% was found when testing speed (elongation rate) changed from 10 mm/min to 400 mm/min. Axial stress-strain relationships of pairs of fine beech and larch roots were measured including failure stress, failure strain, and fatigue behaviour of thick beech roots. From these measuring results, it was found that:

- (1) stress-strain values of root pairs are closer to each other than those found in their diameter classes
- (2) number of loading cycles before root failure depends on the percentage stress level
- (3) diameter of thick roots ( $D = 4-12$  mm) has no effect on failure stress and failure strain. Earlier experimental results however showed that diameter of thin roots (less than 4 mm) relates very well with failure stress and failure strain
- (4) plastic strain increment decreases with increasing number of loading cycles and increases with increasing percentage stress level
- (5) overall stiffness modulus decreases with increasing percentage stress level.

## **5 SOIL REINFORCEMENT BY ROOTS**

### **5.1 INTRODUCTION: FIBRE REINFORCEMENT**

#### **5.1.1 Composite materials**

Composite materials may exist as an artificial (i.e. man made) or a natural product. The history of man-made composite materials is dated to the ancient times where the Chinese and Egyptians used bamboo and chopped straws respectively, as reinforcements in most of their constructions. A composite material such as reinforced concrete beam is a typical example of man-made composite material, whilst wood can be cited as an example of naturally occurring composite product. According to Agarwal and Broutman (1980) a composite material can be anything consisting of two or more distinct parts, constituents or phases. They indicated that it is only when the constituent phases have significantly different physical properties (i.e., composite properties are noticeably different from the constituent properties) that a material can be recognized as a composite. Their description of composite materials therefore eliminates such materials that contain only unwanted elements or impurities from being classified as composites. For example, metals which very often may contain alloying elements and plastics which generally contain small quantities of fillers, lubricants, etc. Two main known phases of composites are: (1) discontinuous phase (embedded in the continuous phase) and (2) continuous phase. The discontinuous phase which is normally harder and stronger than the continuous phase is commonly referred to as a reinforcement or reinforcing material, whereas the continuous phase is termed as a matrix. Geometry of a reinforcement is considered very important as its dimensions determine its ability to contributing its properties to the composite. Classification of composite materials based on geometry of a representative unit of the reinforcement is shown in figure 5.1. Pictorial representations of some components in the above classification are shown in figure 5.2. Within this classification fibre is considered as a very important reinforcing material because of its long dimensions which are known to be effective in preventing growth of incipient cracks. Further discussions in this section will therefore be focussed mainly on fibre composites.

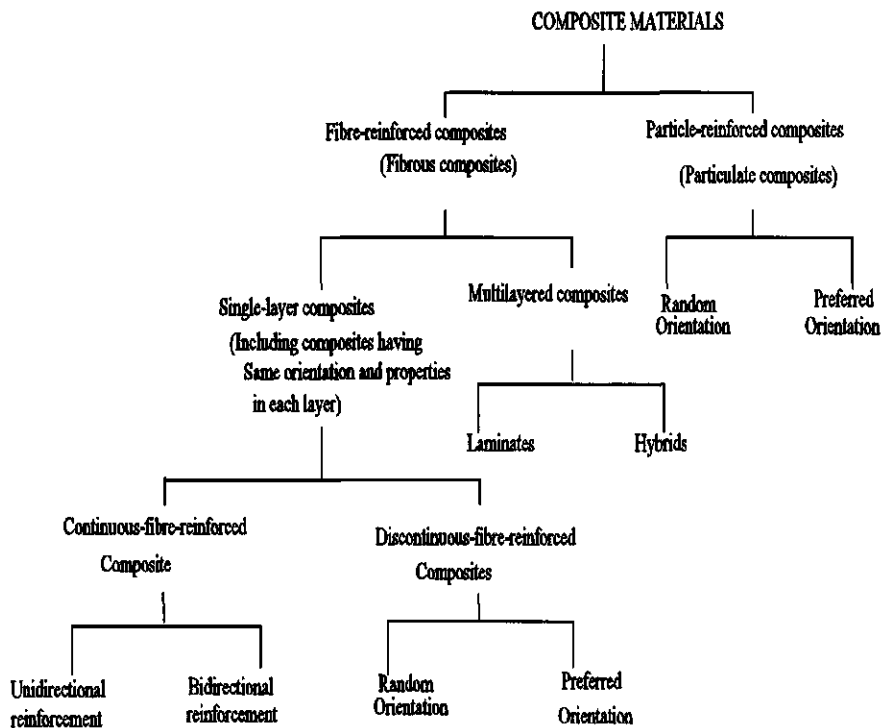


Figure 5.1 Classification of composite materials.

Source: Agarwal and Broutman (1980)

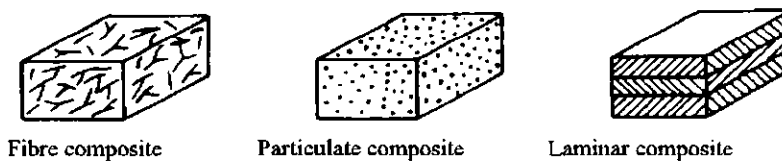


Figure 5.2 Types of composite materials.

Source: Vinson and Sierakowski (1986)

Fibre composites can be grouped into two broad classes: (1) single-layer composite and (2) multi-layer composite. The former may consist of one layer of fibrous composite with the same orientation, whilst the latter may consist of several layers of fibrous composites with varying orientation. Single-layer composites with long fibres are known as continuous-fibre-reinforced composites whilst those with short fibres are termed discontinuous-fibre-reinforced composite. Continuous-fibre-composites with fibres aligned in one direction are called unidirectional composites. A schematic diagram of a typical unidirectional composite is shown by figure 5.3. When fibre directions are mutually perpendicular to each other they are termed as bidirectional composites. This arrangement provides extra strength to the composite. An example of bidirectional composite is a woven fabric (see section 5.1.3.1).

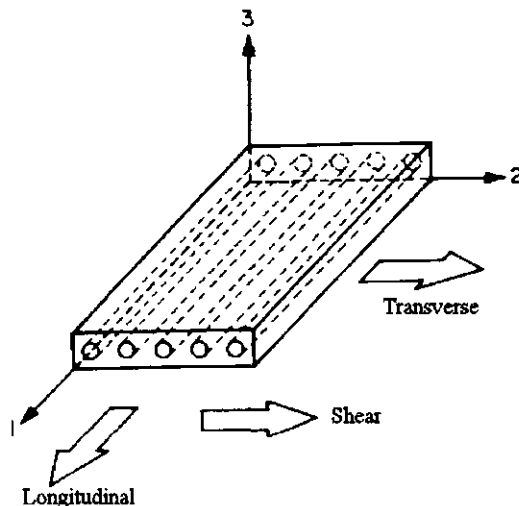


Figure 5.3 Schematic representation of unidirectional composite.

Source: Agarwal and Broutman (1980)

In general, reinforcements are principal load-carrying members and their inclusion is basically to improve upon the mechanical properties of the matrix. The surrounding matrix keeps the fibres in their desired location and orientation, and also acts as a load transfer medium between them. This load transmission is however controlled by the interfacial bond between the matrix and the fibres. The matrix also protects the reinforcements from environmental damages. Beside providing strength the reinforcements may also enhance stiffness of the composites.

Vinson and Chou (1975) listed a number of factors which generally affect the strength of composite materials. These consisted of the following:

- (1) direction of load application in relation to orientation of the reinforcement
- (2) volume fractions of the component materials
- (3) nature and effect of interfacial bonding.

Increase in strength and stiffness provided by fibres in composites is maximum only when the fibres are parallel to loading direction. Strength qualities of composites are determined by the relative amounts of their constituents. The stress-strain curve of a composite will therefore move closer to the stress-strain curve of the fibre if volume fraction of the fibre is comparatively high, and will move closer to that of the matrix if the volume fraction of the fibre is comparatively low. A typical example illustrating the stress-strain relationships of composite and its constituents is as shown in figure 5.4. Volume fractions of the matrix and fibre in a composite may be evaluated by equations 5.01 and 5.02 respectively.

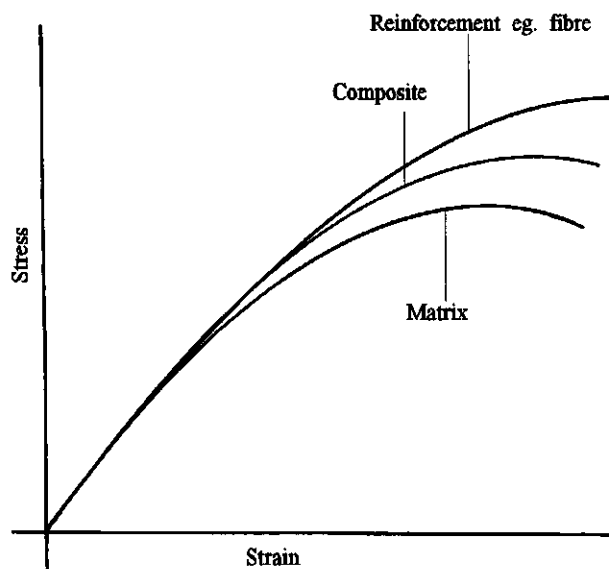


Figure 5.4 Characteristic stress-strain curves of composite and its constituents.

$$V_m = v_m / v_c \quad 5.01$$

$$V_{fb} = v_{fb} / v_c \quad 5.02$$

where,

$V_m$  = volume fraction of matrix

$v_m$  = volume of matrix

$V_{fb}$  = volume fraction of fibre

$v_{fb}$  = volume of fibre

$v_c$  = volume of composite ( $v_{fb} + v_m$ ).

Agarwal and Broutman (1980) estimated the tensile stress of unidirectional composites (in the longitudinal direction) by making the following assumptions: (1) uniform in properties and diameter, (2) continuous; parallel throughout composite and (3) perfect bonding between fibres and matrix so that no slippage occurs at the interface.

The above assumptions implied that the strain experienced by fibre, matrix, and the composite, are equal. Total strength of the composite can therefore be calculated from equation 5.03.

$$\sigma_c = \sigma_{fb} A_{fb} / A_c + \sigma_m A_m / A_c \quad 5.03$$

where,

$A_c$  =  $A_{fb} + A_m$

$A_c$  = cross-sectional area of composite

$A_{fb}$  = cross-sectional area of fibre

$A_m$  = cross-sectional area of matrix

$\sigma_c, \sigma_{fb}, \sigma_m$  = tensile stresses of composite, fibre and matrix respectively.

### 5.1.2 Failure

Material failure may be classified into two main groups: (1) static failure, for example, fracture and distortion and (2) dynamic failure, for example, fatigue and creep. For the purpose of this thesis dynamic failure will be discussed. Failure of materials under the action of repeated stresses is commonly referred to as fatigue, and has been under investigation for more than 200 years. Implying, that fatigue is old but very important failure phenomenon. Details of this phenomenon can be found in most books dealing with strength of engineering materials. In metals, fatigue may result from slip occurring along certain crystallographic directions. Under sufficiently high repeated stresses, this slip may

be accompanied by local crystal fragmentation leading to the formation of submicroscopic cracks, which eventually grow into visible cracks of a macroscopic type. Number of cycles to failure of most materials is known to depend on factors such as stress level, stress state, mode of cycling and material composition. In most materials there exists a limiting stress below which a load can be repeatedly applied for indefinitely large number of times without causing failure. Models used in predicting life of composites structures subjected to fatigue loadings have been studied by Schaff (1997). He noted that life of composites decreases more rapidly when the loading sequence is repeatedly changed after only a few loading cycles. Typical example of a material under action of repeated loading is as shown in figure 5.5.

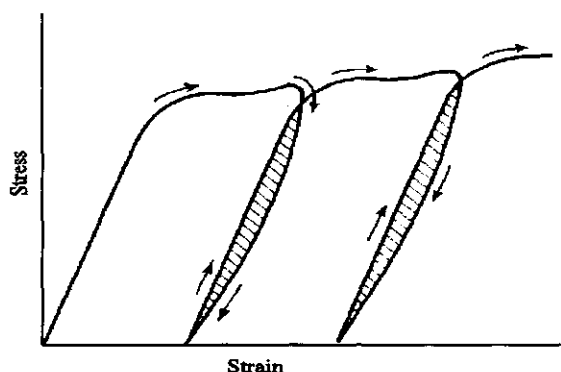


Figure 5.5 Stress-strain curve of material under action of repeated loading

Source: Davis et al. (1982)

Unlike fatigue, creep occurs under the application of a constant load, and is associated with gradual flow or change in dimension. Its complementary effect is relaxation, that is the reduction of stress with time under a given extension. Problem of creep has become of considerable technical importance owing to its influence on design of equipment for high temperature service. Kabir (1988) divided creep data into two groups: (1) in-isolation and (2) in-soil tests. According to his report, in-isolation test data may be used to obtain design parameters for materials which are unaffected by soil in confinement, while in-soil tests may be used for obtaining design parameters for materials whose properties are significantly altered when confined in soil.

### 5.1.3 Soil reinforced by geotextiles

#### 5.1.3.1 Introduction

Gray and Ohashi (1983) classified materials used in soil reinforcement into two main groups. They consisted of: (1) ideally inextensible and (2) ideally extensible materials (table 5.1). The former consists of high modulus metal strips and bars, while the latter is made up of relatively low modulus natural fibres, plants roots and polymeric fabrics. In geotechnical engineering the polymeric fabrics are commonly referred to as geotextiles (Giroud and Noiray, 1981) and are made from petroleum products such as polyester, polyethylene and polypropylene.

Table 5.1 Comparative behaviour of soil reinforcements.

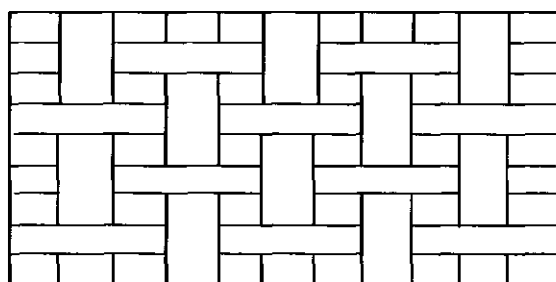
Reinforcements	Stress-deformation behaviour of reinforcement	Role and function of reinforcement
Ideally <i>inextensible</i> inclusions (metal strips, bar, etc.)	Inclusions may have rupture strains which are less than the maximum tensile strains in the soil without inclusions, under the same stress conditions. Depending on the ultimate strength of the inclusions in relation to the imposed loads; these inclusions may or may not rupture.	Strengthens soil (increases apparent shear resistance) and inhibits both internal and boundary deformations. Catastrophic failure and collapse of soil can occur if reinforcement breaks.
Ideally <i>extensible</i> inclusions (natural and synthetic fibres, roots, fabrics, geotextiles)	Inclusions may have rupture strains larger than the maximum tensile strains in the soil without inclusions. These inclusions cannot rupture no matter their ultimate strength or the imposed load.	Some strengthening ...but more importantly provides greater extensibility (ductility) and smaller loss of post peak strength compared to soil alone or to reinforced earth.

Source: Gray and Ohashi (1983)

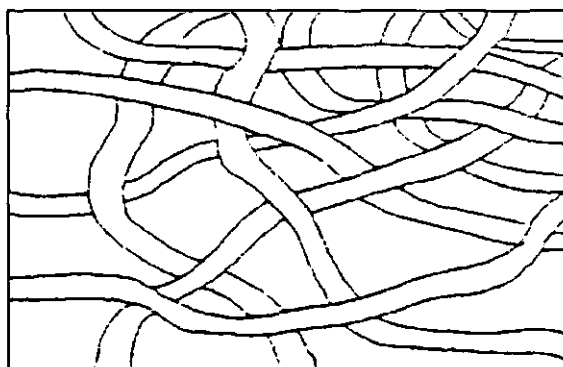
In 1953, geotextiles were used by the Dutch in reconstructing dykes destroyed by tidal storms and later by the French for load distribution and as non-contamination sheets



(Gourc, 1993). However, their usage did not reach popularity until quite recently (Simonini, 1996; Ju and Son, 1996; Leshchinsky, 1993; Lopes, 1996).



(a)



(b)

Figure 5.6 Types of geotextiles: (a) woven and (b) non-woven.

Source: Provencher (1992)

Provencher (1992) classified geotextiles into two main groups: (1) woven and (2) non-woven geotextiles. Woven geotextiles consist of strips of few millimetres in width, arranged at right angles (figure 5.6 (a)) thereby offering resistance in directions of both length and width. Closely woven geotextiles may further impede the flow of water through it. On other hand, non-woven geotextiles (figure 5.6 (b)) may consist of many randomly-interlaced fibres which may be bonded either by fusion or mechanical means. Unlike woven, non-woven geotextiles promote greater elongation before tearing and also have the ability to offer uniform resistance in all directions.

Effects of soil environment on geotextiles used in soil reinforcement have been studied by Jewell and Greenwood (1988). Physical damage include: (1) tearing, (2) pierced holes and (3) abrasion of the yarns. Some of these damages may cause reduction of the cross-section of geotextiles, thereby locally raising stress and reducing the time to cause stress-rupture at the damage section when supporting load. Apart from the above factors, the following factors may also reduce the strength of geotextiles in the soil: (1) oxidation, (2) hydrolysis, (3) alkaline attack and (4) ultraviolet light. In construction, geotextiles may perform one or more functions such as: (a) drainage, (b) separation, (c) filtration and (d) reinforcement. When used in filtration, or separation, it allows free flow of water whilst keeping various soil layers separate (McKyes, 1985; Das, 1995). Beneficial effects of geotextiles in soil reinforcement are derived from increase of tensile strength and shear resistance of the soil.

Examining the mechanics of reinforced embankments, Jewell (1988) mentioned that increase in soil shearing resistance by reinforcing materials may be achieved by reducing the forces causing failure and increasing the forces resisting failure. These fundamental actions of reinforcements were illustrated by figure 5.7 (a) for a direct shear test on reinforced soil. The reinforcement force  $P_R$  at an orientation  $\theta$  in the soil acts to reduce the applied shear loading  $S_s$  that the soil must support on the soil shear surface  $A_s$  and also increase the normal effective stress  $\sigma_n$  on the soil shear surface so that greater frictional shearing resistance is mobilized (equations 5.04 and 5.05). With regards to embankments, Jewell (1988) pointed out, that since the foundation soil may not be able to support lateral tensile forces generated by the fill material, an important role of the reinforcement when used will be to carry the generated outward shear stresses and provide inward shear stresses to restrain the foundation soil from lateral displacement (figure 5.7 (b)). This role, among other things, will depend on the longitudinal stiffness  $\xi_r$  (equation 5.06) of the reinforcing material.

$$S_s = S_{yx} - [(P_R \sin \theta) / A_s] \quad 5.04$$

$$\sigma_n = \sigma_{yy} + [(P_R \cos \theta) / A_s] \quad 5.05$$

$$\xi_r = E_r A_r \quad 5.06$$

where,

$E_r$  = elastic modulus of the reinforcement

$A_r$  = cross-sectional area of the reinforcement.

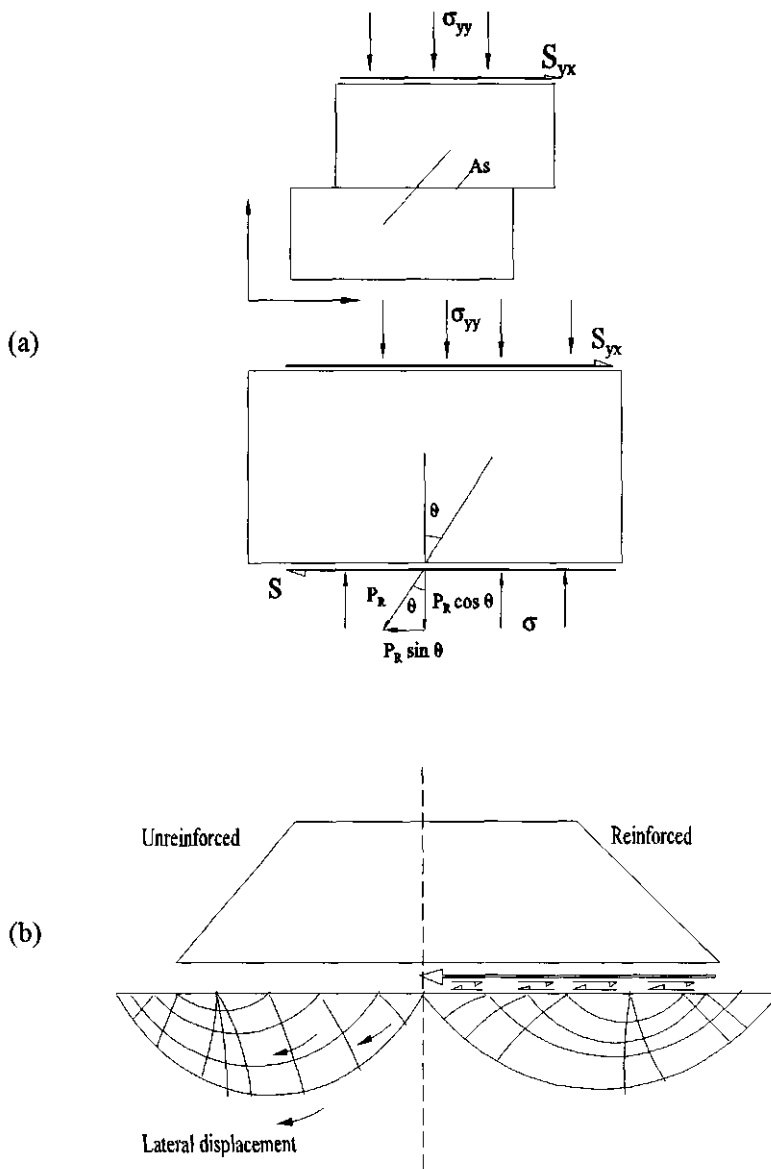


Figure 5.7 Role of reinforcements in: (a) improving soil shear resistance and (b) restraining outward shear stresses in embankment.

Source: Jewell (1988)

A popular way of explaining the action of reinforcing materials used in reinforced soils, is by the concept of tension-membrane effect (Sellmeijer et al, 1982; Gourc, 1993; Houlsby and Jewell, 1990; Giroud and Noiray, 1981). That is, when loaded, the reinforcement in the region of the applied load becomes curved (figure 5.8) thereby causing reduction in the magnitude of the vertical stresses applied to the subgrade. This reduction in vertical stresses is brought about by the combined effects of the curvature and tension in the reinforcing material. An essential benefit of the above reinforcing phenomena or actions is an increase in bearing capacity of the soil (i.e., value of contact pressure that can be applied to the soil without causing failure).

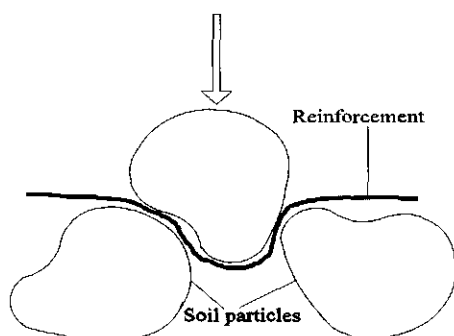


Figure 5.8 Resistive action exhibited by the reinforcing material when the reinforced section of the soil is loaded.

Source: Adapted from Hoare (1979)

Bearing capacities of both reinforced and unreinforced soil have been studied by a number of people including Fannin and Sigurdsson (1996), Sitharam et al. (1996), Das (1995), Mandal and Dixit (1990), Florkiewicz (1990), Higuchi and Watari (1990), Ju and Son (1996), Koga and Aramaki (1988), Mckyes (1985), Hirano (1990), Vesic (1977) and Hvorslev (1970). Among the well known theories describing mode of soil failure when subjected to a bearing pressure are those, proposed by Prandtl and Terzaghi (figure 5.9). For shallow foundations Terzaghi formulations are usually applied (Roberts, 1977). Ultimate bearing capacity of soil  $q_u$  is estimated by equation 5.07, however some correction factors may be applied when loading is considered to be circular, square or continuous.

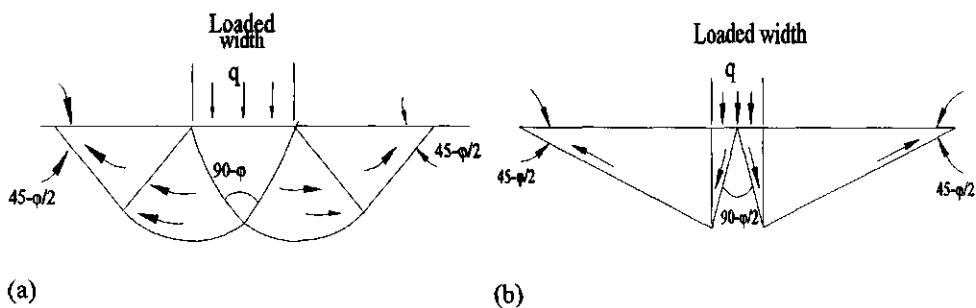


Figure 5.9 Mode of soil failure under a bearing load assumed by: (a) Prandtl and (b) Terzaghi.

Source: Roberts (1977)

In situations where reinforcements are used, improvement of bearing capacity at failure,  $q_{ur}$  is assessed by using bearing capacity ratio, BCR (equation 5.08). Values of 1.24 and 1.54 have been published (Koga and Aramaki, 1988) for surface and embedded footings respectively. Bearing capacity numbers  $N_\gamma$ ,  $N_c$ ,  $N_q$ , may be derived by equations 5.09 to 5.11. Methods of soil reinforcements are basically classified into three main groups: one layer, multi-layers and mattress-type (figure 5.10).

$$q_u = c N_c + q N_q + 0.5 \gamma B N_\gamma \quad 5.07$$

$$BCR = q_{ur} / q_u \quad 5.08$$

$$N_\gamma = 2 (N_q + 1) \tan \phi \quad 5.09$$

$$N_c = (N_q - 1) \cot \phi \quad 5.10$$

$$N_q = \tan^2 [45 + 0.5 \phi] e^{\pi \tan \phi} \quad 5.11$$

where,

$c$  = cohesion of the soil

$\gamma$  = unit weight of soil

$\phi$  = friction angle of the soil

$q_{ur}$  = ultimate bearing capacity at failure of reinforced ground

$B$  = loaded width.

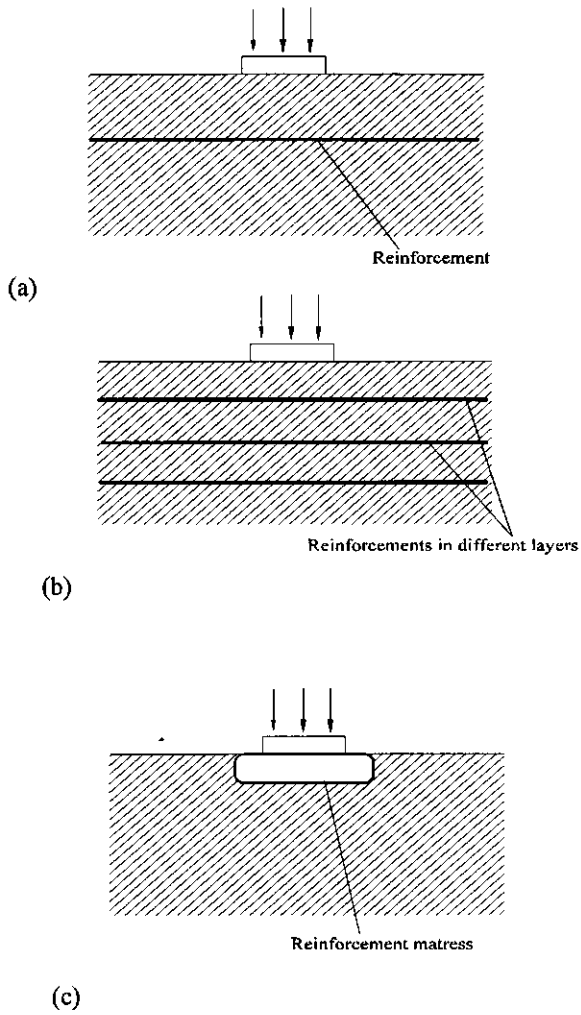


Figure 5.10 Methods of soil reinforcement: (a) single layer, (b) multi-layer and (c) mattress-type.

Source: Modified from Ju and Son (1996)

### 5.1.3.2 Soil-geotextile interface properties

Interface properties of soil-reinforcement interaction play an essential role in the prediction of the performance of reinforced structures (Matichard, 1993). Common properties used in the description of interface behaviour are adhesion and friction angle, and may be investigated either by pullout or shear tests.

The same apparatus, commonly a shear box (Wu et al., 1988; Abe and Ziemer, 1991) may be used for both the friction and pull-out tests. The basic difference between these tests has been mentioned by Woods (1994). In friction tests, a layer of soil placed on a geotextile is submitted to horizontal displacements while the geotextile remains attached to a supporting medium (can be either a layer of soil or a rigid plate, figure 5.11 (a)), whereas in pull-out test, the geotextile is subjected to a tensile force and moves between two layers of soil (figure 5.11 (b)).

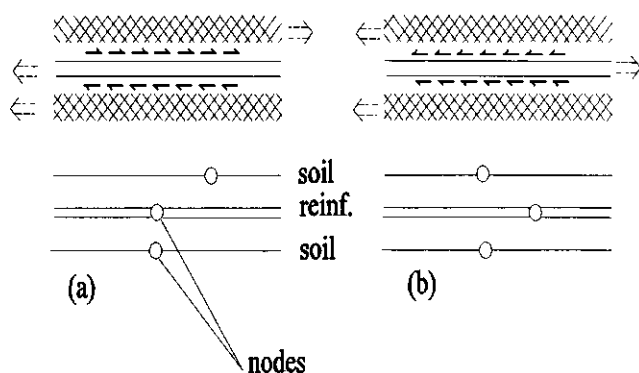


Figure 5.11 Interface behaviour: (a) friction and (b) pullout.

Source: Modified from Woods (1994)

A new laboratory device (ring simple shear apparatus) for studying and measuring friction between sand and reinforcing elements has been presented by Lerat and Unterreiner (1996). The main principle governing the use of this apparatus (figure 5.12) is to evolve a rigid steel cylinder in an annular soil sample.

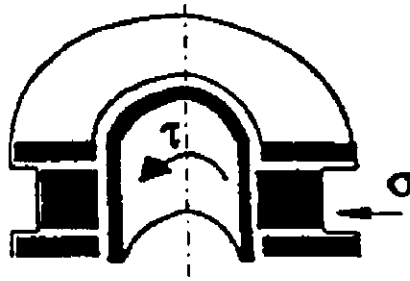


Figure 5.12 Principle of ring simple shear test.

Source: Lerat and Unterreiner (1996)

Pullout tests have been discussed by a number of researchers including Adanur et al. (1996), Lopes (1996), Chang et al. (1996), Woods (1994), Leshchinsky (1993), Gourc (1993), Matichard (1993), Wu et al. (1988), Mitchell and Villet (1987). Experimental systems of pull-out tests range from simple boxes (figure 5.13 (a)) to more advanced set-ups such as those shown in figure 5.13 (b) and 5.13 (c). In pull-out experiments, the normal pressure and interface friction at the soil-geotextile interface is assumed to be constant along the length of the geotextile. Usually large pull-out boxes are used to minimize the influence of lateral, base, and top boundaries. At the mid-height of pull out boxes are two apertures: one in the front wall and the other in the back wall of the box to permit the pull out of the reinforcement and passage of inextensible wires that are used for the displacement measurements. Pullout force is transmitted by means of a device (for example, a hydraulic system) which permits the application of constant displacement rate, whilst confinement stresses are applied by placing masses (load) on top of the pull out box. Pullout force may be measured by a load cell, whilst displacement along the length of the geotextile (i.e., including frontal displacement) be measured by a potentiometers or dial gauges. Electric vibratory hammer or manual compactor may be used in pullout experiments to compact the soil to the required density.



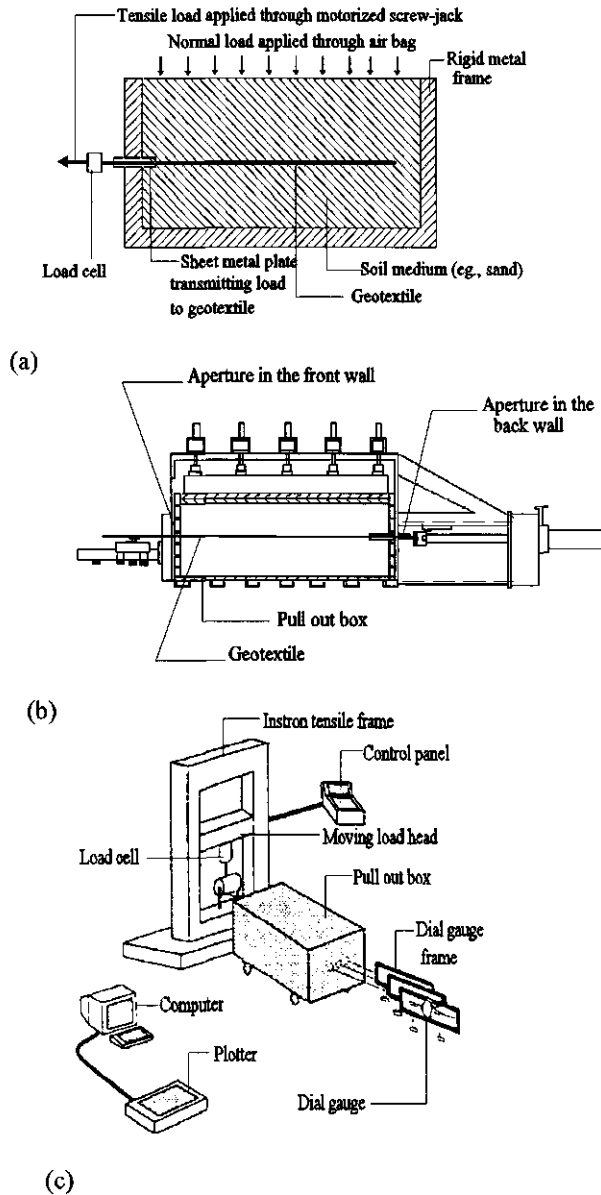


Figure 5.13 Schematic representations of pullout experiments: (a) simple (after Leshchinsky, 1993), (b) intermediate (after Lopes, 1996) and (c) advanced (after Adanur et al., 1996).

According to Lopes (1996), displacement measurements in pull-out test involving extensible materials (for example, geo-synthetics) may have two components: one corresponding to friction strain on the soil-reinforcement interface; and the other due to the elongation of the inclusion, thus measurement results need to be carefully interpreted.

Common approaches used in predicting pullout capacities have been discussed by Mitchell and Villet (1987). They consist of analyses that consider: (1) only friction, (2) only passive resistance and (3) both friction and passive resistance. In friction analyses, pullout capacity  $P_f$  is calculated in terms of apparent or effective coefficient of friction  $\mu_e$  and surface area  $A_r$  of the reinforcement (5.12), whereas in passive analyses, it is assumed that only a small proportion of the resistance is developed through friction and pullout force  $P_p$  is defined in terms of passive resistance anchorage factor  $N_p$  (or bearing capacity factor), and surface area of reinforcement in bearing  $a_b$  (5.13). In the third approach pullout force  $P_T$  is calculated as a sum of the pullout forces developed in the friction and passive analysis (5.14).

$$P_f = \mu_e \gamma z A_r \quad 5.12$$

$$P_p = N_p z \gamma n a_b \quad 5.13$$

$$P_T = z \gamma [\mu_e A_r + N_p n a_b] \quad 5.14$$

where,

$\gamma$  = unit weight of soil

$n$  = number of transverse bearing members behind the failure surface

$z$  = depth to reinforcement

$P_T$  = total pullout force.

Jewell (1990), on the other hand, described the interaction between soil and reinforcements in terms of friction angle  $\phi$  of the soil and bond coefficient  $f_b$  (equation 5.15). The bond coefficient governs the rate of load transfer between the reinforcement and the soil. For geotextiles, Jewell (1990) quoted the bond coefficient to range between 0.0 and 1.0 (in his earlier design charts for slope reinforcement a value of 0.5 was specified).

$$P_{bond} = 2 W_r L_{bond} \sigma_n f_b \tan \phi \quad 5.15$$

where,

- $P_{bond}$  = maximum bond force (kN)
- $W_r$  = width of reinforcement
- $L_{bond}$  = length of reinforcement
- $\sigma_n$  = effective stress normal to the reinforcement.

Fair degree of disagreement can be found among various researchers concerning the magnitude of coefficient of friction between soil and the geotextile. Whilst some maintain that the coefficient of friction in the soil-geotextile interface exceeds that of soil, others argue that the frictional coefficient is in fact less than that of the soil.

Work done by Gourc (1993) indicates that coefficient of friction between soil and geotextiles in granular soils may be approximated by equation 5.16. Values of friction angles reported by some authors are as compiled in table 5.2 below.

$$\tan \phi_g / \tan \phi > 2/3 \quad 5.16$$

where,

- $\phi_g$  = soil-geosynthetic angle of friction
- $\phi$  = soil angle of friction.

In a related study Bengough et al. (1997) stated that frictional properties of metals used in soil reinforcement can be related to that of tree roots (i.e., friction between root and soil). In order to study the frictional resistance encountered by tree roots in soil, soil-metal friction in a number of different soils were investigated. Angles of soil-metal friction were found to range from 27° to 35° for all the soil samples (texture of these soil samples ranged from sandy loam to silty clay). These values are close to those mentioned in table 5.2 for sandy soils.

Table 5.2 Skin friction angle of different reinforcing fibres in sand.

Fibre type	Diameter (mm)	Skin friction angle (°)	Source
Parachute cord	3.2	40	Shewbridge and Sitar (1989)
Wood rods	3.2	35	
Wood dowels	7.8	35	
Bungy cord	3.2	40	
Aluminum rods	9.5	24	
Steel rods	3.2	24	
Buna-N (rubber, ASTM 200)	1.1	30	Maher and Gray (1990)
Reed (Phragmites communis)	1.0	30	
Palmyra (Borassus flabelliformis)	1.2	30	Gray and Ohashi (1983)
Plastic (PVC)	2.2	23	
Copper wire	1.0	21	

Apart from friction coefficient between the soil and reinforcement, representation of soil-reinforcement interface is another aspect of soil-reinforcement modelling that has generated disagreement among scientists. The main argument concerns the physical existence of shear band or zone (Gourc, 1993). The shear zone is discussed in section 5.2.2

Work done by Rowe and Soderman (1987) showed that in soil-reinforcement modelling, interface elements can be introduced by the use of joint elements, nodal-compatibility slip elements or substructuring. Joint elements allow relative deformation of the soil and reinforcement prior to failure of the interface. On the other hand, nodal compatibility slip element, which initially may be formulated in terms of normal and tangential springs with high stiffness ensures compatible displacement between a pair of dual nodes, one attached to the soil and one attached to the reinforcement, until a Mohr-Coulomb failure criterion is reached. Rowe and Soderman (1987) however pointed out that as the stiffness of joint element increases it tends to a nodal-compatibility slip element. Also, they proposed three

possible failure mechanisms that need to be considered in modelling soil-reinforcement interface behaviour:

- (1) if there is insufficient anchorage capacity, failure will occur at the soil reinforcement interface above and below the reinforcement as the reinforcement is pulled out of the soil
- (2) if the shear strength of the soil reinforcement is less than the shear strength of the soil alone, then failure may occur by sliding of the soil along the upper surface of the reinforcement, as the upper soil mass moves relative to both the reinforcement and the underlying soil (this rarely occurs)
- (3) the soil below the reinforcement (usually soft foundation) may be squeezed out from beneath the lowest reinforcement layer.

Failure of reinforced soil structures continues to be a major topic of discussion among geotechnical or civil engineers. Mallick (1988) discussed the total failure of the reinforced structure resulting from failure of individual and adjacent reinforcements. Mitchell and Villet (1987) pointed out the effects of friction angle (depend on soil type) on stability of reinforced soil structures. According to their report, lower soil friction angle will lead to: (1) higher internal horizontal earth pressure to be restrained by the reinforcements, (2) lower apparent friction coefficient and bearing value for frictional and passive reinforcement systems respectively.

Coutts (1983) used a theoretical model to explain the occurrence of root breakage in soil. Initially he considered an unbranched root of uniform diameter buried in the soil over an indefinite length under tensile load from one end A (figure 5.14 (a)). The following assumptions were made with regard to his model: root is stretched by tensile force at A; soil-root resistance is proportional to the distance AB; and at a point along the root, root-soil resistance will be equal to the applied load. He indicated, that maximum strain and therefore failure, will occur at A where there is no root-soil resistance ( $R_{rs}$ ). On the other hand, if the root tapers from the point of application of the force (Fig. 5.14 (b)) strain distribution will be determined both by  $R_{rs}$  and the cross-section area of the root. Under a given load, strain will increase with distance from A as the root decreases in diameter, but will decrease again as root-soil resistance increases with distance from A. The root then breaks at a point between A and B where maximum strain occurs. According to his report, increase in root thickness or a decrease in  $R_{rs}$  (e.g., by wind loosening) will move

the point of breakage outwards away from the tree, whereas factors which increases root-soil resistance such as drying of the soil, will cause the roots to break nearer to the base. Where roots show branching (figure 5.14 (c)),  $R_{rs}$  will exceed the tensile strength of the soil. He pointed out that if the amount of root material diminishes to give  $R_{rs} < \text{soil strength}$ , strain will first cause fracture of the soil (because of its low elasticity), causing the force to act on the roots as in figure 5.14 (c). Roots afterward break and project themselves from the broken soil surface.

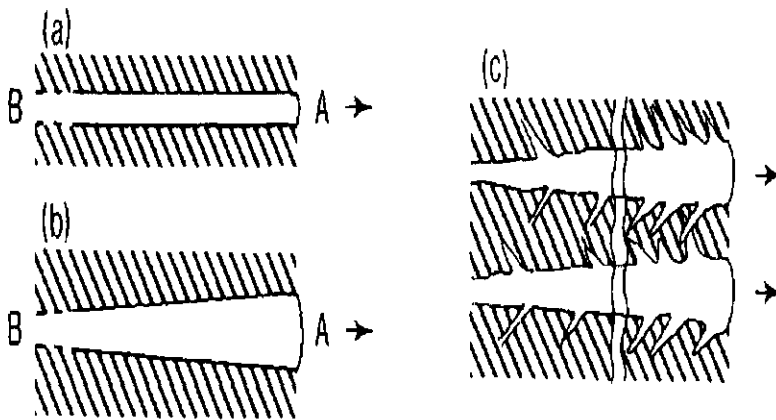


Figure 5.14 Behaviour of roots and soil (shaded) when horizontal force is applied at A.

Source: Coutts (1983)

### 5.1.3.3 Modelling soil reinforced by geotextiles

Several modelling techniques such as earth pressure theory, boundary elements, theory of elasticity, finite difference, finite element, limit equilibrium have been used in the analyses of reinforced soil structures (Woods, 1994), for example slopes and embankments. However, the most widely used of these methods are Limit Equilibrium Analysis (LEA) and Finite Element Methods (FEM). Their acceptance and usage as modelling tools can partly be attributed to the simplicity (Rowe and Soderman, 1985) of the former and the capacity of the latter to deal with more complex situations. One of the

basic differences between LEA and FEM is that in LEA material stress-strain relationship plays no special role whilst it does in FEM. A brief discussion of the two methods are therefore presented.

Limit equilibrium analysis has been used in the design of earth structures for about 70 years (Leshchinsky, 1993). Apart from its simplicity (i.e., relatively simple input data), the following attractive features have also been identified: (1) modelling of reinforcement can intuitively be comprehended and (2) reasonability of results of the analysis can be easily assessed based on experience, or through simplified charts. Inclusion of reinforcement in LEA is considered to be straightforward. For a test-body assumed to be at the verge of failure, the reinforcement forces are integrated into the limiting equilibrium equations (equations are based on the rupture surface) and a global factor of safety is calculated. After examination of many such test-bodies, required layout and strength of the reinforcement is determined so that a design safety factor is attained. Current safety factor of about 1.3 is commonly used, and may be defined by equation 5.17.

$$F = S_s / S_e \quad 5.17$$

where,

- $S_s$  = available shear strength of soils
- $S_e$  = shear strength required for equilibrium
- $F$  = factor of safety.

Different approaches of LEA have been documented: kinematic theorem (Michalowski, 1997), friction circle (Hassiotis et al., 1997); two-part wedge analysis and logarithmic spiral analysis (Jewell, 1990), shakedown analysis and method of slices (Ohtsuka et al., 1996). Most of these methods are used in stability analysis of reinforced slopes.

Applicability of the kinematic theorem requires that the materials (i.e., soil and reinforcement) be perfectly plastic and the deformation be governed by the normality rule. The theorem states that "the rate of work done by traction and body forces is less than or equal to the energy dissipation rate in any kinematically admissible failure mechanism". Considering two-part wedge and logarithmic spiral analyses, Jewell (1990) pointed out

that the former adapts better to problems of potential failure cutting out sharply between reinforcement layers than the latter. With method of slices, the equilibrium equations on the slice blocks are solved based on the assumption that the forces between blocks are at a limit state. The shakedown method is usually employed for the stability assessment against repeated loads. However, it was demonstrated by Ohtsuka et al. (1996) that the method can in fact also be used to study the effect of mechanical properties of reinforcements. The main feature of this method deals with residual stress which corresponds to plastic strain. Of the above LEA approaches, friction circle method is considered as the most convenient method in the analysis of pile-reinforced homogeneous slope (Hassiotis et al., 1997). Although LEA is commonly used in slope stability and embankment analysis, some scientists are still sceptical about the use of this technique in predicting embankment deformations, safety factor, and reinforcement strains. This has been attributed to the inability of LEA to: (1) adequately model the complete interaction of composite soil-geotextile system alone (Rowe and Soderman, 1985) and (2) to present stress relief produced by excavation and the interaction between the soil and the reinforcement (Matsui and San, 1988).

Table 5.3 Finite element analysis: applications and variables.

Application	Primary	Associated	Secondary
Stress analysis	Displacement, Rotation	Force, Moment	Stress Failure criterion Error estimates
Heat transfer	Temperature	Flux	Interior flux Error estimates
Potential flow	Potential function	Normal velocity	Interior velocity Error estimates
Navier-Stokes	Velocity	Pressure	Error estimates

Source: Akin (1986)

FEM is considered as a more sophisticated analytical modelling approach than LEA (Leshchinsky, 1993). It was first introduced in the 1950's (Fagan, 1992) and for the last two decades, has become a common tool in most engineering works (table 5.3).



With regards to reinforced soil structures, it is considered as the most suitable method capable of making rational predictions of in-service deformation and likely collapse mechanism. Potentially it may be used to check the influence of: reinforcement stiffness, reinforcement creep and interactions between system components (Woods , 1994). Its success has been partly attributed to its ability to handle truly arbitrary geometry, deal with general boundary conditions, include nonhomogeneous materials, and describe processes with fewer simplifying assumptions than needed by other available analytical methods. The main disadvantage of the use of FEM is the large amount of data and computations that are involved. However, increasing computing technology and power these days have facilitated the growth of FEM and flourished the market with FEM computer packages or programs (e.g., PLAXIS, DIANA, SLOVIA, etc.), which are being used today by people, many of whom have very little, or no experience at all in numerical methods.

In FEM, the boundary and interior of the region under study are subdivided by lines (or surfaces) into a number of discrete sized subregions called finite elements. This process of sub-division of the region of interest is commonly referred to as mesh generation and the resultant mesh. Two-dimensional analysis of continua is generally based on the use of either triangular or quadrilateral elements (figure 5.15 (a)). Generally the larger the number of nodes defining an element, the better the results (i.e., more accurate). A typical two-dimensional mesh depicting reinforced soil under a footing is as shown in figure 5.15 (b). Mathematical procedures concerning FEM have been presented by authors such as Fenner (1975), Huston et al. (1984), Atkin (1986), Cook et al. (1989) and Barneveld (2000).

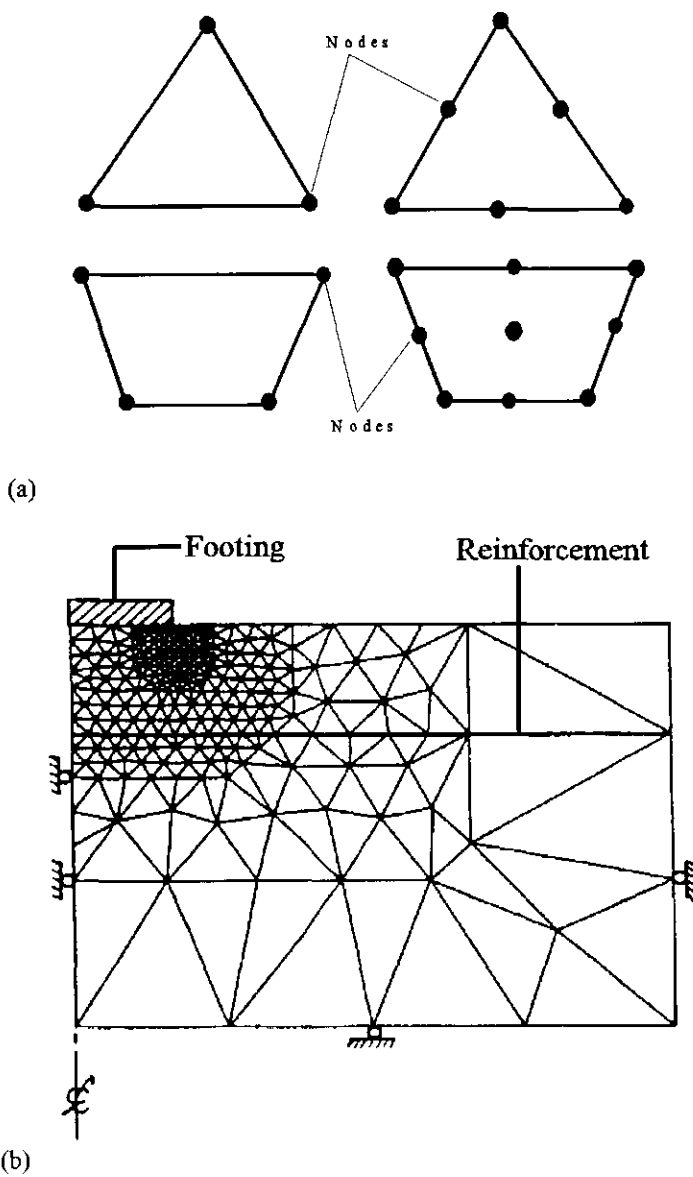


Figure 5.15 · Finite element methods: (a) triangular and quadrilateral elements and (b) mesh.

Source: Adapted from Burd and Brocklehurst (1990)

Finite element approaches used in modelling the behaviour of reinforced soil are classified into two main groups: (1) discrete and (2) composite representations. In the discrete representation, the soil, individual reinforcement members, any component of the system are all modelled distinctly, whilst in the composite representation, the reinforced soil structure is considered as a composite. The discrete approach is usually used to obtain information about the way in which the soil and reinforcement interact.

## 5.2 MODELLING SOIL-ROOT REINFORCEMENT

### 5.2.1 Soil-root models

Soil stability improvement by tree roots has often been explained in terms of: (1) root activities in soil, for example, association with fungi, absorption of minerals and water from the soil, addition of organic matter to the soil, etc. and (2) mechanical reinforcement based on root properties such as shear resistance, tensile resistance, etc. The latter commonly appears in soil-root reinforcement models because in most circumstances they can be quantified. O'Sullivan and Simota (1995) reported of three basic criteria that must generally be satisfied by models: (1) they should have few parameters as possible, (2) parameters should be well defined and accessible (i.e., either measured or estimated) and (3) should adequately be documented.

Improvement in soil's load carrying ability might be enhanced by the presence of roots (Koolen, 1996; Heij and Koolen, 1993). Earlier investigations conducted by Willatt and Sulistyaningsih (1990) on loamy soil showed an increase in both bearing capacity and shear vane resistance by the presence of tree roots (table 5.4). Vane shearing resistance and bearing capacity were measured with Eijkelkamp self recording vane-tester and penetrometer (electrically driven, with a speed of 0.9 mm/sec) respectively. According to an article published by Wästerlund (1989), presence of roots may cause about 50-70% increase in soil's strength.

Table 5.4 Bearing capacity and shearing resistance of loamy soil (kPa) with or without paddy rice plants after 70 days of emergence.

Irrigation treatments	Bearing capacity (kPa)		Shearing resistance (kPa)	
	with plants	without plants	with plants	without plants
Puddled soil, irrigated each week with 30 mm of water	73.3	15.1	2.6	1.5
Nonpuddled soil irrigated each week with 30 mm water	395.4	193.7	10.6	5.1

Source: Willatt and Sulistyaningsih (1990)

Goss (1987) reported an increase in soil's bulk density around growing roots (table 5.5).

Table 5.5 Increase in soil bulk density around growing roots.

Soil type	Initial bulk density (g/cm <sup>3</sup> )	Density around root (g/cm <sup>3</sup> )
Fine sand	1.40	1.50
Loam	1.50	1.53
Clay	1.21	1.26

Source: Goss (1987)

A root-platform/soil interaction model which approximates the support provided by the root system to sustain the mass of shoot system (aerial parts) has been presented by Henwood (1973). In this model, densely packed root and soil mass served as a footing much as those used on the bottom of concrete columns in standard construction practice (figure 5.16).

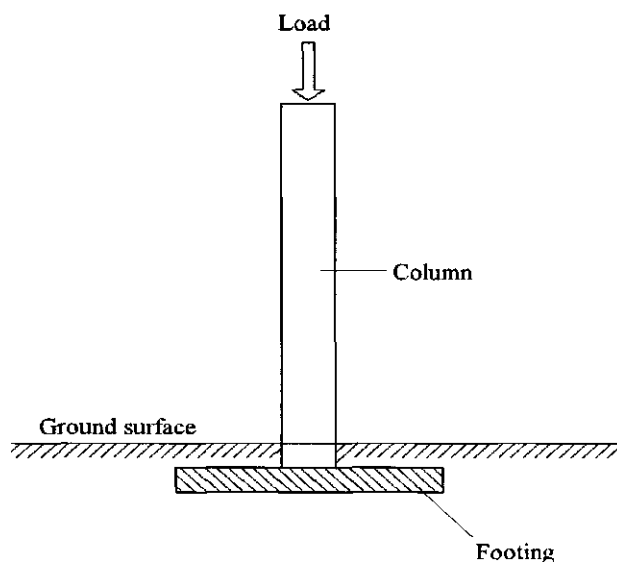


Figure 5.16 Schematic diagram of footing/column construction.

Source: Henwood (1973)

He indicated that under condition of zero eccentricity of loading, soil directly under the centre of the footing will possess high bearing pressures, with pressure decreasing towards the edges.

Slope stability by roots of woody vegetation has been documented by Waldron (1977). According to his observation vegetation removal by logging, wildfire or brush clearing is often seen to be followed by a high frequency of landslides. This soil instability was attributed to reduced or total absence of roots activities in the soil resulting from clearing of vegetation or logging. He indicated, that root reinforced soils can be analysed as composite materials in which fibres of relatively high tensile strength are embedded in a matrix of lower tensile strength. This concept conforms to the technique of reinforced earth in which true cohesion is imparted to soil by linear reinforcing elements. His model (figure 5.17) was based on Coulomb equation in which soil shearing resistance  $S_u$  is developed by cohesive and frictional forces (equation 5.18). In this model roots were treated as flexible and elastic.

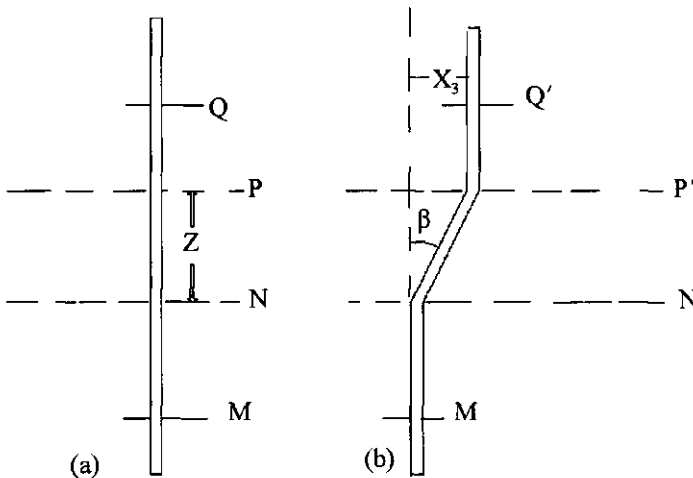


Figure 5.17 Model of a flexible, elastic root extending vertically across a horizontal shear zone of thickness  $Z$ : (a) undisturbed soil and (b) upper mass of soil above  $N$  displaced at a distance  $X_3$ .

Source: Waldron (1977)

$$S_r = c + \sigma_n \tan \varphi \quad 5.18$$

where,

$c$  = soil cohesion

$\sigma_n$  = normal stress

$\varphi$  = angle of internal friction of the soil.

Seven assumptions were made by Waldron (1977):

- (1) soil shearing occurs in a horizontal zone of thickness,  $Z$ , which is penetrated by vertical roots (figure 5.17) and  $Z$  does not change during shear
- (2) roots are flexible, of uniform diameter ( $D$ ), and are linearly elastic with modulus  $E$
- (3) soil friction angle  $\varphi$  is unaffected by roots so that the Mohr-Coulomb equation for root-permeated soil ( $S_r$ ) is given by equation 5.19
- (4) the tensile strain of the roots is not large, so that the loaded root length,  $L$ , approximates  $L_0$ , the length the loaded section would be if it were unstressed
- (5) the tensile stressed section of root extends equal distances from  $N$ , i.e.,  $NM = NQ$
- (6) the soil puts tension on the root by tangential stresses  $\tau$  which have a maximum value at incipient slippage of  $\tau'$
- (7) all longitudinal displacements of the root, including elastic tensile strain, mobilize the maximum tangential stress  $\tau'$ .

$$S_r = c + \Delta S_a + \sigma_N \tan \varphi \quad 5.19$$

where,

$\Delta S_a$  = contribution of roots to soil shear resistance.

According to Waldron (1977), when the upper mass of soil in figure 5.17 is displaced a distance ' $X_3$ ', the root segment  $MQ$  will be extended to a new length  $MQ'$ , and the average tensile stress in the stressed length of the root will depend on the elastic modulus and strain. Length of root under tension ( $MQ'$ ) after displacement and the root axial stress at  $N$  were expressed in terms of the variables  $Z$ ,  $D$ ,  $E$ ,  $\tau'$ ,  $\beta$  (see equations 5.20 and 5.21). Root contribution to increase in soil shear strength  $\Delta S_a$  was estimated by equation 5.22 when forces tangential and normal to the horizontal plane at  $N$  are considered. From purely frictional considerations, the maximum tangential stress  $\tau'$  was estimated by equation 5.23. Waldron's model showed, that  $\Delta S_a$  is proportional to the fraction of shear

cross sectional area occupied by roots (a result which was also verified by his experiments). He found that reinforcing effect of roots on inhomogeneously repacked soils is greater than on uniformly moulded soils. His model, however, did not account for roots' strain beyond elastic limits, breakage, or slip through the soil.

$$L = T_N D / 2 \tau' \quad 5.20$$

$$T_N = K_2 (\sec \beta - 1)^{0.5} \quad 5.21$$

$$\Delta S_a = a_r T_N (\sin \beta + \cos \beta \tan \phi) \quad 5.22$$

$$\tau' = \mu \sigma_n \quad 5.23$$

where,

$T_N$  = tensile stress at point N

$K_2 = (4\tau'ZE / D)^{0.5}$

$a_r$  = fraction of shear cross section filled by roots ( $A_r / A$ )

$A_r$  = total root cross section at the shear plane

$A$  = total soil shearing cross section

$\mu$  = coefficient of friction

$\sigma_n$  = stress normal to the root surface

$D$  = root diameter.

Work done by Waldron and Dakessian (1982) showed that effects of plant roots on slope's stability may result from their influence on: (1) soil shear resistance at failure and (2) weight of the soil block. Magnitude of root reinforcement was assessed by conducting direct shear measurement on twelve different root species. Ratio of shear resistance at 25 mm displacement of rooted and root-free soil samples were used in the estimation of root reinforcement. Their study showed that roots cannot significantly increase the soil's shearing resistance unless many of them grow into and through potential shear surfaces. In this case deep rooted vegetation will be more effective than shallow rooted vegetation. Removal of soil water by transpiration decreases the weight of the soil block and increases soil shear resistance at failure as the matric potential is reduced. In situations where rooted soils remain unsaturated (matric potential less than zero), root/soil tangential resistance to slipping will tend to increase thereby mobilizing more of the root potential for reinforcement.



Waldron's model was extended by Waldron and Dakessian (1981) to include situations where roots tend to stretch, slip or break when loaded in tension and the soil around is sheared. This was investigated using different root diameters (i.e., 0.1- 0.5 mm for barley, and 0.25- 6.0 mm for pine). Effect of shear zone thickness was investigated by simulation. Comparison of model simulations and experimental results revealed, that magnitude of  $\Delta S_a$  is strongly dependent on the strength of soil-root bond  $\tau'$ . In clay loam, values of  $\tau'$  were reported to be  $100 \text{ g cm}^{-2}$  in the absence of root hairs and ranged between 300 and  $600 \text{ g cm}^{-2}$  where root hairs exist. It was pointed out by Waldron and Dakessian that even if soil shearing causes roots to slip through the soil they will continue to contribute a reinforcing increment. This reinforcing effect will however be lost if soil shearing causes the tensile stress in the root to reach the rupture stress. Contribution of soil reinforcement provided by roots was given as the sum of those imparted by non-slipping  $S_1$  and slipping  $S_2$  roots (see equation 5.24). Root slippage was mentioned as the most common condition limiting reinforcement or strengthening of saturated fine-textured soil by roots.

$$\Delta S_a = S_1 + S_2 \quad 5.24$$

Waldron's model was based on partial mobilization of fibre (roots) tensile strength during shear without any constraint on the distribution of the reinforcing fibres (Gray and Ohashi, 1983). In their study on reinforcement effects, Gray and Ohashi (1983) used theoretical models based on limiting equilibrium of forces to: (1) examine the influence of natural (eg. roots) and synthetic fibre inclusions on the shear strength of sand, (2) identify important test parameters and fibre/sand variables. Their models accounted for the influence of such variables as fibre modulus, diameter, initial fibre orientation, elongation during shear, skin friction between fibre and sand, angle of internal friction, and relative density of the soil. Fibres used in their study were assumed to be long, elastic, extending an equal length over either side of a potential shear plane, and thin enough to offer little if any resistance to shear displacement from bending stiffness. Increase in shear strength resulting from inclusion of fibre reinforcement oriented perpendicularly and at an acute angle with respect to the shear zone were estimated from equations 5.25 and 5.26 respectively. These fibre orientations are illustrated in figure 5.18.

$$S_r = t_R [\sin \theta + \cos \theta \tan \varphi] \quad 5.25$$

$$S_r = t_R [\sin (90-\psi) - \cos (90-\psi) \tan \varphi] \quad 5.26$$

$$\psi = \tan^{-1} \{1 / [k_1 + (\tan^{-1} \alpha)^{-1}]\} \quad 5.27$$

where,

$$t_R = (A_R / A) \sigma_{fs}$$

$S_r$  = shear strength increase from fibre reinforcement

$\varphi$  = angle of internal friction of sand

$\theta$  = angle of shear distortion

$\alpha$  = initial orientation angle of fibre with respect to shear surface

$k_1$  = shear distortion ratio ( $k_1 = x/z$ )

$x$ , = horizontal component of shear displacement

$z$  = thickness of shear zone

$\sigma_{fs}$  = tensile stress developed in the fibre at the shear plane.

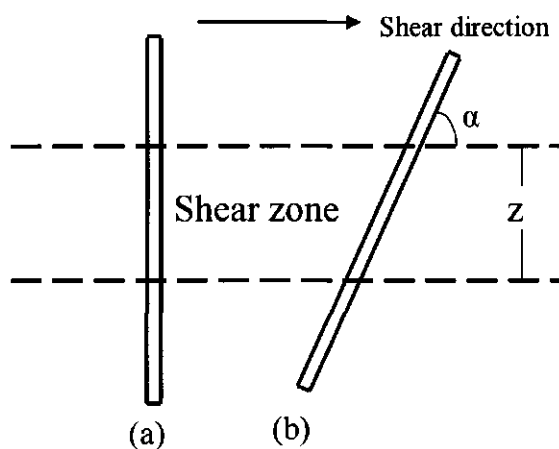


Figure 5.18 Fibre orientation to the shear zone: (a) perpendicular and (b) orientation at an angle  $\alpha$ .

Source: Gray and Ohashi (1983)

Direct shear tests were conducted to verify these models. Diameters and lengths of fibres used ranged from 1-2 mm and 20-250 mm, respectively. From their study it was found that an initial fibre orientation of 60° with the shear surface was optimum for maximum shear strength increase.

Terwilliger and Waldron (1991) argued that although models presented by Waldron (1977) and Waldron and Dakessian (1981) may represent maximum reinforcement potentials of roots in soils, they will have limited applicability since these models concentrate on soil conditions directly under the plant stems (that is, where roots would usually be densest and thickest). Studying the effects of roots on soil slippage on unstable hillside, they found that reinforcement potential of tree roots may depend not only on vegetation characteristics but also on the properties of the soil upon which the vegetation is growing.

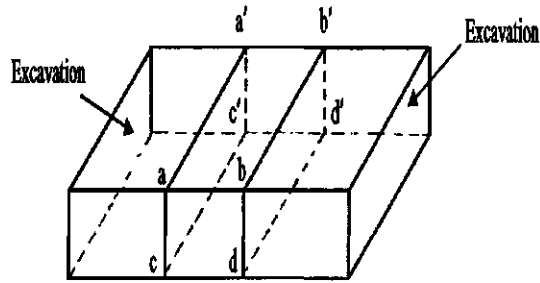
Using representative distributions of root-strength values, Terwilliger and Waldron (1991) proposed a slope model that provides an initial estimate of the average effect of roots reinforcement on hillside. The following assumptions were made:

- (1) slippage is assumed to occur on a plane that is parallel to a smooth sloping earth surface
- (2) unit of soil that moves is assumed to be a parallelogram with vertical head and toe walls
- (3) entire soil mantle would be saturated above a likely failure surface
- (4) cohesion less soil
- (5) root displacement during shear being equal to the total displacement necessary to mobilize shear strength during shear test
- (6) roots would tend to straighten and be pulled in tension during failure, but would possess the same tensile-stress developed during failure.

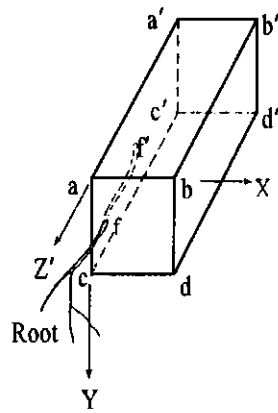
In comparison to forest soils, distribution of roots reinforcement in grasslands are found to be relatively uniform. Work done by Maher and Gray (1990) showed that increase in the aspect ratio (i.e., length/diameter) of a reinforcing material will result in a higher contribution of the material to increase in shear strength of the soil. This therefore makes long thin roots more important in soil reinforcement than short thick roots.

Using analytical models Wu et al. (1988) showed that resistance offered by a tree root in the soil-root system could be analysed as a pile on an elastic-plastic support (for small shear displacements) or as a cable (for large shear displacements). Their proposed models were partly based on roots that were cut off by the sides of a shear apparatus during shear displacement. In-situ shear experiments were conducted in the laboratory to verify the models. With their in-situ shear experiments, roots were considered to run in a direction parallel to the ground surface. Implying that the shear direction in case will be perpendicular to the ground surface. The side plates of the shear apparatus acc'a' and bdd'b' were forced into the ground and the soil behind the plates (i.e., falls outside the shear box) was excavated (see figure 5.19 (a)). Roots leaving the shear box at f' are therefore cut off by the side plate acc'a' (figure 5.19 (b)). One of the basic difficulties associated with the use of the models proposed by Wu et al. (1988) is that the displacement the root had undergone at the end of shear displacement will have to be known in order to decide whether the pile or the cable solution should be used. Accurate estimation of this displacement is almost impossible in most situations.

Other difficulties that are generally associated with the determination of root contribution to increase in soil strength include: (1) the variability of shear strength measurement resulting from differences in rooting density and soil properties, (2) accurate estimation of the shear width (see section 5.22). From the above it will be concluded that although various attempts have been made to quantify the contribution of roots to increase in soil strength, these attempts have not been completely successful.



(a)



(b)

Figure 5.19 In situ shear experiment: (a) excavation around the shear plates and (b) cut-off root.

Source: Adapted from Wu et al. (1988)

### 5.2.2

#### Shear zone

Estimation of the width of the shear zone is considered as one of the essential steps in soil-root modelling because root contribution to increase in soil strength is known to be affected by the size of this zone (Shewbridge and Sitar 1989; Shewbridge and Sitar, 1990). Until now, various methods have been used in the estimation of the width of the shear zone because there appears to be no standard prediction method available. Shewbridge and Sitar (1990) numerated four factors which may affect the width of the shear zone in testing devices: (1) reinforcement stiffness, (2) concentration of the reinforcement, (3) magnitude of soil-reinforcement bond and (4) level of deformation constraints imposed by the testing device.

Earlier study conducted by Shewbridge and Sitar (1989) on shear zone deformation patterns in reinforcement soil composites showed, that deformation pattern of a reinforcing material is curvilinear and symmetric about the centre of the shear zone, and can be described by an exponential decay function.

Studying the mechanics of how tree roots reinforce soil, Abe and Ziemer (1991) observed the deformation of roots and the development of the shear zone through a glass-sided shear box (figure 5.20). This was achieved by placing 1 cm wide belts of white sand on the bottom glass of the apparatus and oriented perpendicular to the direction of shear. Fine sand with a dry density of  $1.47 \text{ g/cm}^3$  and a moisture content of 19.5% by weight was used in the experiments. For each test, a total of 90.5 kg of sand was placed and compacted in the shear box in five 18.1 kg layers. Finally 250 kg of lead shot was placed on top of the sand to keep the overburden stress distribution uniform throughout the test. The normal stress on the bottom glass was  $0.0964 \text{ kg/cm}^2$ . Straight roots without branches, bends or visible defects were placed in the shear box in three vertical layers and sheared across a vertical plane. The number of roots used in each test was either 0, 3, 6 or 9 with diameters ranging between 8.2 to 14.0 mm. Roots in the sheared sand affected the development of the shear zone by relative movement among sand particles. Deformation of the white sand bands showed three sheared zones  $Z_1$ ,  $Z_2$ , and  $Z_3$ . These are shown in figure 5.20.

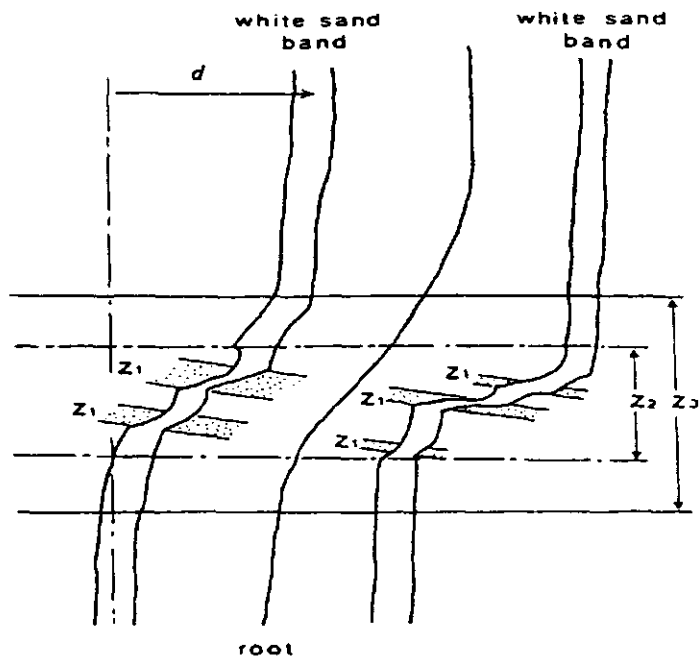


Figure 5.20 Mapped shear zones.

Source: Abe and Ziemer (1991)

These shear zones have different strains with the largest strain,  $Z_1$ , emanating from the middle of the shear zone. This zone, however, becomes more indistinct with increasing concentration of roots. Shear zone varied between 8 and 16 cm. The model uses root strain to estimate the shear stress of soil reinforced by roots. The following assumptions were made: (1) roots are linearly elastic, (2) observed root shape can be approximated by an exponential function and (3) movements of physical points on the root axis are parallel to the shear surface, implying that short elements of the root will be elongated axially.

Though the shapes of the above deformed roots in the sheared soil agreed with model proposed by Shewbrige and Sitar (1989), they disagreed with the model published by Waldron (1977) where roots bend abruptly at boundaries between the shear zone and

outer undisturbed zone. Hypothetical root deflections and corresponding shear zone values developed during shear experiments conducted by Terwillinger and Waldron (1991) are shown in table 5.6.

Table 5.6 Root deflections and corresponding zones of shear (Z) assumed to mobilize during soil failure.

Root deflection (mm)	Z (mm)
5 - 8	10
9 - 12	20
13 - 16	30
17 - 20	40
21 - 24	50
25 - 28	60
29 - 32	70
33 - 36	80
37 - 40	90
41 - 44	100
45 - 49	110
> 50	120

Source: Terwillinger and Waldron (1991)

In general, the shear band or development of the shear zone is of little importance in soil-wheel systems. This is because these systems involve the so-called stable soil behaviour.



### 5.3

### SOIL-ROOT AND VEHICLE MECHANICS

Literature on soil deformation by field traffic has been presented by many authors including Bailey et al. (1986), Bailey et al. (1988), Petersen (1993), Gupta and Visvanathan (1993) and Chi et al. (1993). Effect of multiple passes has been discussed by Pollock et al. (1986) and Kirby et al. (1997). Load-sinkage relation is commonly represented by equation 5.28 (Turner, 1984; Hvorslev, 1970).

$$P = b y^m \quad 5.28$$

where,

- $P$  = unit normal load
- $y$  = sinkage
- $m$  = sinkage exponent
- $b$  = sinkage modulus.

Hvorslev (1970), however, revealed that routine plate sinkage tests conducted on plastic clay and fine sand at the U.S. Army Engineer Waterways Experimental Station (WES) produced results that were not consistent with this equation. Therefore, equation 5.29, that adequately predicts the vertical displacement  $\delta$  of a circular rigid plate, resting on the surface of a semi-infinite elastic solid, was proposed.

$$\delta = \frac{0.5 \sigma \pi R (1.0 - v^2)}{E_s} \quad 5.29$$

where,

- $E_s$  = modulus of elasticity of the solid
- $v$  = Poisson's ratio
- $R$  = radius of plate.

Koolen (1986) reported of a simplified model that describes the stress matrix between the contact surface of deflected wheels (or tracks) and the soil. This model consists of a soil volume element in the form of micro cube loaded by principal stresses  $\sigma_1$ ,  $\sigma_2$  and  $\sigma_3$  (figure 5.21).  $\sigma_1$  relates to vertical wheel load (through tyre inflation pressure and carcass stiffness) transmitted to the soil.

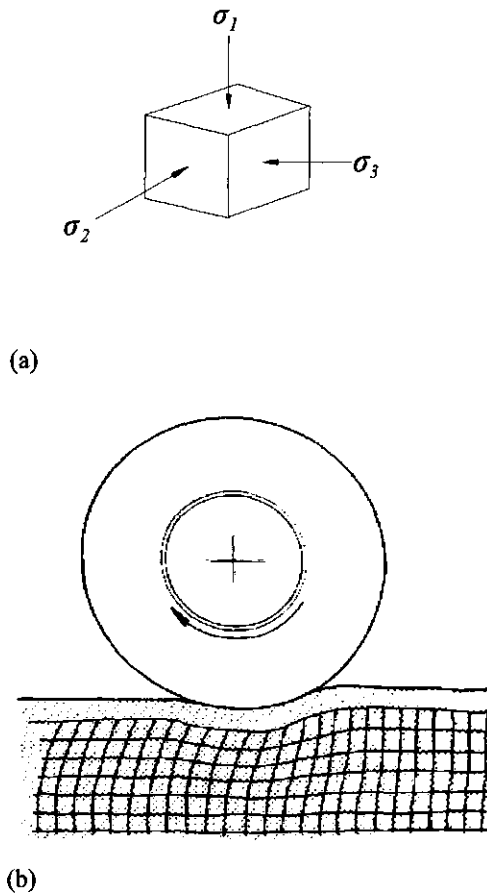
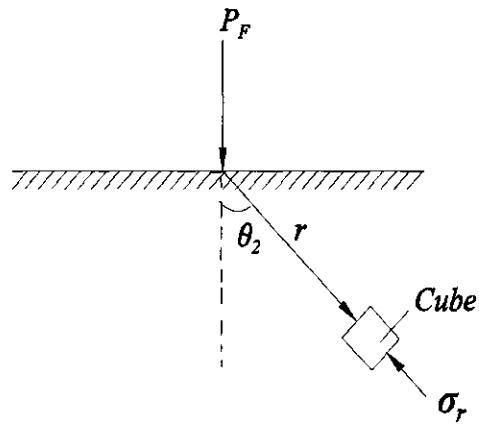


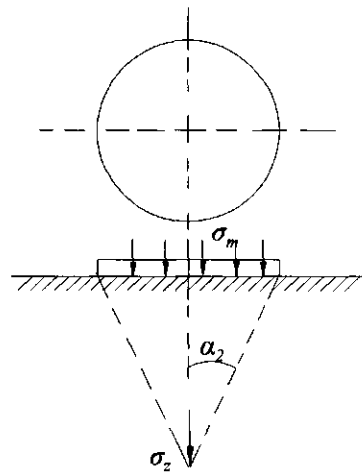
Figure 5.21 A soil volume-element under loading by principal stresses (a) and an example of soil-wheel interaction involving a large number of soil volume-elements (b).

Source: Koolen (1986)

A number of methods by which  $\sigma_1$  may be estimated have been discussed by Koolen and Kuipers (1983). Among these are (1) vertical point-load method (figure 5.22 (a)) and (2) circular loaded area method (figure 5.22 (b)).



(a)



(b)

Figure 5.22 Estimation of the normal stress ( $\sigma_1$ ) in a tyre-soil system:  
(a) vertical point load and (b) circular loaded area.

Source: Koolen and Kuipers (1983)

The vertical point-load method was based on the theory of Boussinesq for a point load on an elastic isotropic semi-infinite soil mass. Considering a small cube in such a position that radius vector  $r$  is perpendicular to one of its sides (figure 5.22 (a)), Boussinesq showed that the only stresses encountered on the cube were those experienced by the sides perpendicular to the radius. The normal stress (principal stress) on the cube was given by equation 5.30. The vertical point-load method predicts the same stress distribution for all soils. To account for different soil properties equation 5.30 was modified to 5.31.

$$\sigma_1 = \frac{3P_F}{2\pi r^2} \cos\theta \quad 5.30$$

$$\sigma_1 = \frac{3P_F}{2\pi r^2} \cos^{v-2}\theta \quad 5.31$$

where,

- $P_F$  = point load
- $r$  = radius vector
- $v$  = concentration factor ( $v$  is equal to 3, 4, 5 for hard, normal and soft soils, respectively).

In the second method (i.e., figure 5.22 (b)) the soil-wheel system was described by a circular area loaded by uniformly distributed normal load. The area of the circle was chosen to be equal to the area of the soil-wheel contact surface, while the stress  $\sigma_m$  on the circular area was considered to be equal to  $\sigma_1$  in the soil-wheel interface. An angle  $\alpha_2$  represents the depth under consideration. The principal stress  $\sigma_z$  induced in the plane by presence of  $\sigma_m$  was given by equation 5.32. This was also modified to account for differences in soil strength by introducing the concentration factor  $v$  (equation 5.33).

$$\sigma_z = \sigma_m (1 - \cos^3 \alpha_2) \quad 5.32$$

$$\sigma_z = \sigma_m (1 - \cos^v \alpha_2) \quad 5.33$$

Though Söhne's procedure is most likely to give realistic results (more detailed than the others), the idea of circular loaded method is commonly used. This assumption was also

adopted by Koolen et al. (1992) and Heij and Koolen (1993) in their analysis of normal stresses under a tyre at shallow depth  $z$  (equation 5.34).

$$\sigma_z = q (1 - \cos^v \{ \arctan [ (1/z) (P_F / \pi q)^{1/2} ] \}) \quad 5.34$$

where,

- $\sigma_z$  = peak stress under a wheel at a depth  $z$  metres [ $\text{kN/m}^2$ ]
- $P_F$  = vertical wheel load [ $\text{kN}$ ]
- $q$  = stress at the contact area between tyre and soil [ $\text{kN/m}^2$ ]. By approximation  $q$  is calculated as 2 \* inflation pressure
- $v$  = concentration factor.

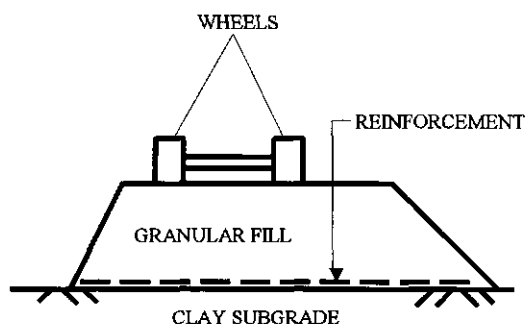


Figure 5.23 Section of reinforced unpaved road.

Source: Houlsby et al. (1989)

The improvement of bearing capacity due to the presence of roots, and stresses set up in the soil by the action of field traffic, may also be estimated using methods suggested by Giroud and Noiray (1981), Sellmeijer et al. (1982), Houlsby and Jewell (1990), Burd and Brochlehurst (1990), Fannin and Sigurdsson (1996) and Sellmeijer (1990) who specifically studied the improvement of unpaved roads reinforced with geotextiles. Unpaved roads are usually used as temporary site access like forestry roads, and may consist of a layer of fill compacted onto the subgrade with a single layer of geotextile or geogrid reinforcement placed at the base of the fill as shown in figure 5.23.

Most mathematical considerations of road reinforcement mechanisms assume the concept of 'tensioned membrane' effect (Giroud and Noiray, 1981; Sellmeijer et al. 1982; Sellmeijer, 1990; Gourc, 1993), that is, as surface rut develops, the reinforcement in the region of the applied load becomes curved. Reduction in the magnitude of the vertical stresses applied to the subgrade then results from the combined effects of the curvature and tension in the reinforcement. Since the above concept is only significant at large rut depths, Houlsby et al. (1989) therefore proposed a new explanation for reinforcement mechanisms that tends to account for improvement in bearing capacities even at very small rut depths.

Although basic mechanisms of soil reinforcement have been accepted by most researchers, mode of soil loading by vehicles continues to be one of the approaches which visibly draws a line between them. By considering the soil-wheel contact area as a circular plate, the loading is assumed to be axisymmetric (Pollock et al., 1986; Milligan et al., 1989; Kirby et al., 1997), otherwise, the plane strain approach is adopted (Fannin and Sigurdsson, 1996; Burd and Brocklehurst, 1990; Milligan et al., 1989). With regard to the former approach, Houlsby and Jewell (1990) argued that if an unpaved road is rutted, it will be inappropriate to consider the loading as axisymmetric. Limit equilibrium design method proposed by Houlsby and Jewell (1990) has been adopted by a number of authors in estimating the stresses set up in a road by the action of a passing vehicle. With this method, wheels are modelled as footing and the induced stresses are calculated using a load spread angle  $\beta$  (figure 5.24). Burd and Brocklehurst (1990) proposed a value of  $22.1^\circ$  for  $\beta$ . Below the centre line of the footing, the vertical stress  $\sigma_v$  due to the presence of a pressure  $P$  at any distance  $z$  in the soil was calculated by equation 5.35.

$$\sigma_v = \gamma z + \frac{PB_1}{B_2 + z \tan \beta} \quad 5.35$$

where,

$B_2$  = half width of plane strain footing

$\gamma$  = unit weight of fill material.

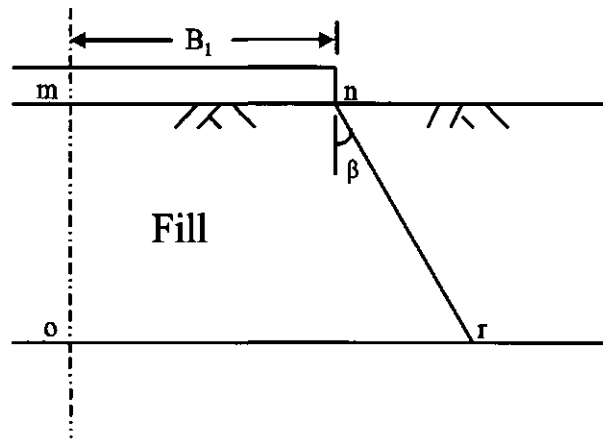


Figure 5.24 Load spread under a strip footing.

Source: Houlsby and Jewell (1990)

Modelling soil reinforcement by roots network is considered to be complex and difficult and hence, will require the use of a sophisticated method such as finite element analyses employing appropriate constitutive equations (Chi et al., 1993; Gray and Ohashi, 1983). In this thesis finite element code known as PLAXIS will be used, therefore some of its relevant features will be briefly discussed.

## PLAXIS: finite element code

PLAXIS stands for Plasticity Axisymmetric (Vermeer, 1991; Brinkgreve and Vermeer, 1998). Its development began in early 1987 at Delft University of Technology, when the Dutch's Department of Public Works needed an easy-to-use finite element code for soil plasticity calculations. PLAXIS was initially developed for the analysis of sea dikes and river embankments in the coastal lowlands of Holland, but has now been extended to cover most areas of geotechnical engineering, hence, has undergone periodic improvement since its development in 1987. In comparison to the earlier versions, the current PLAXIS version (version 7.0) is considered to be more user friendly (i.e., easy to use) and allows for full automatic mesh generation when geometry of the problem under investigation is drawn. Mesh generation takes full account of position of points and lines in the geometry model, so that exact position of layers, loads and structures are reflected by the finite element mesh. This mesh generation is based on a robust triangulation principle that searches for optimized triangles. Two main triangle elements are used: 6-noded triangle elements (default) and 15-noded triangle elements. The 6-noded triangle element contains 3 stress points whilst 15-noded triangle element contains 12 stress points (figure 5.25).

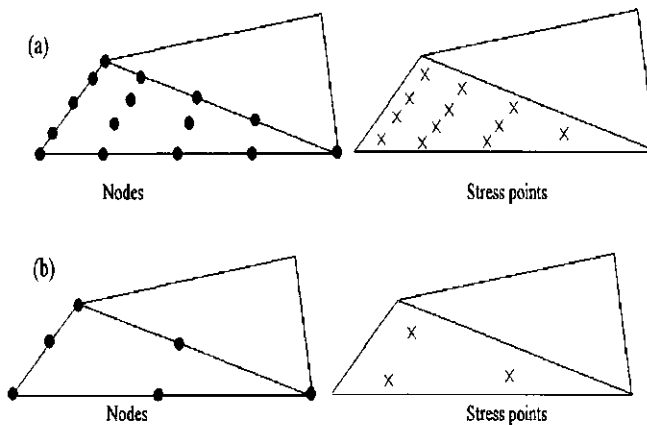


Figure 5.25 Triangular elements and their corresponding stress points: (a) 15-noded and (b) 6 noded.

Source: Brinkgreve and Vermeer (1998)



In PLAXIS, behaviour of reinforced soil structures, for example, embankments, walls, etc., are studied by the use of geotextiles. These geotextiles are considered as slender objects with a normal stiffness but no bending stiffness. Thus, they can sustain only tensile forces and no compression. Geotextiles are simulated as 3 or 5 noded line elements (figure 5.26 (a)) depending on the type of the soil elements that were initially used in the program. When 6-noded soil elements are employed, each geotextile element is defined by 3 nodes or are defined by 5-nodes when 15-noded soil elements are used. Material property required of geotextile as input is its longitudinal stiffness (see equation 5.06). In PLAXIS, geotextiles may also be used in combination with anchors, for example, node-to-node (figure 5.26 (b)) and fixed-end (figure 5.26 (c)) anchors, to simulate ground anchorage. These anchors are considered as elasto-plastic spring elements.

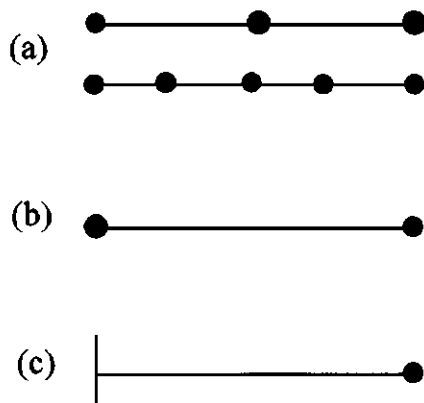


Figure 5.26 Soil reinforcement elements: (a) geotextiles, (b) node-to-node anchors and (c) fixed-end anchor.

Source: Brinkgreve and Vermeer (1998)

During bearing capacity analysis, PLAXIS adopts a special procedure where load increments are automatically added until a prescribed load is reached (figure 5.27). Two main situations are encountered in bearing capacity calculations: (1) failure before reaching the prescribed load (Fig.5.27 (b)) and (2) reaching prescribed load (figure 5.27 (c)).

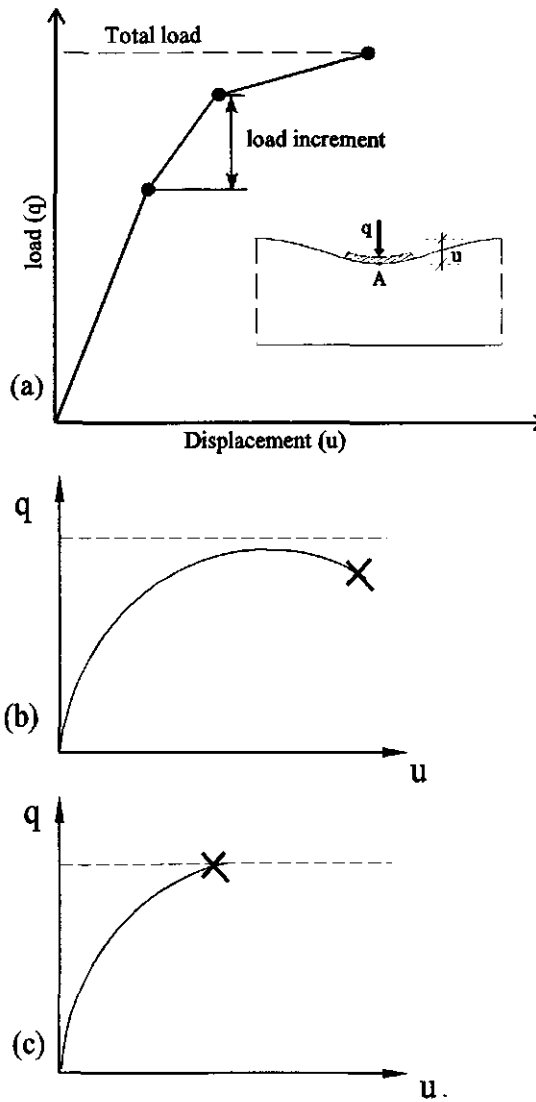


Figure 5.27 Bearing capacity analysis: (a) automatic load increment; (b) failure before reaching prescribed ultimate level and (c) reaching prescribed ultimate level.

Source: Bonnier (1998)

It is possible to model interaction between the reinforcements and the soil using interface elements which may be deduced from the soil properties using a reduction factor  $R_{inter}$ . Suggested values of  $R_{inter}$  provided by PLAXIS for various interface elements are given in table 5.7.

Table 5.7 Suggested values of interface elements given by PLAXIS.

Interface	$R_{inter}$
Sand/steel	0.67
Clay/steel	0.5
Sand/concrete	1.0-0.8
Clay/concrete	1.0-0.7
Soil/geotextile	0.9-0.5

Source: Brinkgreve and Vermeer (1998)

## **5.4 SIMULATING REINFORCEMENT EFFECTS OF TREE ROOTS IN A SOIL-WHEEL SYSTEM**

### **5.4.1 Introduction**

Among the paramount steps used in finite element analysis are: (1) selection of an appropriate constitutive model and (2) ensuring accuracy of input data. Constitutive models describe the stress-strain relationships of the materials under consideration. Work done by Chi et al. (1993) revealed some basic criteria that need to be considered in the selection of these models. These include: (1) accuracy of the model at representing various aspects of soil behaviour and (2) convenience in parameter determination and model implementation. Information on how soil input data can be obtained for use in finite element modelling has been presented by Kirby et al. (1997), Chi et al. (1993), Koolen and Van den Akker (2000), Petersen (1993), Bailey and Johnson (1989), Bailey et al. (1984), Bailey et al. (1988), Liu and Evett (1984).

Constitutive models which are commonly used include the following:

- (1) hyperbolic model
- (2) Mohr-Coulomb model
- (3) Van den Akker's model (in SoCoMo)
- (4) Cam-clay model
- (5) Drucker-Prager model.

The hyperbolic model uses generalized Hooke's law to predict deviatoric stress and volumetric strain under triaxial compression. Principal advantages of this model is its ability to represent stress-strain behaviour of a wide variety of soils (ranging from clay, and silt through sand) and be used for unsaturated and saturated soils, as well as drained or undrained loading conditions. Basic component of the model is the tangent Young's modulus of elasticity, which is given by equation 5.36 (Chi et al., 1993).

$$E_t = K_t P_a \left( \frac{\sigma_3}{P_a} \right)^{n_t} \left( 1 - \frac{R_f(1-\sin\phi)(\sigma_1 - \sigma_3)}{2 * c * \cos\phi + 2\sigma_3 \sin\phi} \right) \quad 5.36$$

where,

- $E_t$  = tangent Young's modulus
- $P_a$  = atmospheric pressure
- $\sigma_1$  = major principal stress
- $\sigma_3$  = minor principal stress
- $c$  = cohesion
- $\phi$  = internal friction angle of soil
- $K_n$  and  $n_t$  = dimension less parameters
- $R_f$  = failure ratio defined as ratio of the maximum failure deviatoric stress obtained in a triaxial tests to the ultimate deviatoric stress obtained from regression analysis.

The Mohr-Coulomb model applies to relatively dense soil that does not compact easily, and can be used in identifying soil regions where plastic flow occurs. Such regions may show severe soil structure deterioration (Koolen and Van den Akker, 2000). Five parameters are required by Mohr-Coulomb's model: (1) Young's modulus of elasticity, (2) Poisson's ratio, (3) cohesion, (4) angle of internal friction and (5) angle of dilatancy.

From values of soil cohesion, angle of internal friction, and pre-consolidation stress, SoCoMo predicts size and location of plastic regions in the soil under wheels of agricultural field vehicles. Important components of SoCoMo include: (1) vertical point load solution and (2) solution for tangential force on a semi-infinite elastic medium. Shear stresses in the soil-wheel interfaces are accounted for by SoCoMo.

The Cam-clay model is a typical example of elasto-plastic model, and may be used in predicting volumetric strain under triaxial compression. In general, the Cam-clay type models in finite element codes result in stress distributions and distributions of soil deformation that distinguish between soil regions where soil behaves according to the laws of elasticity, Coulomb's law of plastic yielding or laws of plastic hardening (Koolen

and Van den Akker, 2000). The modified Cam-clay model describes the stress-strain relationships of the Normal Consolidation Line (NCL) and Swelling Line (SL) and may be defined in terms of specific volume and mean normal pressure (equations 5.37 and 5.38).

$$\ln\left(\frac{v_a}{v_b}\right) = \lambda_c^* \times \ln\left(\frac{P_a}{P_b}\right) \quad 5.37$$

$$\ln\left(\frac{v_a}{v_b}\right) = \kappa_c^* \times \ln\left(\frac{P_a}{P_b}\right) \quad 5.38$$

where,

- $v_a$  and  $v_b$  = specific volumes at states a and b respectively;
- $P_a$  and  $P_b$  = corresponding mean and normal stresses (kPa);
- $\lambda_c^*$  and  $\kappa_c^*$  = slopes of the NCL and SL respectively plotted on log- log scale (figure 5.28).

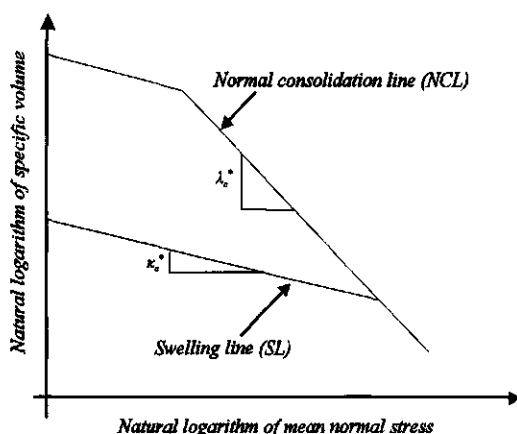


Figure 5.28 Determination of parameters for Cam-clay model.

Source: Chi et al. (1993)

In PLAXIS, the Cam-clay model is officially referred to as the PLAXIS Cap model and the normal consolidation line and swelling line are defined in terms of volumetric strain and logarithm of the mean effective stress (equations 5.39 and 5.40). Some of the characteristics of the PLAXIS Cap model are: (1) distinction between primary loading and unloading/reloading, (2) remembering pre-consolidation stress and overconsolidation. PLAXIS Cam-clay model requires: (1) Poisson's ratio, (2) compression index, (3) rebound index, (4) cohesion, (5) angle of internal friction, (6) soil dilatancy angle and (7) pre-consolidation stress. The compression and rebound indices may also be referred to as modified compression index and modified swelling index, respectively.

$$\epsilon_v - \epsilon_v^0 = -\lambda^* \ln \left( \frac{P}{P^0} \right) \quad 5.39$$

$$\epsilon_v^e - \epsilon_v^{e0} = -\kappa^* \ln \left( \frac{P}{P^0} \right) \quad 5.40$$

where, the index 0 refers to a reference condition and

- $\epsilon_v$  = volumetric strain
- $P$  = mean normal stress
- $\lambda^*$  = slope of the NCL plotted on normal versus logarithm scale
- $\kappa^*$  = slope of the SL plotted on normal versus logarithm scale.

Unlike the models already discussed, Drucker-Prager's model uses the Drucker-Prager failure criterion stated in equation 5.41. Common methods used in determining soil parameters for modelling in finite element analysis include: (1) triaxial compression, (2) uniaxial compression and (3) direct shear. Typical example of results obtained in a drained triaxial compression test is as shown in figure 5.29.

$$f_f = \sqrt{I_1} - k_2 I_2 - k_3 \quad 5.41$$

where,

- $f_f$  = failure function
- $k_2$  and  $k_3$  = dimension less parameters
- $I_1 = 1/6[(\sigma_1 - \sigma_2)^2 + (\sigma_1 - \sigma_3)^2 + (\sigma_2 - \sigma_3)^2]$
- $I_2 = \sigma_1 + \sigma_2 + \sigma_3$

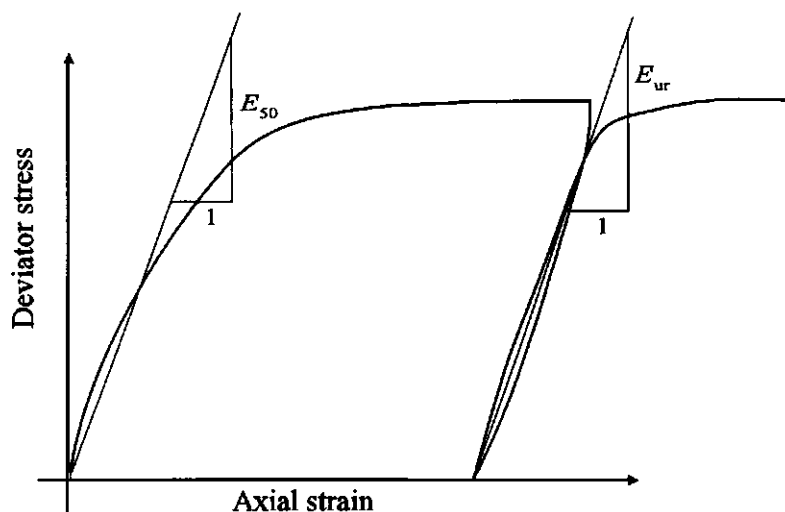


Figure 5.29 Typical results from triaxial compression test.

Source: Brinkgreve and Vermeer (1998)

In the above test the cell pressure is held constant and the sample is loaded until failure occurs. In order to arrive at a suitable value of Young's modulus for finite element analysis,  $E_{50}$  is often adopted. This is the value of secant Young's modulus when the deviator stress is exactly 50% of the failure value. Soil parameters provided by Koolen and Van den Akker (2000) on compactible Lobith loam and practically incompressible wet dense Wageningen silty clay loam can be used in the Mohr-Coulomb model and Cam-clay model respectively (table 5.8). Other studies conducted by Chi et al. (1993) on Mawcook Gravel-sandy loam and Ste-Rosalie Clay have provided the needed soil parameters for models such as the hyperbolic model and Cam-clay model (see table 1, appendix III).

Coefficient of lateral earth pressure  $K_0$  for most agricultural and wet agricultural clayey soils has been reported to be 0.5 and 0.9 respectively, whilst cohesion is quoted to range between 9 to 140 kPa. Minimum value of cohesion  $c$  is estimated by equation 5.42.



$$c = \chi s_w \tan \varphi \quad 5.42$$

where,

- $\chi$  = degree of saturation  
 $s_w$  = suction in the soil water  
 $\varphi$  = angle of internal soil friction.

Table 5.8. Soil parameters derived from compactible Lobith loam and wet dense Wageningen silty clay loam.

Soil Parameters	Soil types	
	Lobith Loam	Wageningen Silty clay loam
Young's modulus, E	-	2.2 MPa
Coefficient of earth pressure, $K_0$	0.5	0.9
Angle of internal friction, $\varphi$	35°	0
Cohesion, c	23 kPa	82 kPa
Poisson's ratio, $\nu$	0.15	0.35
$\lambda^*$	0.07	-
$\kappa^*$	0.0047	-
water content, w	20 %	18 %

Source: Koolen and Van den Akker (2000)

The main objective of this study will be to demonstrate the effects of tree roots in the soil-wheel system using PLAXIS. Specifically this will involve: (1) simulating the deformation (rut formation) induced by single passage of a forestry vehicle on soil between two tree rows which are 5 m apart with roots from the trees forming a mat in the soil, (2) studying stresses in the soil under the wheels at different depths, (3) effects of varying soil depth, (4) bending resistance of individual roots and (5) inclusion of interface element. Average wheel width and contact pressure will be taken to be 0.5 m and 200 kPa (2 bars) respectively. Centre to centre distance between pairs of the vehicle wheels will also be taken to be 2.5 m. The problem is as illustrated in figure 5.30.

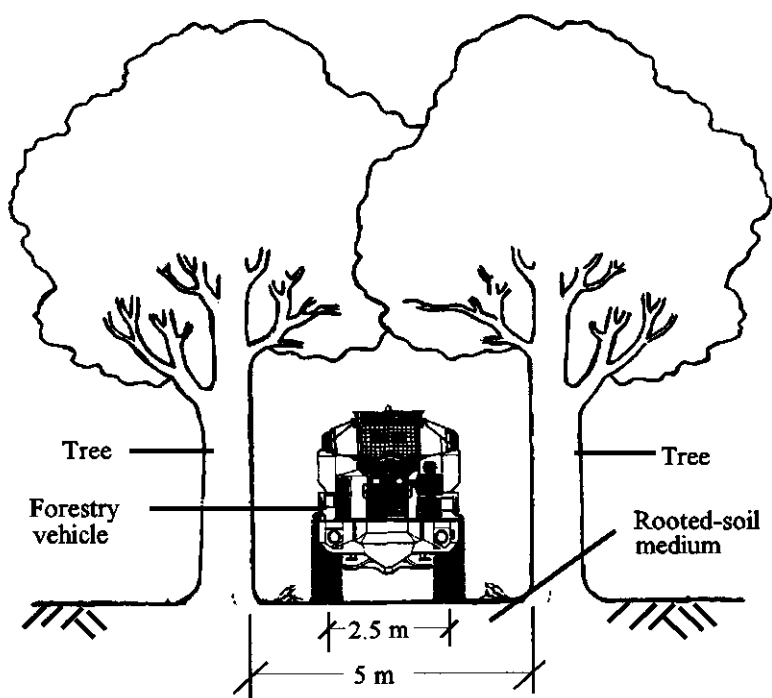


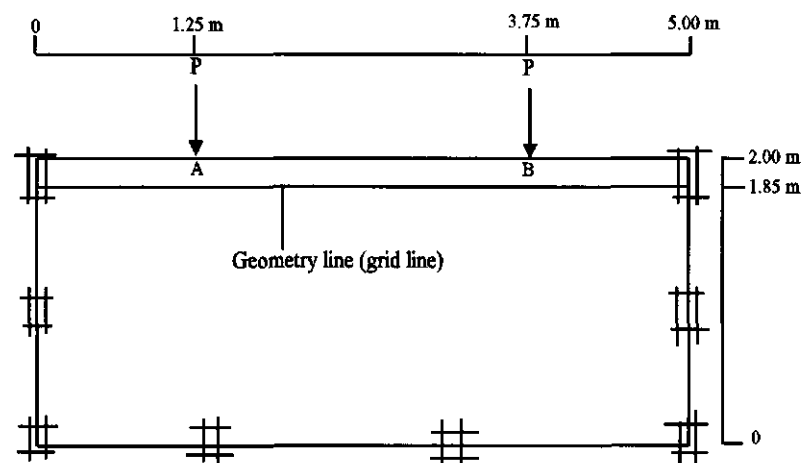
Figure 5.30 Illustrating soil-vehicle interaction.

## **5.4.2 Methods**

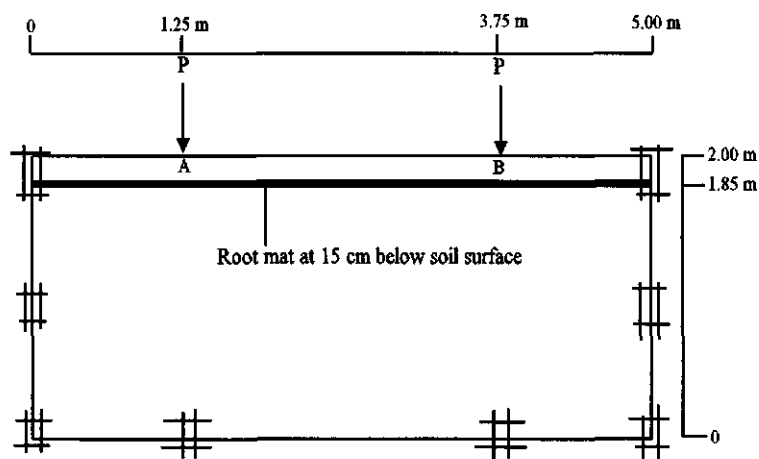
### **5.4.2.1 Reference case**

The problem illustrated above (i.e., figure 5.30) was considered as a two-dimensional problem, hence making it ideal to be handled in PLAXIS (version 7.0). Two main situations that were investigated involved: (1) soil volume without roots (root-free soil) and (2) soil volume containing roots (rooted-soil).

Effects of tree roots on rut formation induced by wheels of forestry vehicles can be studied by: (1) considering roots acting as a geotextile mat with no bending stiffness placed at a particular depth in the soil and (2) roots smeared at the upper soil layer forming a uniform stiff soil-root layer. In the latter situation, a combined modulus of elasticity has to be calculated for the stiff soil-root layer. In this study the former option was adopted, and was accomplished by considering a rooted top layer of 0.3 m thickness with root concentration of 0.015% (i.e., root intensity = 0.0015). This therefore formed a mat of 0.0045 m thickness and cross sectional area  $A_r$  of 0.0045 m<sup>2</sup> per metre (parallel to direction of travel), at a depth of 15 cm below the soil surface. The mat was modelled as 5 noded line elements with normal stiffness, but no bending stiffness. Bottom and sides of the soil meshes were fixed including ends of the root mat. Geometry of the meshes including boundary conditions are as illustrated in Fig. 5.31. This was considered as a reference case. Grid line was inserted in the root-free mesh (depth = 15 cm) to ensure that changes detected in rooted soil mesh after loading is solely due to the effects of root mat inclusion, and not partly due to differences of meshes.



(a)



(b)

Figure 5.31 Geometry and boundary conditions: (a) root-free soil and (b) rooted soil.

Stiffness of the root mat  $\xi$  was calculated by equation 5.43. Initial stiffness modulus of the root mat  $E_{\text{initial}}$  was estimated by considering values of overall stiffness modulus  $E_{\text{overall}}$

found in our earlier experiments on beech roots (see Makarova et al., 1998). From the aforementioned article  $E_{\text{initial}}$  of the root mat was estimated to be approximately  $10^6$  kPa (using  $E_{\text{initial}} \approx 5 E_{\text{overall}}$ ), hence giving  $\xi$  to be  $4500 \text{ kN m}^{-1}$ .

$$\xi = E_{\text{initial}} A_r \quad 5.43$$

Soil behaviour was considered as drained, and was modelled as plane strain, using 15-noded triangular elements. PLAXIS Cam-clay constitutive model was used taking soil parameters on compactible Lobith loam provided in table 5.8. Initial stresses in the soil were generated by using  $K_0$ -procedure. Dry and wet weights of the soil were taken to be  $13 \text{ kN m}^{-3}$  and  $15 \text{ kN m}^{-3}$  respectively. Contact pressure,  $P$  (magnitude =  $200 \text{ kPa}$ ), imposed on the soil by action of the vehicle at points A and B was considered as strip loading with width equal to  $0.5 \text{ m}$  (i.e., vehicle's wheel width =  $0.5 \text{ m}$ ). Soil condition before loading was considered as normally consolidated, hence, Overconsolidation ratio (OCR) and Pre-overburden pressure (POP) were taken to be equal to  $1.0$  and  $0.0$  respectively.

Additional assumptions that were made included the following: (1) effect of surface cover such as fallen leaves, weeds, branches, etc., are neglected, (2) soil condition is uniform and same both in root-free-soil and rooted-soil, implying that increase in bearing capacity is due to the presence of roots only and (3) roots mat is considered as a geotextile mat with uniform thickness. PLAXIS updated mesh procedure for studying deformation induced on reinforced structures was adopted. From simulation results, stresses beneath the wheels at different depths of the root-free soil were compared to that of rooted-soil, whilst axial stress in roots mat was compared to tensile stress of roots measured in the laboratory. Load-displacement curves of the centre point of the rut bottom in both root-free and rooted soils were plotted. Effects of roots in the soil-wheel system were estimated as the difference in conditions in root-free and rooted soils.

#### 5.4.2.2 Other cases

Effect of varying mesh height  $h$  on the load-displacement curve of the root-free soil was investigated by considering values of  $h$  equal to  $3 \text{ m}$ ,  $2 \text{ m}$ , and  $1 \text{ m}$ . Simulations were

performed by developing three study cases to represent each of the above. Size of the initial soil mesh was taken to be 5 m wide and 3m high having 3 layers of 1 m high (Fig. 5.32).

**Study case 1** - soil layers A, B, and C were assigned the same soil parameters (see parameters for compactible Lobith loam in table 5.8). This represented a mesh height of 3 m.

**Study case 2** - soil layer C was made much stiffer by having values of soil cohesion and pre-consolidation stress ten times as high as that assigned to layers A and B specified in study case 1 (all other soil parameters were maintained). In this case, mesh height was equal to 2 m.

**Study case 3** - soil layers B and C were made stiffer than layer A (as described in study case 2), hence representing a mesh height of 1 m.

Further, effect of varying mesh width on the load-displacement curve was simulated by considering mesh width equal to 4 m, 5 m and 6 m.

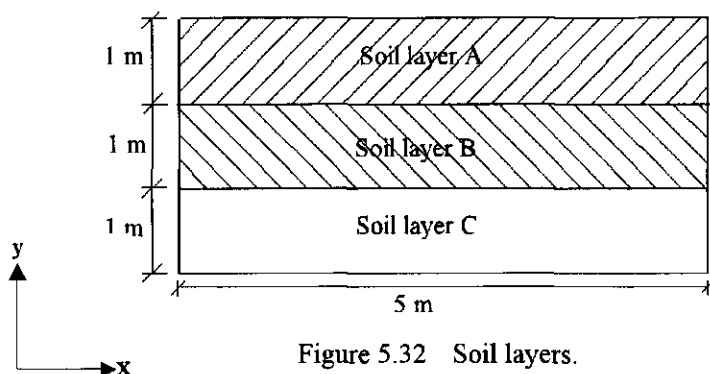


Figure 5.32 Soil layers.

In the rooted soil mesh, the following aspects of the soil-root system were also studied:

- (1) effect of varying root mat's stiffness  $\xi_{\text{root}}$  (with bending stiffness of root mat = 0)
- (2) bending resistance of individual roots
- (3) depth of placement of root mat
- (4) inclusion of interface elements between root mat and soil.

### 5.4.3 Results

#### 5.4.3.1 Reference case

Load-displacement curves showing relationship between load application and formation of ruts are shown in figure 5.33. Improvement in load bearing capacity of the soil as a result of the inclusion of roots was estimated as the difference in applied load needed to cause the same rut depth in both the rooted and root-free soils. At a rut depth of 0.1 m, improvement in load bearing capacity of the soil due to the inclusion of the root mat was estimated to be approximately 10%. This is indicated by the broken lines.

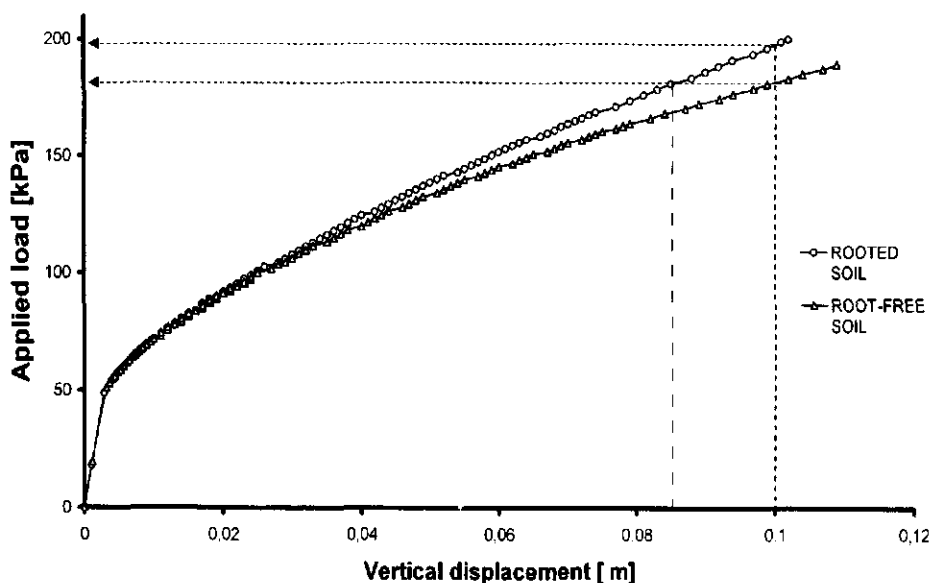


Figure 5.33 Load-displacement curves of rooted and root-free soils.

Inspection of plastic points within the meshes showed that compaction occurs both within the root-free and rooted soils after deformation. Deformed meshes and diagrams showing directions of principal stresses in the soil are as shown in figure 5.34 and figure 5.35 respectively.

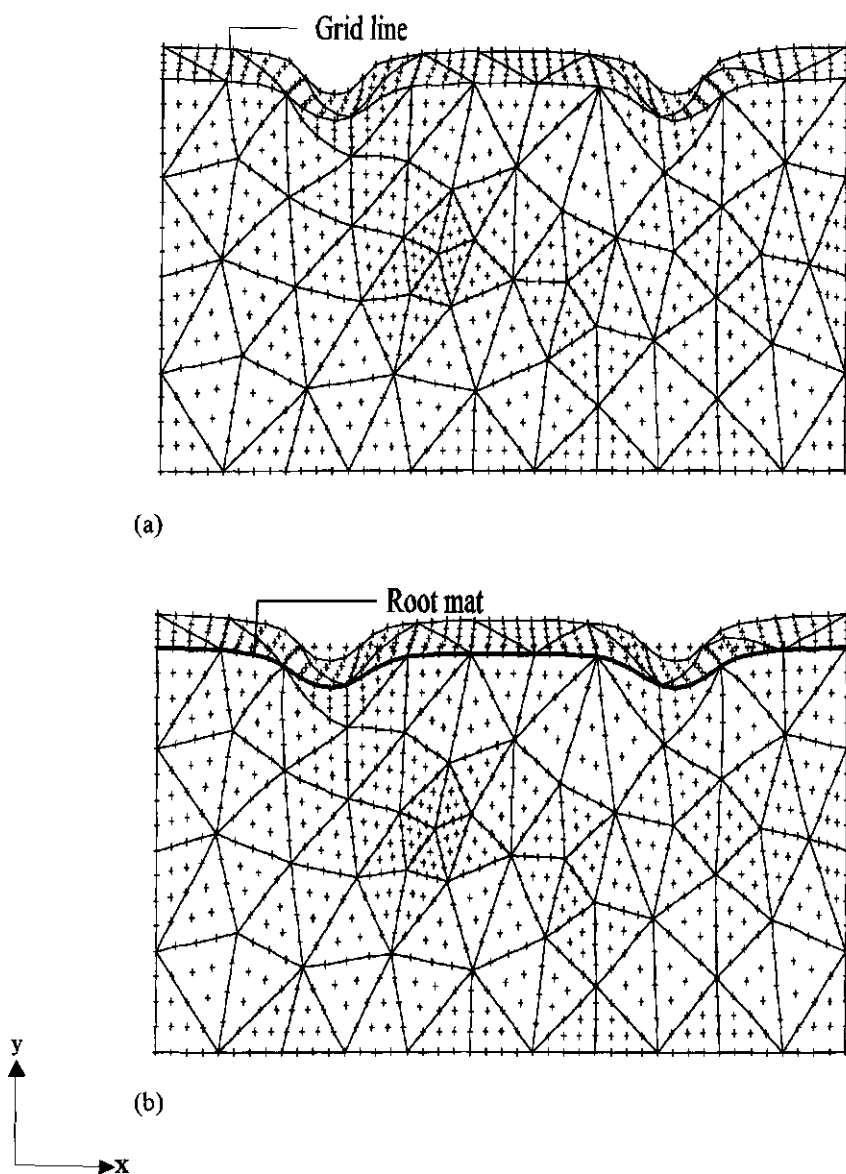
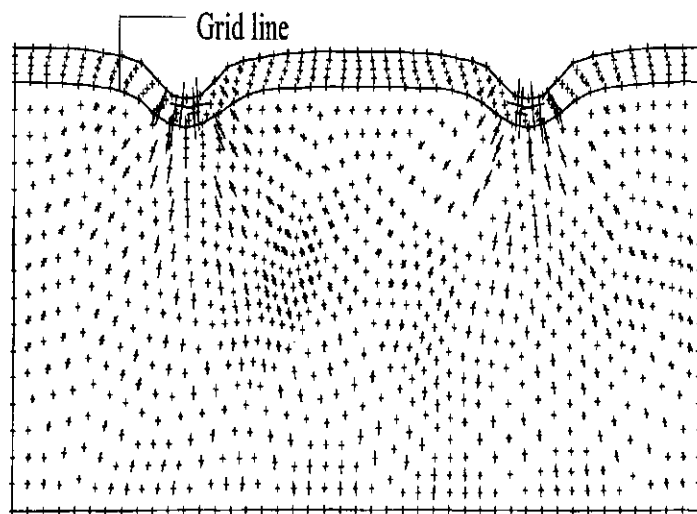
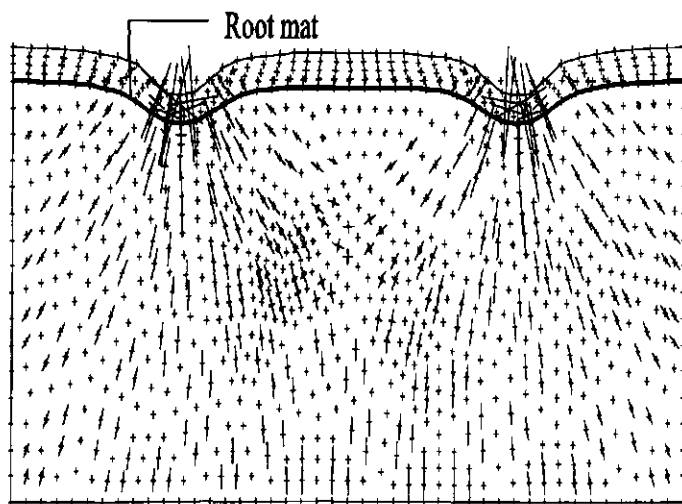


Figure 5.34 Deformed mesh: (a) root-free soil and (b) rooted soil.





(a)



(b)

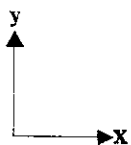


Figure 5.35 Direction of principal stresses: (a) root-free soil and (b) rooted soil.

Comparison of stresses under the centre of the vehicle wheel in the root-free soil and rooted soil was done by considering vertical stresses below the grid line in the former and root mat in the latter. This is shown in figure 5.36.

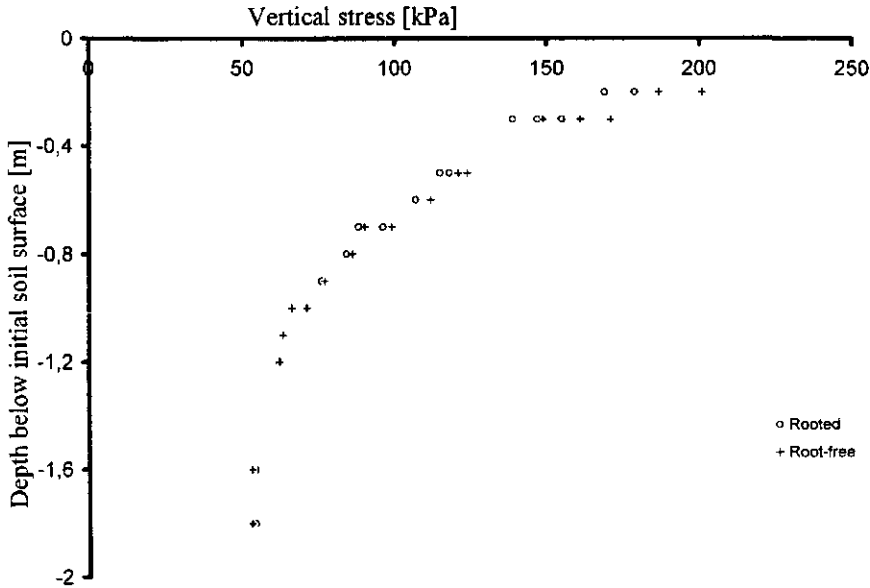


Figure 5.36 Vertical stresses under the centre of a wheel plotted against depth below the initial soil surface.

Figure 5.37 shows the axial force exhibited by the root mat. An extreme axial force of  $29.44 \text{ kN m}^{-1}$  was found by PLAXIS. Extreme tensile stress in the root mat was therefore calculated by dividing the extreme axial force (calculated from PLAXIS) by the thickness of root mat. This was found to be  $6.54 \text{ MPa}$ . This value of the calculated tensile stress of the root mat indicates that indeed failure stress of the root mat was not attained during the simulation.

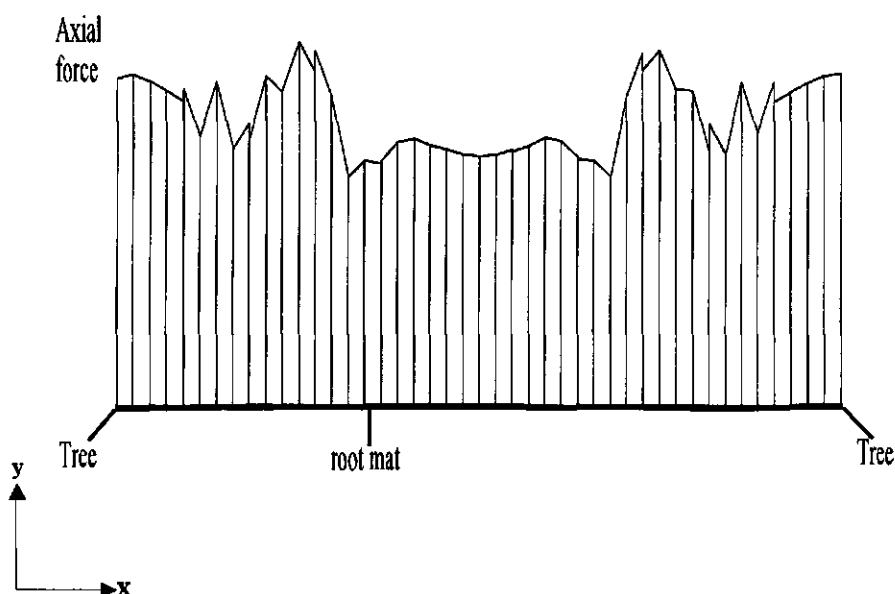


Figure 5.37 Axial force in root mat plotted against distance between two trees.

#### 5.4.3.2 Other cases

From the simulation results it was found that depth of rut formed in the soil depended on the height of the soil mesh. The highest rut depth was therefore observed in study case 1 where mesh height was equal to 3 m. This was followed by study case 2 (mesh height = 2 m), and then study case 3 (mesh height = 1 m), for the same applied load. These are shown in figure 5.38. Reinforcement effect of the root mat was found to increase with increasing root mat stiffness (figure 5.39). Under this circumstance rut depth tends to decrease.

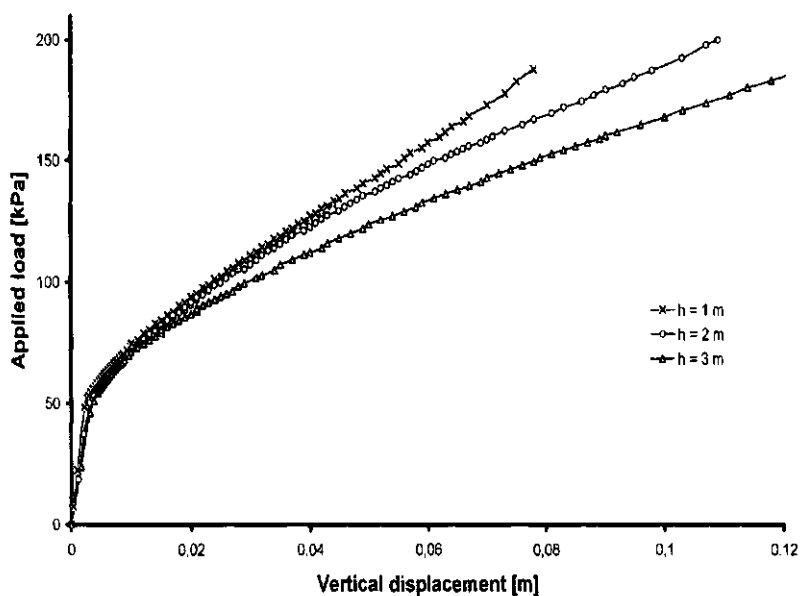


Figure 5.38 Effect of mesh height on rut formation in the root-free soil.

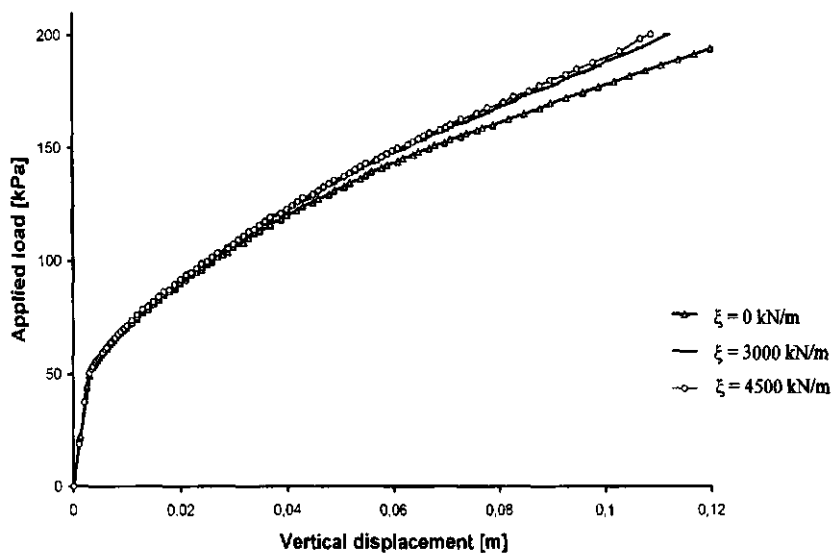


Figure 5.39 Effect of increasing root mat stiffness  $\xi$  on rut formation in the rooted soil.

Magnitude of soil reinforcement was found to decrease with increasing depth of placement of the root mat from initial soil surface. This is shown in figure 5.40.

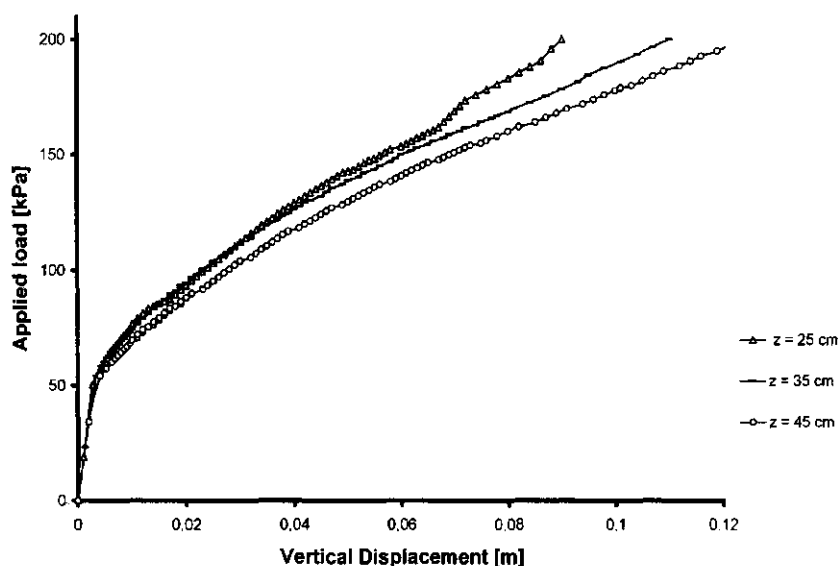


Figure 5.40 Effect of root reinforcement with respect to increasing depth of placement of root mat  $z$  from the initial soil surface

Further calculations were done to simulate roots with non-zero bending resistance (i.e., thick roots). Bending resistance of individual root was studied by modelling the root as a horizontal beam rather than as a geotextile. One thick root per metre of the distance perpendicular to the ruts was considered. The beam was given a bending resistance equal to the bending resistance of the root when its diameter is equal to 0, 5, 8, 10, 15 and 20 cm respectively. The horizontal beam was fixed at both ends (i.e., the left and right grid sides). Relationship between rut depth and root thickness is shown in figure 5.41. Vertical stresses in the soil under the centre of the vehicle's wheel (specifically below the root) were also found to decrease with increasing thickness of the root. Figure 5.42 shows the vertical stresses under the centre of the imposed load in the rooted soil with a root thickness of 15 cm and the root-free soil. This figure shows that at a depth of 30 cm below the initial soil surface, stresses developed in the rooted soil are reduced to about 50% of

the stresses developed in the root-free soil. Introduction of interface elements in the simulations involving the rooted soils did not produce much effect on the load-displacement curves. This may be attributed to the lower magnitude of applied load used.

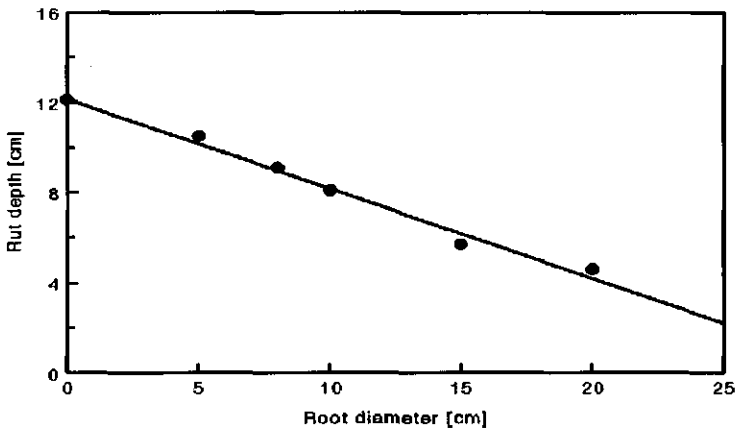


Figure 5.41 Effect of increasing root thickness on rut formation below the centre of a vehicle wheel.

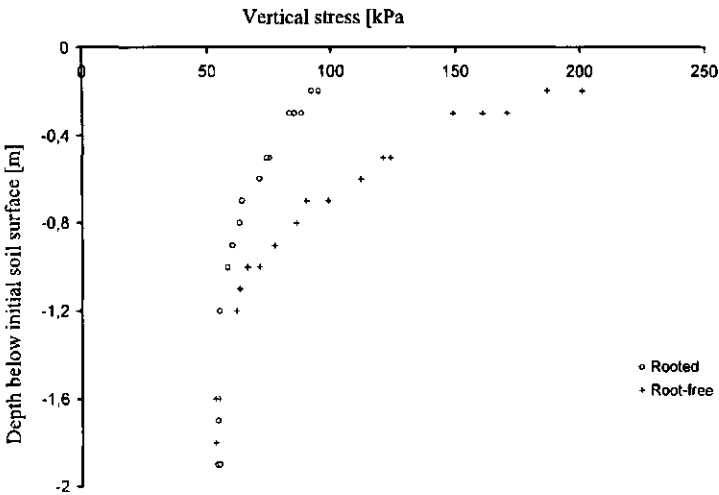


Figure 5.42 Vertical stresses under the centre of a vehicle wheel in the a rooted soil (root thickness = 15 cm) plotted against depth below initial soil surface.

Simulations conducted in this study were mainly based on a single passage of a forestry vehicle on a soil which may be rooted or without roots (root-free). In these investigations, updated mesh analysis was used to ensure that influence of geometry change of the mesh on equilibrium conditions during deformation are automatically accounted for by PLAXIS. Mesh height and width correspond to soil depth and distance between tree rows respectively. In the rooted soil, combined effect of the roots in the soil was initially modelled as root mat exhibiting tension membrane effect. In this regard the root mat acts to reduce the magnitude of vertical stresses which might be imposed on the sub-grade by the presence of the wheel load (see section 5.1.3.1). To achieve this it was necessary to provide firm anchorage of the root mat outside the loaded area (figure 5.31).

The assumptions made in section 5.4.2 ensured that increase in bearing capacity in the rooted soil was due solely to the presence of the roots mat. In fact, such condition is almost impossible to achieve in the laboratory or field due to factors such as differences in rooting density, presence of organic matter, etc. Considering load-displacement curves of the rooted and root-free soils, it was realised that tensile strength in the root mat was not effectively mobilized until a point was reached where a certain magnitude of load is applied. After this point, higher load was required to be applied to the rooted soil in order to produce the same rut depth as that induced in the root-free soil. These characteristics exhibited by the load-displacement curves indicate that mobilization of tensile strength in the roots mat actually becomes effective at increasing load application or rut depth.

This finding is in agreement with results on reinforced soils published by a number of researchers including Burd and Brocklehurst (1990), Gourc (1993). Extreme longitudinal stress of the root mat calculated by PLAXIS was found to be lower than the longitudinal failure stress found in beech roots. Longitudinal failure stress of beech roots found by Liu (1994) in the laboratory produced a value of  $24 \pm 1.58$  MPa, which is approximately four times higher than the stress value calculated from PLAXIS. This therefore justifies the use of an initial elastic modulus for the simulated roots.

Increasing the thickness of the root may be considered to be equivalent to increasing the concentration of the reinforcement. Simulation of the bending effect of roots (i.e., with

non-zero bending resistance) conducted in this study showed that an increase in root thickness was associated with a decrease in rut depth. This signifies an increase in the soil strength. This finding confirmed some of the previous studies published by Gray and Ohashi (1983). It is however in contrast to the findings published by Shewbridge and Sitar (1989) who suggested that increasing strength of reinforced soils may not necessarily be caused by increase in concentration of the reinforcement. Large reduction in vertical stresses observed in the rooted soil under the root may be attributed to increase in root bending resistance brought about by increase in root thickness.

From this studies it was also found that the magnitude of reinforcement provided by roots depended on the depth of placement of the root from the initial soil surface. Increase of soil strength provided by the root was found to be completely lost when its depth of placement exceeded 45 cm. In studying the effect of mesh height on the rut formation (in the root-free soil), it was necessary to divide the soil mesh into three layers in order to minimize effects resulting from patterns of the mesh grid. Unlike mesh height, mesh width did not show any remarkable effect on rut formation. Introduction of an interface between the soil and the root mat had very little effect on the load-displacement curve. This may be due to the small magnitude of input load (i.e., wheel load).

#### 5.4.5 Conclusions

From the above analysis, it is concluded that the presence of a root mat in the soil increases the soil's load bearing capacity, and the effects can adequately be modelled by PLAXIS. Improvement of about 10% was found at rut depth of 0.1 m considering wheel load, wheel width, and root mat stiffness of 200 kPa, 0.5 m and 4500 kN m<sup>-1</sup> respectively. Extreme longitudinal stress of beech root mat calculated by PLAXIS in the reference case was found to be 6.54 MPa. Laboratory measurements conducted by Liu (1994) found the longitudinal failure stress of beech roots to be  $24 \pm 1.58$  MPa. This is approximately 4 times the stress value calculated from PLAXIS, implying that the FEM (Finite Element Methods) calculations, carried out in this thesis, are justified. Simulation of the bending resistance of an individual root showed that root thickness plays an important role in root contribution to improving the bearing capacity of the soil. Rut depth and vertical stresses in the soil under the centre of load application (i.e., wheel) were found to decrease with



increasing thickness of the root mat. At a depth of 30 cm below the initial soil surface, stresses in the rooted soil (root thickness = 15 cm) were found to be reduced by about 50% of that found in the root-free soil. Inclusion of interface element had no remarkable effect on the load-displacement curves of the rooted soil. The study also showed the following: (1) reinforcement effect increases with increasing stiffness of the reinforcing material and decreases with increasing depth of placement of the reinforcement from the initial soil surface and (2) rut depth increases with increasing mesh height.

Though mechanized field operation has contributed immensely towards production in agriculture, some of its processes have been subjected to constant criticisms due to their impact on the environment, especially true for forest soils. The extent of damage caused to the soil by these processes are commonly associated with factors such as the type of machinery involved (size and weight), prevailing soil conditions, etc. However, beside these processes, there also exist some factors such as bush fire, population pressure, and unsustainable forest practices that have been identified as equally (if not more) disastrous to the soil. In this study attempts were made to throw more light on the role played by tree roots in stabilizing or improving soil strength. This role among others has contributed tremendously to an increase in root studies within the last two decades. This thesis also revealed that, although increase in soil strength may depend on mechanical properties of the reinforcement (which in this study are roots), important associated soil factors such as soil water, soil organic matter, activities of soil micro-organisms, etc. (see chapter 2) need to be thoroughly considered.

The contribution of tree roots to increase in soil strength is clearly manifested in soft forest soils where a rut easily forms during the passage of field vehicles. Investigations on the suitability of roots for use as soil reinforcements have shown that root potential for reinforcing the soil will depend among others on the root mechanical properties and factors associated with root dimensions, distribution, etc. Mechanical properties of roots being used in soil-root models consisted of tensile and shear properties. Published data on root mechanical properties has however shown wide variations and spread both within the same root species and among different root species. Interestingly, these strength values are seen to conform to a particular range (i.e., within certain minimum and maximum values) which makes it less difficult in proposing an average strength value that will be suitable for use in models involving roots.

Laboratory measurements of the tensile strength of roots are seen to be a tedious operation considering the high potential of root failure close to the clamping devices and root slippage. In such instances, the experimental results are discarded and new experiments are required to be performed. Attempts have been made to provide answers to a number of research questions raised at the beginning of this study. Comparisons of the spread of

failure stress values within root pairs and their associated diameter classes showed that stress values within root pairs are closer to each other than in their corresponding diameter classes. This outcome provided the opportunity to use the idea of root pairs to measure failure stresses and maximum stresses of roots which have been very illusive during the past years. Average failure stress of roots with diameters in the range of 4.0 mm to 12.0 mm was found to be 20 MPa (standard deviation = 4.1 MPa). From these experiments, the root diameter did not show a pronounced effect on failure stresses and failure strains. Cyclic loading experiments conducted with the roots showed that the number of loading cycles before root failure depends on the applied stress level. Plastic strain increment of individual root pieces was found to decrease with an increasing number of loading cycles and increases with an increasing percentage stress level. On the other hand, overall stiffness modulus was found to increase with increasing number of loading cycles and to decrease with increasing percentage stress level. Investigating the effect of elongation rate on tensile stress values, it was found that root tensile values increased for about 8-20% for an increase in the rate of elongation from 10 mm/min to 400 mm/min. These results will play a crucial role especially in soil-root deformation models because in such models it will be expected that tensile properties of the root are measured in such a way that the rate of elongation used is very close to what is experienced by roots in forest soils when passed over by a field vehicle. Although this would be very difficult to achieve on tensile measuring machines in most laboratories, at least attempts could be made to use the highest elongation rate allowable. Other factors known to affect results of measured root strength properties include: (1) season, (2) diameter of thin roots, (3) clamping procedure and (4) root preparation before measurement.

In this thesis the finite element code known as PLAXIS (version 7.0) was used in conducting the simulations. Finite element approach was used because of its versatility. In addition to the above, PLAXIS version 7.0 takes precedence over other softwares due to its: (1) full automatic mesh generation ability and (2) improved user interface, etc. Modelling the soil-wheel system is generally seen to be complex and difficult, and the accuracy of its output depends highly on the application of appropriate constitute equations. The information on the performance of soil reinforced by geotextiles/fibres was therefore necessary due to the limited information found on the study of soil reinforced by tree roots. Their associated models/equations (see chapter 5) were as a matter of fact rich sources of information which played useful roles in designing the PLAXIS simulation

model used in this thesis.

Simulations performed in this thesis were exclusively based on single loading of rooted/root-free forest soil. Part of the PLAXIS calculations illustrated the stresses set in the soil due to the action of the passing wheel load. In practice, it is clearly seen that such loading will be repetitive. This was however not considered in this study. In future studies it should be possible to model repetitive soil loading by PLAXIS. With regards to soil-vehicle interactions, different modelling approaches or methods are often likely to be encountered. It was noticed that such situations are unavoidable since some researchers try as much as possible to keep their formulations simple either to make the modelling situation clearer or to avoid the complex calculations that might develop. Such occurrences were also noticed during the soil-root reinforcement simulations. Among the basic controversies encountered was the choice of soil loading. By considering the soil-wheel contact area as a circular plate, the loading is taken to be axisymmetric, otherwise plane strain is assumed. However it has been argued in some published papers concerning soil-vehicle interactions that such loading could not be treated as axisymmetric if there is an evidence of soil deformation by the vehicle's wheels. The plane strain approach used in this thesis therefore represents a simplification of the loading that would occur in practice.

Results obtained from the simulations showed that improvement in soil bearing capacity provided by tree roots can adequately be modelled by PLAXIS. In these simulations, interest was placed on the situation where no significant slippage occurs between the root mat and the soil. Initial stiffness of the root mat,  $E_{\text{initial}}$ , was estimated from overall stiffness modulus,  $E_{\text{overall}}$ , found in previous root experiments.  $E_{\text{initial}}$  was taken to be approximately 5 times  $E_{\text{overall}}$  (ie.,  $E_{\text{initial}} \approx 5 E_{\text{overall}}$ ). Simulation results showed that the presence of a root mat in the soil greatly improves the soil bearing capacity. Improvement of about 10 % was found at a root depth of 0.1 m considering wheel load, wheel width and root mat stiffness of 200 kN/m<sup>2</sup>, 0.5 m and 4500 kN/m respectively. Extreme longitudinal stress of beech root mat calculated by PLAXIS in the reference situation was found to be 6.54 MPa. Laboratory measurements conducted by Liu (1994b) found the longitudinal failure stress of beech roots to be  $24 \pm 1.58$  MPa and therefore justifies the initial elastic modulus used for the simulated roots, because in the laboratory root experiments root failure occurred during loading, whilst that was not the case in the

simulations reported in this thesis. Simulation of bending effect of the root showed, that root thickness plays an important role in the root mat contribution to improving the soil bearing capacity. Increasing thickness of root was found to decrease rut depth. Vertical stresses beneath the root mat were also found to decrease with increasing root thickness. At a depth of 30 cm below the initial soil surface, stresses developed in the rooted soil (root thickness = to 15 cm) were found to be reduced by about 50% of the stresses developed in the root-free soil. In the above bending simulations, the elastic modulus in bending was estimated from elastic modulus in tension. This was due to the fact that the scatter of data on elastic modulus was so large that elastic modulus in bending could not be differentiated from elastic modulus in tension. Inclusion of interface element and varying width of the mesh had no remarkable effect on the load-displacement curve. The study also showed the following: (1) reinforcement effect increases with increasing stiffness of the reinforcement and decreases with increasing depth of placement of the reinforcement from the soil surface and (2) rut depth increases with increasing mesh height (soil depth). Although the models/equations discussed at the beginning of this study were helpful in designing the above soil-root reinforcement simulations, it was still considered impractical to compare data from the above models with the simulation output produced by PLAXIS because of the simple nature of their formulations. Some of these weaknesses are discussed below.

This study revealed that in soil-fibre systems, a limiting value of pull out resistance can theoretically be studied from the knowledge of the normal stress exerted on the reinforcement (see equation 5.12 to 5.14). However such simple calculations may not wholly be applicable to the soil-root reinforcement systems because: (1) the effective normal stress may be altered by soil-root interaction and (2) roots surfaces may not be smooth, that is, may contain root hairs. Pull out experiments were not carried out in this thesis because it was found that the resemblance between root pull out and soil-root behaviour in the soil-wheel systems was very poor. Roots contributions to improvement in soil strength have been studied using two main approaches: (1) bearing capacity approach (adopted in this thesis) and (2) soil-root in-situ shear strength approach. In the latter, the root contribution to an improvement in soil strength is calculated as an increase in shear strength resulting from the root inclusion. Under such a condition it is expected that indirect roles played by soil factors such as soil organic matter, mycorrhiza, mucilages and exudates produced by soil microorganisms, etc., are eliminated. However

most of the models used in the estimation of root contribution to increase in soil strength failed to take the above soil factors into account. It therefore seems reasonable to believe that since these effects are not isolated, the estimated increase in soil strength may not be due to roots alone, but also to certain unknown factors which may include those mentioned above. In these in-situ experiments, estimation of root contribution to soil strength is partly based on the development of the shear zones which are known to be of very little importance in soil-wheel systems due to the so called stable soil behaviour. Apart from the above factors, results of soil-root in-situ shear experiments are also known to be influenced by the dimensions of the test apparatus. The model provided by Houlsby and Jewell (1990), (see equation 5.43) can not be wholly applied, because in their model the principal function of the reinforcement is to carry shear stresses which would otherwise be applied to the soft sub-grade soil. Under this condition the developed shear stresses in soil automatically put the reinforcement into tension which makes the roughness of the reinforcement very important rather than anchorage as seen in this thesis. Comparison of curves from pressure-sinkage data (i.e., equations 5.36 and 5.37) and PLAXIS output showed great differences (Barneveld, 2000). The above sinkage equations are normally developed for small rut depths.

## **Further studies**

A number of questions still remains to be answered regarding the loading of soil-root systems. For example: (1) what strain can a root undergo before its biological functions are affected or completely disrupted? (2) the effect of a decreasing root diameter during elongation on soil-root interfacial stresses; etc. Apart from these, very little information is currently available on the effect of root: (1) patterns, (2) dimensions, (3) shape and (4) surface structures e.g., hair, mycorrhiza, etc., on its contribution to soil reinforcement.

During thickening of roots, soil closer to these roots may be compacted. On the other hand, when water is absorbed by roots, the surrounding soil may dry and shrink. These activities by roots may affect soil strength, but very little studies have been conducted on these issues. In practice, soil-root reinforcement should be analysed as a three-dimensional problem. Achieving this in simulations used to be very complex and will also be limited by computer resources. Current advances in computer technology have however enhanced the possibility of moving from 2-dimensional modelling to 3-

dimensional modelling. These 3-dimensional modelling techniques will improve simulation results and should be considered in future studies.

## REFERENCES

- Abe, K. and R.R. Ziemer, 1991. *Effect of tree roots on a shear zone: modelling reinforced shear stress*. Can. J. For. Res., Vol. 21: 1012-1019.
- Adanur, S., S. Mallick and H. Zhai, 1996. *Analysis of geotextile-soil interaction in pull-out tests*. In: H. Ochiai, N. Yasufuku, and K. Omine (eds), *Earth reinforcement*, Balkema, Rotterdam, Vol. 1: 3-8.
- Agarwal, B.V. and L.J. Broutman, 1980. *Analysis and performance of fiber reinforced composites*. New York, Wiley, 355 pp.
- Akin, J.E., 1986. *Finite element analysis for Undergraduate*. Harcourt Brace Javanovich, New York, 319 pp.
- Atkinson, D., 1983. *The growth, activity and distribution of the fruit tree root system*. In: D. Atkinson, K.K.S. Bhat, M.P. Coutts, P.A. Mason, and D.J. Read (eds), *Developments in Plant and Soil Sciences*, vol 7, Martinus Nijhoff / Dr. W. Junk Publishers, 23-35.
- Bailey, A.C., C.E. Johnson, R.L. Schafer, 1984. *Hydrostatic compaction of agricultural soils*. Transactions of the ASAE: 952-955.
- Bailey, A.C., C.E. Johnson, R.L. Schafer, 1986. *A model for Agricultural soil compaction*. J. Agric. Engng Res., 33: 257-262.
- Bailey, A.C., T.A. Nichols and C.E. Johnson, 1988. *Soil stress determination under wheel loads*. Transactions of the ASAE, Vol. 31(5): 1309-1314.
- Bailey, A.C. and C.E. Johnson, 1989 *A soil compaction model for cylindrical stress states*. Transactions of the ASAE, Vol 32(3): 822-825.
- Barneveld, A., 2000. *FEM based soil stress and strain analyses aimed at plant growth factors*. PhD. Thesis, Wageningen University, Wageningen, The Netherlands, 222 pp.
- Barracough, P.B., A.H. Weir and Kuhlmann, 1991. *Factors affecting the growth and distribution of winter wheat under UK field conditions*. In: McMichael, B.L. and H. Persson (Eds.), *Developments in agricultural and managed-forest ecology 24: Plant roots and their environment*, 410-417.
- Beekman, F., 1987. *Soil strength and forest operations*. PhD. Thesis, Wageningen Agricultural University, Wageningen, The Netherlands, 167 pp.
- Bell, A.D., 1991. *Plant form*. Oxford University Press, New York, 341 pp.



- Bengough, A.G., C.E. Mullins and G. Wilson, 1997. *Estimating soil frictional resistance to metal probes and its relevance to the penetration of soil by roots*. European Journal of Soil Science, 48: 603-612.
- Berrie, G.K., A. Berrie and J.M.O. Eze, 1987. Tropical Plant Science. John Wiley and Sons, Inc., New York, 410 pp.
- Blackwell, P.G., K. Rennolls and M.P. Coutts, 1990. *A root anchorage model for shallowly rooted sitka spruce*. Forestry, 63: 73-91.
- Bowen, A.D. and A.D. Rovira, 1991. *The rhizosphere: The hidden half of the hidden half*. In: Y. Waisel, A. Eshel, and U. Kafkafi (Eds), Plant roots: The hidden half. Marcel Dekker Inc., New York, 641-669.
- Böhm, W., 1979. Methods of studying root systems. Springer-Verlag, Berlin, 141 pp.
- Bragg, P.L., G. Govi and R.Q. Cannell, 1983. *A comparison of methods, including angled and vertical minirhizotrons, for studying root growth and distribution in a spring oat crop*. Plant and Soil, 73: 435-440.
- Brinkgreve, R.B.J. and P.A. Vermeer (Eds), 1998. Plaxis. Finite element code for soil and rock plasticity. Balkema, Rotterdam.
- Burd, H.J. and C.J. Brocklehurst, 1990. *Finite element studies of the mechanics of reinforced upaved roads*. In: G. den Hoedt Geotextiles, geomembranes and related products, Balkema, Rotterdam, 217-221.
- Cannon, W.A., 1911. The root habits of desert plants. Carnegie Institution, Washington, 96 pp.
- Chang, D.T., C. Chen and Y. Fu, 1996. *The creep behaviour of geotextiles under confined and unconfined conditons*. In: H. Ochiai, N. Yasufuku, K. Omine (eds), Earth reinforcement, Balkema, Rotterdam, Vol. 1: 19-24.
- Chen, T.C., R.H. Chen, Y.S. Lee and J.C. Pan, 1996. *Dynamic reinforcing effect of reinforced sands*. In: H. Ochiai, N. Yasufuku, K. Omine (eds), Earth reinforcement, Balkema, Rotterdam, Vol. 1: 25-28.
- Chen, L.T. and H.G. Poulos, 1997. *Piles subjected to lateral soil movements*. Journal of Geotechnical and Geoenvironmental Engineering, Vol. 123, No. 9, September, 802-811.
- Chi, L., S. Tessier, E. Mckyes, C. Laguë, 1993. *Modelling mechanical behaviour of agricultural soils*. American Society of Agricultural Engineers, 36(6): 1563-1570.
- Chi, L., S. Tessier, C. Laguë, 1993. *Finite element modelling of soil compaction by liquid manure spreaders*. American Society of Agricultural Engineers, 36(6): 637-644.

- Clowes, F.A.L., 1968. *Anatomical aspect of structure and development*.  
In: Whittington, W.J. (Editor), Root growth, Butterworths, London, 3-19.
- Commandeur, P.R. and M.R. Pyles, 1991. *Modulus of elasticity and tensile strength of Douglas-fir roots*. Can. J. For. Res., Vol. 21: 48-51.
- Cook, R.D., D.S. Malkus, M.E. Plesha, 1989. Concepts and applications of finite element analysis. John Wiley and Sons, New York, 629 pp.
- Coutts, M.P. and G.J. Lewis, 1983. *When is the structural root system determined in Sitka Spruce?* Plant and Soil, 71: 155-160.
- Coutts, M.P., 1983. *Root architecture and tree stability*. Plant and Soil, 71: 171-188.
- Coutts, M.P., 1986. *Components of tree stability in Sitka Spruce on peaty gley soil*. Forestry Vol. 59, No. 2: 174-197.
- Craul, P.J., 1993. Urban soil in landscape design. John Wiley and Sons, Inc., 385 pp.
- Das, B. M., 1995. Principles of foundation engineering. PWS Publishing company, Boston, 828 pp.
- Davis, H.E., G.E. Troxell, G.F.W. Hauck, 1982. The testing of engineering materials. McGraw-Hill Book Company, New York, 478 pp.
- De Willigen, P. and M. van Noordwijk, 1987. Roots, plant production and nutrient use efficiency. Landbouwniversiteit, Wageningen, 280 pp.
- De Groot, M.T., G. den Hoedt, A.H.J. Nijhof, 1988. *Dutch progress in the standardization of geotextile test methods*. International geotechnical symposium on Theory and Practice of Earth Reinforcement, Fukuoka, Japan, 75-80.
- Deans, J.D. and Ford, E.D., 1983. *Modelling root structure and stability*. Plant and Soil, 71: 189-195.
- Desai, N.B., H.N. Shah, L.M. Shah and H.P. Pandya, 1988. *Creep behaviour of indigenous geosynthetic material*. Proceedings of the Geotextiles Conference held at the Indian Institute of Technology: Reinforced soil and geotextile. Bombay, India, 8-9 December, A.11 - A.15.
- Duncan, J.M., 1996. *State of the art: Limit equilibrium and finite-element analysis of slopes*. Journal of Geotechnical Engineering: 577-593.
- Esau, K., 1977. Anatomy of seed plants. John Wiley and Sons, New York, 550 pp.
- Ess, D.R., D.H. Vaughan, J.V. Perumpral, 1988. *Crop residue and root effects on soil compaction*, Transactions of the ASAE, Vol. 41(5): 1271-1275.

- Fagan, M.J., 1992. Finite element analysis: Theory and practice. John Wiley and Son, Inc., New York, 315 pp.
- Fannin, R.J. and O. Sigurdsson, 1996. *Field observations on stabilization of unpaved roads with geosynthetics*, Journal of Geotechnical Engineering, 544-552.
- Fenner, R. T., 1975. Finite element methods for engineers. The Macmillan Press, London, 171 pp.
- Fitter, A.H., 1991. *Root system architecture*. In: D. Atkison (ed) Plant root growth, an ecological perspective, Blackwell scientific publications, London, 229-243.
- Florkiewicz, A., 1990. *Bearing capacity of subsoil with a layer of reinforced earth*. In: G. den Hoedt (ed), Geotextiles, Geomembranes and related products, Rotterdam, pp. 162.
- Fogel, R., 1983. *Root turnover and productivity of coniferous forests*. In: D. Atkinson, K.K.S. Bhat, M.P. Coutts, P.A. Mason, and D.J. Read (eds) Developments in Plant and Soil Sciences, vol 7, Martinus Nijhoff / Dr. W. Junk Publishers, 75-85.
- Foster, R.C., A.D. Rovira and T.W. Cook, 1983. Ultrastructure of the root-soil interface. The American Phytopathological Society, U.S.A., 157 pp.
- Foth, H. D., 1990. Fundamentals of soil science. John Wiley and Son, New York, 360 pp.
- Froehlich, H.A., 1989. *Soil damage, tree growth, and mechanization of forest operations*. Proceedings Seminar FAO/ECE/ILO on the impact of mechanization of forest operations on the soil, Louvain La Neuve, Belgium, 11-15 th September, 77-82.
- Fusseder, A., 1983. *A method for measuring length, spatial distribution and distances of living roots in situ*. Plant and Soil, 73: 441-445.
- Gerard, C.J. P. Sexton and G. Shaw, 1982. *Physical factors influencing soil strength*. Agronomy Journal, Vol. 72: 875-879.
- Gill, W.R. and G.E. Vanden Berg, 1967. Soil dynamics in tillage and traction. Agricultural handbook No. 316, ARS, United States Department of Agriculture, 511 pp.
- Giroud, J. and L. Noiray, 1981. *Geotextile-reinforced unpaved road design*. Journal of the Geotechnical Engineering Div. Proceedings ASCE, Vol. 107, No. GT9: 1233-1254.
- Gliński, J. and J. Lipiec, 1990. Soil physical conditions and plant roots. CRC Press, Florida, 250 pp.
- Goss, M.J., 1987. *The specific effects of roots on the regeneration of soil structure*. In: G. Monnier, and M.J. Goss (editors), soil compaction and regeneration. Published for the commission of the European Communities by A.A. Balkema, Rotterdam, The Netherlands, 145-155.

- Gourc, J.P., H. Perrier and G. Riondy, 1982. *Cyclic loading of a two layer soil system reinforced by geotextile*. Second International Conference on Geotextiles, Vol 2, August 1-6, U.S.A., 399-404.
- Gourc, J.P., 1993. *Keynote lecture: Geosynthetics in embankments, review of theory and practice*. In: H. Ochiai, S. Hayashi and J. Otani (eds), *Earth reinforcement Practice*, Balkema, Rotterdam, 773-797.
- Gray, D.H. and H. Ohashi, 1983. *Mechanics of fiber reinforcement in sand*. Journal of Geotechnical Engineering, vol. 109, No. 3, March, 335-351.
- Gray, D.H., 1991. *Deformation characteristics of reinforced sand in direct shear: Discussion*. Journal of Geotechnical Div., ASCE, 117(11), 1810-1811.
- Greacen, E.L., K.P. Barley and D.A. Farrell, 1969. *The mechanics of root growth in soils with particular reference to the implications for root distribution*. In: Whittington, W.J. (editor), *Root growth*, Butterworths, London, 256-268.
- Greenland, D.J., 1979. *Physics and chemistry of the interface*. In: J.L. Harley and R.S. Russell (eds), *The soil-root interface*, Academic Press, London, 83-98.
- Gupta, C.P. and R. Visvanathan, 1993. *Dynamic behaviour of saturated soil under impact loading*. ASAE, Vol. 36(4): 1001-1007.
- Hamazah, M., B.L. Haines and R.L. Todd, 1983. *A technique for estimating fine root production in the forest ecosystem*. Plant and Soil, 73: 421-423.
- Hoare, D.J., 1979. *Laboratory study of granular soils reinforced with randomly oriented discrete fibres*. International conference on soil reinforcement: reinforced earth and other techniques. Paris 20-21 March, 47-52.
- Harper, J.L., M. Jones and N.R.S. Hamilton, 1991. *Root evolution and problems of analysis*. In: D. Atkison (ed) *Plant root growth, an ecological perspective*, Blackwell scientific publications, London, 3-22.
- Hassiotis, S., J.L. Chameau and M. Gunaratne, 1997. *Design method for stabilization of slopes with piles*. Journal of Geotechnical and Geoenvironmental Engineering, Vol. 123, No. 4, April, 314-323.
- Heij, W. and A.J. Koolen, 1993. *The influence of roots on stress transmission in forest soil*. Proceedings IUFRO meeting S3.0.4, Auburn University, Auburn, AL, U.S.A.
- Henderson, J., 1990. *Damage-controlled logging in managed tropical rain forest in Suriname*. PhD. Thesis, Wageningen Agricultural University, Wageningen, 204 pp.
- Henwood, K., 1973. *A structural model of forces in buttressed tropical rain forest trees*. Biotropica, 5(2): 83-93.

- Hess, C.E., 1968. *Internal and external factors regulating root initiation*. In: W.J. Whittington, (Ed.), *Root growth*, Butterworths, London, 42-53.
- Hettiaratchi, D.R.P. and C.A. Ferguson, 1973. *Stress-deformation behaviour of soil in root growth mechanics*. *J. agric. Engng Res.*, 18: 309-320.
- Higuchi, Y. and Y. Watari, 1990. *Planning and the design method for earth spreading using geotextile on the very soft ground*. In: G. den Hoedt (ed), *Geotextiles, Geomembranes and related products*, Balkema, Rotterdam, pp. 165.
- Hildebrand, E.E., 1989. *The influence of soil compaction on soil function in forest sites*. Proceedings Seminar FAO/ECE/ILO on the impact of mechanization of forest operations on the soil, Louvain La Neuve, Belgium, 11-15 th September, 149 - 159.
- Hirano, I., 1990. *Test on trafficability of a low embankment on soft ground reinforced with geotextiles ground*. In: G. den Hoedt (ed), *Geotextiles, Geomembranes and related products*, Balkema, Rotterdam, 227-232.
- Hird, C.C., 1986. *Stability charts for reinforced embankments on soft ground*. *Geotextiles and Geomembranes*, 4: 107-127.
- Hofer, R., 1991. *Root hairs*. In: Y. Waisel, A. Eshel, and U. Kafafi (eds), *Plant roots the hidden half*. Marcel Dekker Inc., New York, 129-148.
- Houlsby, G.T., G.W.E. Milligan, R.A. Jewell and H.J. Burd, 1989. *A new approach to the design of unpaved roads - Part 1*. *Ground Engineering*, 22(3): 25-29.
- Houlsby, G.T. and R.A. Jewell, 1990. *Design of reinforced unpaved roads for small rut depths*. In: G. den Hoedt (ed), *Geotextiles, Geomembranes and related products*, Balkema, Rotterdam, 171-176.
- Huston, R.L. and C.E. Passerello, 1984. *Finite element methods: An introduction*. Marcel Dekker Inc., New York, 295 pp.
- Hvorslev, M.J., 1970. *The basic sinkage equations and bearing capacity theories*. Technical report M-70-1, U.S. Army Engineer Waterways Experiment Station, Vicksburg, Mississippi, 43 pp.
- Jackson, B.D., 1971. *A glossary of botanic terms*. Hafner Publication Co. Inc., New York, 481 pp.
- Jeffery, R.S. and D.D. Barry, 1997. *Life prediction methodology for composite structures. Part I - Constant amplitude and two-stress level fatigue*. *Journal of composite materials*, Vol. 31, No. 2: 129-157.
- Jeffery, R.S. and D.D. Barry, 1997. *Life prediction methodology for composite structures. Part II - Spectrum fatigue*. *Journal of composite materials*, Vol. 31, No. 2: 158-181.

- Jewell, R.A., 1988. *The mechanics of reinforced embankments on soft soils*. Geotextiles and Geomembranes, 7: 237-273.
- Jewell, R.A. and J.H. Greenwood, 1988. *Long term strength and safety in steep soil slopes reinforced by polymer materials*. Geotextiles and Geomembranes, 7: 81-118.
- Jewell, R.A., 1990. *Revised design charts for steep reinforced slopes*. In: Shercliff, D.A (ed), reinforced embankments: theory and practice, London, Telford, 1 - 27.
- Jones, C.J.F.P., 1988. *Predicting the behaviour of reinforced soil structures*. International Geotechnical Symposium on Theory and Practice of Earth Reinforcement, Fukuoka Japan, 5-7 October, 535-540.
- Jones, J.W., P. Jones, P.A. Everett, 1987. *Combining expert systems and agricultural models: a case study*. ASAE, 1308-1313.
- Jones, A.C., W.L. Bland, J.T. Ritchie and J.R. Williams, 1991. *Simulation of root growth*. In: Hanks, J. and Ritchie, J.T. (Eds), Modelling plant and soil systems, Madison, Wisconsin, U.S.A., 91-123.
- Ju, J.W. and S.J. Son, 1996. *Bearing capacity of sand foundation reinforced by geonet*. In: H. Ochiai, N. Yasufuku, K. Omine (eds), Earth reinforcement, Balkema, Rotterdam, 603-608.
- Juvinall, R.C., 1967. *Engineering consideration of stress, strain, and strength*. McGraw-Hill book Company, New York, 580 pp.
- Kabir, M.H., 1988. *Creep behaviour of geotextile*. *Proceedings of the International Geotechnical Symposium: Theory and practice of earth reinforcement*. Fukuoka, Kyushu, 5-7 October, 111-116.
- Kirby, J.M., B.G. Blunden and C.R. Trein, 1997. *Simulating soil deformation using a critical-state model: II. Soil compaction beneath tyres and tracks*. European Journal of Soil Science, 48: 59-70.
- Klein, L. and B. Franklin, 1994. *Natural resources consumption*. In: Hammond, A.L., D. Estes, and R.T. Livernash (Editors), World Resources 1994-95, Oxford University Press, New York, 3-26.
- Koga, K. and G. Aramaki, 1988. *Finite element analysis of grid reinforcement*. International Geotechnical Symposium on Theory and Practice of Earth Reinforcement, Fukuoka Japan, 5-7 October, 407-411.
- Kolesnikov, V., 1971. *The root system*. Mir publishers, Moscow, 268 pp.
- Koolen, A.J. and H. Kuipers, 1983. *Agricultural soil mechanics*. Springer-Verlag, Berlin, 241 pp.

- Koolen, A.J., 1986. *Deformation and compaction of elemental soil volumes and effects on mechanical soil properties*. Soil & Tillage Research, 10: 5-19.
- Koolen, A.J., 1989. *Strategies to avoid or to reduce detrimental impacts: working techniques for avoiding damage*. Proceedings Seminar on Impact of Mechanization of Forest Operations to the Soil, 11-15 September, 1989, Louvain-la-Neuve, Published by the Ministry of Agriculture, Brussels, Belgium, 235-244.
- Koolen, A.J., P. Lerink, D.A.G. Kurstjens, J.J.H. van den Akker and W.B.M. Arts, 1992. *Prediction of aspects of soil-wheel systems*. Soil & Tillage Research, 24: 381-396.
- Koolen, A.J., 1994. *Soil-machine relations*. Proceedings Forsitrisk Seminar, July 4-8, Feldafing, Fed. Rep. Germany, 11 pp.
- Koolen, A.J., 1996. *Towards inclusion of soil reinforcement by plant roots in soil-vehicle mechanics*. Of-road/machine and Vehicle in Theory and Practice, Proceedings 1st International Conference September 23-24, Wroclaw, Poland, 199-203.
- Koolen, A.J. and J.J.H. van den Akker, 2000. *On the use of agricultural soil data required in soil deformation models*. In: R. Horn, J.J.H. van den Akker and J. Arvidsson (Eds), Subsoil compaction, distribution, Processes and consequences. Catena Verlag GmbH, Germany, 118-125.
- Köstler, J.N., E. Brückner, H. Biebelriether, 1968. *Die Wurzeln der Waldbäume*. Verlag Paul Perey, Hamburg, 284 pp.
- Kramer, P.J. and T.T. Kozlowski, 1960. *Physiology of trees*. McGraw-Hill Book Company Inc., 642 p.
- Kuiper, L.C. and M.P. Coutts, 1992. *Spatial disposition and extension growth of the structural root system of douglas-fir*, For. Ecol. Manage, 47: 111-125.
- Larson, W.E., G.R. Blake, R.R. Allmaras, W.B. Voorhees and S.C. Gupta (Eds), 1989. *Mechanics and related processes in structured agricultural soils*. Proceedings of the 2nd Workshop, St. Paul, Minnesota, 1988. Nato ASI series. Series E: Applied Sciences, Vol. 172. Kluwer, Dordrecht, 273 pp.
- Lerat, P. and P. Unterreiner, 1996. *Experimental analysis of friction between sand and reinforcing elements using ring simple shear tests*. In: H. Ochiai, N. Yasufuku, K. Omine (eds), Earth reinforcement, Balkama, Rotterdam, 77- 81.
- Leshchinsky, D. and D.S. Smith, 1988. *Reinforcement against deep-seated failure: Stability analysis*. International Geotechnical Symposium on Theory and Practice of Earth Reinforcement, Fukuoka Japan, 5-7 October, 419-424.

- Leshchinsky, D., 1993. *Keynote lecture: Issues in geosynthetic-reinforced soil*. In: H. Ochiai, S. Hayashi and J. Otani (eds), *Earth reinforcement Practice*, Balkema, Rotterdam, 871-889.
- Lichtenegger, E. and L. Kutschera-Mitter, 1991. *Spatial root types*. In: McMichael, B.L. and H. Persson (Eds.), *Developments in agricultural and managed-forest ecology 24: Plant roots and their environment*, 359-365.
- Liu, C. and J.B. Evett., 1984. *Soil properties: testing, measurement, and evaluation*. Prentice-Hall, Inc., Englewood Cliffs, New Jersey, 315 pp.
- Liu, J. and Y. Xu, 1992. *The dynamics of grassland soil*. Proceedings of an International Conference of Agricultural Engineering. Oct., Beijing.
- Liu, J., A.J. Koolen and W. Heij, 1994. *The tensile strength of beech and larch roots*. Proceedings 6<sup>th</sup> European ISTVS Conference, Vienna, Austria, September 28-30.
- Liu, J., 1994a. *Roots reinforcing soil*. MSc. thesis Wageningen Agricultural University.
- Liu, J., 1994b. *The effect of dynamic characteristics of beech and larch root strength on trafficability*. 6<sup>th</sup> European ISTVS conference, Vienna, Austria, September 28-30, 12 pp.
- Lôhmus, K., R. Lasn and T. Oja, 1991. *The influence of climatic and soil physical conditions on growth and morphology of Norway spruce roots*. In: McMichael, B.L. and H. Persson (Eds.), *Developments in agricultural and managed-forest ecology 24: Plant roots and their environment*, 233-239.
- Lopes, M.L., 1996. *Pull-out tests for the assessment of soil-geogrids interaction-influence of some mechanical and physical parameters*. In: H. Ochiai, N. Yasufuku and K. Omine (Eds.), *Earth reinforcement*, Balkema, Rotterdam, 89-93.
- MacGregor, C.W., 1950. *Mechanical properties of materials*. In: M. Hetényi (ed), *Handbook of experimental stress analysis*, John Wiley and Sons Inc., New York, 1- 27.
- Macleod, R.D., 1991. *The root apical meristem and its margins*. In: Y. Waisel, A. Eshel and Kafkafi, U. (eds), *Plant roots: the hidden half*. Marcel Dekker Inc, New York, 75-102.
- Maher, M.H. and H. Gray, 1990. *Static response of sands reinforced with randomly distributed fibers*. *Journal of Geotechnical engineering*, vol. 116, No. 11, November, 1661-1677.
- Makarova, O.V., P. Cofie and A.J. Koolen, 1998. *Axial stress-strain relationships of fine roots of beech and larch in loading to failure and in cyclic loading*. *Soil & Tillage Research*, 45: 175-187.
- Mallick, P.K., 1988. *Fiber-reinforced composite*. New York, Marcel Dekker, 469 pp.



- Mandal, J.N. and R.K. Dixit, 1990. *An analytical approach to the design of soil geosynthetic systems*. In: G. den Hoedt (ed), Geotextiles, Geomembranes and related products, Balkema, Rotterdam, pp. 161.
- Matichard, Y., 1993. *Discussion leader's report: Testing and materials*. In: H. Ochiai, S. Hayashi, and J. Otani (eds), Earth reinforcement, Balkema, Rotterdam, 901-903.
- Matkin, E.A. and P. Smart, 1987. *A comparison of tests of soil structural stability*. Journal of Soil Science, 38: 123-135.
- Matsui, T. and K.C. San, 1988. *Finite element stability analysis method for reinforced slope cutting*. International Geotechnical Symposium on Theory and Practice of Earth Reinforcement, Fukuoka Japan, 5-7 October, 317-322.
- McKyes, E., 1985. Soil cutting and tillage. Developments in Agricultural Engineering 7. Elsevier, Amsterdam, 217 pp.
- Michalowski, R.L. and A. Zhao, 1996. *Failure of fiber-reinforced granular soils*. Journal of Geotechnical engineering, Vol. 122, No. 3, March, 226-234.
- Michalowski, R.L., 1997. *Stability of uniformly reinforced slopes*. Journal of Geotechnical and Geoenvironmental engineering, Vol. 123, No. 6, June, 546-555.
- Migunga, G.A., 1995. *Tropical forest soil compaction: Effects of multiply log skidding tractor passes on surface soil bulk density at Sao Hill, Tanzania*. Proceedings of a Symposium organised by IUFRO, XX IUFRO World Congress, 6-12 August, Tampere, Finland, 1-3.
- Milligan, G.W.E., R.A. Jewel, G.T. Houlby and H.J. Burd, 1989. *A new approach to the design of reinforced unpaved roads - part II*. Ground Engineering, Vol. 22 (8): 37 - 42.
- Mitchell, J.K. and W.C.B. Villet, 1987. Reinforcement of earth slopes and embankments. National Cooperative Highway Research Program Report 290. Transportation Research Board, Washington D.C., 323 pp.
- Morton, W.E. and J.W.S. Hearle, 1976. Physical properties of textile fibres. The Textile Institute Heinemann, London, 660 pp.
- Nagao, A. and T. Kitamura, 1988. *Field experiment on reinforced earth and its evaluation using FEM analysis*. International Geotechnical Symposium on Theory and Practice of Earth Reinforcement, Fukuoka Japan, 5-7 October, 329-334.
- Nichols, T.A., A.C Bailey, C.E. Johnson, R.D. Grisso, 1987. *A stress state transducer for soil*. Transactions of the ASAE, Vol. 30(5): 1237-1241.

- Nielsen, K.F., 1974. *Root and root temperatures*. In: Carson, E.W., *The plant root and its environment*, Proceedings of an Institute sponsored by the Southern Regional Educational Board, held at Virginia Polytechnic Institute and State University, July 5-16, 1971, University Press of Virginia, U.S.A., 293-333.
- O'Sullivan, M.F. and R.M. Ritchie, 1993. *Tree stability in relation to cyclic loading*. *Forestry*, Vol. 66(1): 69-82.
- O'Sullivan, M.F. and C. Simota, 1995. *Modelling the environment impacts of soil compaction: a review*. *Soil & Tillage Research*, 35: 69-84.
- Ohtsuka, S., E. Yamada, M. Matsuo, 1996. *Bearing capacity analysis of reinforced ground*. In: H. Ochiai, N. Yasufuku, K. Omine (eds), *Earth reinforcement*, Balkema, Rotterdam, Vol. 1, 647-652.
- Oliver, C.D. and B.C. Larson, 1990. *Forest stand dynamics*. McGraw-Hill Inc., U.S.A., 467 pp.
- Parry, T.O., 1993. *Size, design, and management of tree planning sites*. In: Watson, G.W. and Neely, D. (Eds), *The landscape below ground*, International Society of Arboriculture, Savoy, U.S.A., 3-15.
- Pearson, R.W., 1974. *Significance of rooting pattern to crop production and some problems of root research*. In: Carson, E.W., *The plant root and its environment*, Proceedings of an Institute sponsored by the Southern Regional Educational Board, held at Virginia Polytechnic Institute and State University, July 5-16, 1971, University Press of Virginia, U.S.A., 247-270.
- Perry, R.L., S.D. Lyda and H.H. Bowen, 1983. *Root distribution of four Vitis cultivars*. In: D. Atkinson, K.K.S. Bhat, M.P. Coutts, P.A. Mason, and D.J. Read (eds) *Developments in Plant and Soil Sciences*, Vol 7, Martinus Nijhoff / Dr. W. Junk Publishers, 63-73.
- Persson, H. Å., 1983. *The distribution and productivity of fine roots in boreal forests*. In: D. Atkinson, K.K.S. Bhat, M.P. Coutts, P.A. Mason, and D.J. Read (eds) *Developments in Plant and Soil Sciences*, Vol 7, Martinus Nijhoff / Dr. W. Junk Publishers, 87-101.
- Petersen, C.T., 1993. *The variation of critical-state parameters with water content for two agricultural soils*. *Journal of soil science*, 44: 397-410.
- Pettit, T., 1984. *Metalwork made simple*. Heinemann, London, 226 pp.
- Pollock, D. Jr., J.V. Perumpral, T. Kuppusamy, 1986. *Finite element analysis of multipass effects of vehicles on soil compaction*. *Transactions of the ASAE*, Vol. 29(1): 45-50.
- Provencher, Y., 1992. *Geotextiles: Another road construction option*. Road and transportation technical note TN-182, Ferric, 6 pp.

- Raper, R.L. and D.C. Erbach, 1990. *Effect of variable linear elastic parameters on finite element prediction of soil compaction*. Transactions of the ASAE, Vol. 33 (3): 731-736.
- Raper, R.L. and D.C. Erbach, 1990. *Prediction of soil stresses using the finite element method*. Transactions of the ASAE, Vol. 33(3): 725-730.
- Raumann, G., 1982. *Geotextiles in Unpaved roads: Design consideration*. Second International Conference on Geotextiles, Vol 2, August 1-6, U.S.A., 417-423.
- Reynolds, E.R.C., 1973. *The development of root systems analysed by growth rings*. Plant and Soil, 71: 167-170.
- Richards, D. and J.A. Considine, 1981. *Suberization and browning of grapewine roots*. In: Brouwer, R. et al. (Eds), *Structure and function of plant roots*, Martinus Nijhoff / Dr. W. Junk Publishers, The Hague, The Netherlands, 117-141.
- Roberts, R., 1977. *Geotechnology: An introduction text for students and engineers*. Pergamon Press, England, U.K., 347 pp.
- Rose, D.A., 1983. *The description of the growth of root systems*. Plant and Soil, 75: 405-415.
- Rowe, R.K. and K.L. Soderman, 1985. *An approximate method for estimating the stability of geotextile-reinforced embankments*. Canadian Geotech. Journal, 22: 392-398.
- Rowe, R.K. and K.L. Soderman, 1987. *Stabilization of very soft soils using high strength geosynthetics: the role of finite element analyses*. Geotextiles and Geomembranes, 6: 53-80.
- Rowe, R.K. and B.L.J. Mylleville, 1994. *Analysis and design of reinforced embankments on soft or weak foundations*. In: J.W. Bull (ed), *Soil Structure interaction: Numerical analysis and modelling*, 231-260.
- Rundel, P.W. and P.S. Nobel, 1991. *Structure and function in desert root system*. In: D. Atkinson (ed) *Plant root growth, an ecological perspective*, Blackwell scientific publications, London, 349-378.
- Russell, E.W., 1961. *Soil conditions and plant growth*. Jarrold and Son Ltd., Norwich, 688 pp.
- Russell, R.S., 1977. *Plant root systems: their functions and interaction with the soil*. McGraw-Hill Book Company Ltd., England, 298 pp.
- Schaff, J.R., 1997. *Life prediction methodology for composite structures. Part 1- constant amplitude and two-stress level fatigue*. Journal of composite materials, 31(2): 129-157.
- Schneemann, J., 1988. *Rooting Patterns of Tropical trees*. Department of Silviculture and Forestry Ecology, Wageningen, The Netherlands, 23 pp.

- Scholand, M., F.A. Austenfeld and D.J. Von Willert, 1991. *Underground biomass and its influence on soil shear strength in a grazed and an ungrazed German coastal marsh*. In: D. Atkison (ed) *Plant root growth, an ecological perspective*, Blackwell scientific publications, London, 341-348.
- Schortemeyer, M., H. Šantrůčková, M.J. Sadowsky, 1997. *Relationship between root length density and soil microorganisms in the rhizospheres of white clover and perennial ryegrass*. *Commun. Soil Sci. Plant Anal.*, 28(19 & 20): 1675-1682.
- Sellmeijer, J.B., C.J. Kenter, C. van den Berg, 1982. *Calculation method for a fabric reinforced road*. Second International Conference on Geotextiles, Vol 2, August 1-6, U.S.A., 393-398.
- Sellmeijer, J.B., 1990. *Design of geotextile reinforced paved roads and parking areas*. In: G. den Hoedt *Geotextiles, geomembranes and related products*, Balkema, Rotterdam, 177-182.
- Shewbridge, S.E. and N. Sitar, 1989. *Deformation characteristics of reinforced sand in direct shear*. *Journal of Geotechnical engineering*, vol. 115, No. 8: 1135-1147.
- Shewbridge, S.E. and N. Sitar, 1990. *Deformation-based model for reinforced sand*. *Journal of Geotechnical engineering*, vol. 116, No. 7: 1153-1170.
- Shewbridge, S.E. and N. Sitar, 1991. *Deformation-based model for reinforced sand: Closure*. *Journal of Geotechnical Div., ASCE*, 117(11): 1812-1817.
- Shewbridge, S.E. and N. Sitar, 1992. *Strain compactibility design method for reinforcement earth walls*. *Journal of Geotechnical Div., ASCE*, 118(2): 318-321.
- Shewbridge, S.E. and N. Sitar, 1996. *Formation of shear zones in reinforced sand*. *Journal of Geotechnical engineering*, vol. 122, No. 11: 873-885.
- Simonini, P., 1996. *A finite element approach to the strength of granular soils reinforced with geosynthetics*. In: H. Ochiai, N. Yasufuku, K. Omine (eds), *Earth reinforcement*, Balkema, Rotterdam, 675-679.
- Sitharam, T.G., B.R. Srinivasa-Murthy, H.B. Raghavendra, 1996. *Tensile force distribution along the reinforcement for reinforced soil foundations*. In H. Ochiai, N. Yasufuku, K. Omine (eds), *Earth reinforcement*, Balkema, Rotterdam, 681-684.
- Smith, D.L.O., 1986. *An apparatus for twisting the soil root ball of a mature tree to measure the shear strength of the underlying soil*. *J. agric. Engng Res.*, 34:149-152.
- Smith, G.D., L.S. Jangawada and K.L. Srivastava, 1991. *Castor roots in a veric inceptisol*. In: McMichael, B.L. and H. Persson (Eds.), *Developments in agricultural and managed-forest ecology* 24: *Plant roots and their environment*, 533-542.

- Soane, B.D. and C. van Ouwerkerk, (Eds.), 1994. Soil compaction in crop production. Elsevier, Amsterdam, 650 pp.
- Sporn, C.R., 1979. The mechanics of soil-root systems: Toward the development of a theory. Discussion paper No. 19, Department of geography, University of Toronto, 70 pp.
- Taylor, H.M. and L.F. Ratliff, 1969. *Root elongation rates of cotton and peanuts as a function of soil strength and soil water content*. Soil science, Vol. 108, No. 2: 113 - 120.
- Taylor, H.M., 1974. *Root behaviour as affected by soil structure and strength*. In: E.W. Carson, The plant root and its environment, Proceedings of an Institute sponsored by the Southern Regional Education Board, held at Virginia Polytechnic Institute and State University, July 5-16, 1971, University Press of Virginia, U.S.A., 271-291.
- Terwilliger, V.J. and L.J. Waldron, 1990. *Assessing the contribution of roots to the strength of undisturbed, slip prone soils*. Catena Vol. 17: 151-162.
- Terwilliger, V.J. and L.J. Waldron, 1991. *Effects of root reinforcement on soil-slip patterns in the transverse ranges of southern California*. Geological Society of America Bulletin Vol. 103: 775-785.
- Troughton, A. and W.J. Whittington, 1968. *The significance of genetic variation in root systems*. In: Whittington, W.J. (Editor), Root growth, Butterworths, London, 296-314.
- Trouse, A.C. Jr., 1988. *Crop root capabilities*. Proc. 11 th Conf. ISTRO, Edinburgh, Scotland, 159 - 164.
- Turner, J.L., 1984. *A semi-empirical mobility model for tracked vehicles*. Transactions of the ASAE: 990-996.
- Usher, G., 1970. A dictionary of botany. Van Nostrand Reinhold Company, London, 408 pp.
- Van den Akker, J.J.H. and A.L.M. van Wijk, 1987. *A model to predict subsoil compaction due to field traffic*. In: G. Monnier and M.J. Goss (eds), Soil compaction and regeneration, Balkema, Rotterdam, 69-84.
- Van Noordwijk, M., 1989. *Tree roots as components of agro-forestry systems*. Reader for IBSRAM/ICRAF Workshop on Research in Soil Management and Agroforestry: Nairobi, 25th November - 3rd December, 9 pp.
- Van Noordwijk, M., G. Lawson, A. Soumaré, J.J.R. Groot and K. Hairiah, 1996. *Root distribution of trees and crops: competition and/or complementarity*. In: C.K. Ong and P. Huxley (eds), Tree-crop interactions: a physiological approach, University Press, Cambridge, U.K., 319-365.
- Vermeer, P.A. (Ed), 1991. Plaxis. Finite element code for soil and rock plasticity. Balkema, Rotterdam.

- Vesic, A.S., 1977. Design of pile foundation. National cooperative highway research program, No. 42, National academic of sciences, Washington, U.S.A., 69 pp.
- Vinson, J.R. and T.W. Chou, 1975. Composite materials and their use in structures. London, Applied Science, 438 pp.
- Vinson, J.R. and R.L. Sierakowski, 1986. The behaviour of structures composed of composite materials. Dordrecht, Martinus Nijhoff, 323 pp.
- Visvassaldis, S., 1958. *The role of auxin and other exudates in mycorrhizal symbiosis of forest trees*. In: K.V. Thimann, et al (eds), *The physiology of forest trees*, The Roland Press Company, New York, 427-445.
- Vogt, K.A., D.J. Vogt and J. Bloomfield. *Input of organic matter to the soil by tree roots*. In: McMichael, B.L. and H. Persson (Eds.), *Developments in agricultural and managed-forest ecology 24: Plant roots and their environment*, 171-190.
- Vos, J. and J. Groenwold, 1983. *Estimation of root densities by observation tubes and endoscope*, Plant and Soil, 74: 295-300.
- Voskamp, W. 1990. *Determination of allowable design strength of polyester reinforced mats*. In: Shercliff, D.A (ed), *reinforced embankments: theory and practice*, Telford, London, 67-81.
- Waisel, Y. and A. Eshel, 1991. *Multiform behaviour of various constituents of one root system*. In: Waisel, Y. Eshel, A. and Kafkafi, U. (Editors), *Plant roots, the hidden half*, Marcel Dekker Inc, New York, pp. 39-52.
- Waldron, L.J., 1977. *The shear resistance of root-permeated homogeneous and stratified soil*. Soil Science Society of America J., 41:843-849.
- Waldron, L.J. and S. Dakessian, 1981. *Soil reinforcement by roots: calculation of increased soil shear resistance from root properties*. Soil Science Vol. 132, No. 6: 427-435.
- Waldron, L.J. and S. Dakessian, 1982. *Effect of grass, legume, and tree roots on soil shearing resistance*. Soil Science Society of America J., 46: 894-899.
- Wästerlund, I., 1986. The Strength of bark on Scots pine and Norway spruce trees. Rapport, Institutionen for Skogsteknik, Sveriges Lantbruksuniversitet, No. 167, 106 pp.
- Wästerlund, I., 1989. *Strength components in the forest floor restricting maximum tolerable machine forces*. Journal of Terramechanics, Vol. 26, No. 2: 177-182.
- Wästerlund, I., 1990. *Soil strength in forestry measured with a new kind of test rig*. Proceedings of the 10 th International Conference of ISTVS, Kobe, Japan.

- Wästerlund, I., 1992. *Extent and causes of site damage due to forestry traffic*. Scand. J. For. Res. 7: 135-142.
- Watson, G.W., 1993. *Root development after transplanting*. In: G.W. Watson, and D. Neely (Eds), *The landscape below ground*, International Society of Arboriculture, Savoy, U.S.A, 54-65.
- Weaver, J. E., 1920. *Root development in the grassland formation*. Carnegie Institution, Washington, 151 pp.
- Whiteley, G.M. and A.R. Dexter, 1984. *Behaviour of roots in cracks between soil peds*. Plant and Soil, 74: 153-162.
- Willatt, S.T. and N. Sulistyaningsih, 1990. *Effect of plant roots on soil strength*. Soil & Tillage Research, 16: 329-336.
- Woods, R.I., 1994. *Reinforced slopes and embankments*. In: J.W. Bull (Editor), *Soil Structure interaction: Numerical analysis and modelling*, E & FN Spon, London, 261-314.
- Woods, F.W., 1991. *Cambial activity of roots*. In: Y. Waisel, A. Eshel and U. Kafkafi (Eds), *Plant roots, the hidden half*, Marcel Dekker Inc, New York, 149-160.
- Wu, T.H., W.P. McKinnel III and Swanston, D.N., 1979. *Strength of tree roots and landslides on Prince of Wales Island, Alaska*. Canadian Geotech. J., 16: 19-33.
- Wu, T.H., D.P. Bettadapura and P.E. Beal, 1988. *A statistical model of root geometry*. Forest Science, Vol. 43, No. 4: 980-997.
- Wu, T.H., R.M. McOmber, R.T. Erb and P.E. Beal, 1988. *Study of soil-root interaction*. J. Geotech. Eng., 144(12): 1351-1375.
- Wu, T.H., P.E. Beal and C. Lan, 1988. *In-situ shear test of soil-root systems*. Journal of Geotechnical Engineering, 114: (12): 1376-1394.
- Yatabe, R., N. Yagi, K. Yokota, 1996. *Stability analysis of slope reinforced by roots networks. Earth reinforcement*. In: H. Ochiai, N. Yasufuku, and K. Omine (eds), *Earth reinforcement*, Balkema, Rotterdam, Vol. 1, 835-839.
- Zhang, Y., 1988. *The limit equilibrium of geotextile reinforced structures*. International Geotechnical Symposium on Theory and Practice of Earth Reinforcement, Fukuoka Japan, 5-7 October, 595-598.

## SUMMARY

Soil mechanics in relation to plant growth has developed significantly, as can be seen from numerous textbooks (Gill and Van den Berg, 1967; Koolen and Kuipers, 1983; McKyes, 1985; Larson et al., 1989; Soane and Van Ouwerkerk, 1994). This thesis generally covers:

- (1) literature review on roots, fundamental soil reinforcement techniques and mechanisms of soil-root reinforcements
- (2) experiments on root mechanical properties
- (3) simulations on root reinforcement effect using a finite element code known as PLAXIS 7.0.

Investigations on the suitability of tree roots for use as soil reinforcements showed that root potential for reinforcing soils will depend on complex combination of:

- (1) root morphology and physiology
- (2) root surface structures
- (3) root mechanical properties
- (4) soil properties.

Experimental results showed that the diameter of thick roots has no significant effect on failure stress and strain. Average failure stress of thick beech roots was found to be 20.0 MPa (Standard Deviation = 4.1 MPa). Cyclic loading experiments conducted with the roots showed, that the number of loading cycles before root failure depends on the applied stress level. Plastic strain increment of individual root pieces was found to decrease with an increasing number of loading cycles and increases with an increasing percentage stress level. On the other hand, overall stiffness modulus was found to increase with an increasing number of loading cycles and decreases with an increasing percentage stress level. In separate experiments, stress-strain values of neighbouring root pieces were found to be closer to each other than those found in comparable root diameter classes. Root strength was also found to increase for about 8-20% for increase in elongation rate from 10 mm m<sup>-1</sup> to 400 mm m<sup>-1</sup>.

Modelling of root reinforcement effects showed, that improvement in soil's bearing capacity provided by tree roots can adequately be modelled by a finite element code such as PLAXIS. In these simulations, interest was placed on the situation where no significant



slippage occurs between the root mat and the soil. Initial stiffness of the root mat,  $E_{\text{initial}}$ , was estimated from overall stiffness modulus,  $E_{\text{overall}}$ , found in previous root experiments.  $E_{\text{initial}}$  was taken to be approximately 5 times  $E_{\text{overall}}$ . Simulation results showed that the presence of a root mat in the soil greatly improves the soils bearing capacity. An improvement of about 10 % was found at a rut depth of 0.1 m considering wheel load, wheel width, and root mat stiffness of 200 kN m<sup>-2</sup>, 0.5 m and 4500 kN m<sup>-1</sup> respectively. An extreme longitudinal stress of the beech root mat calculated by PLAXIS in the reference situation was given as 6.54 MPa.

Laboratory measurement of the longitudinal failure stress of beech roots was found by Liu (1994) to be  $24 \pm 1.58$  MPa. This value is approximately 4 times the value found from PLAXIS and therefore justifies the use of an initial elastic modulus for the simulated roots. Simulation of the bending effect of the root showed, that root thickness plays an important role in improving the bearing capacity of the soil. Increasing thickness of the root was found to be associated with decrease in rut depth as well as reduction in vertical stresses under the root. Inclusion of interface element and varying width of the mesh had no remarkable effect on the load-displacement curve. The study also showed the following:

- (1) reinforcement effects increases with increasing stiffness of the reinforcement and decreases with increasing depth of placement of the reinforcement from the soil surface
- (2) rut depth increases with increasing mesh height (soil depth). In practice soil-root reinforcement should be analysed as a three dimensional problem. These three dimensional modelling techniques will improve simulation results and should be considered in future studies.

## APPENDIX I

### DEFINITION OF BIOLOGICAL TERMS

*Adventitious roots*- are applied to roots developing on stems or leaves, i.e. not forming part of the primary root system (Bell 1991).

*Dicotyledonous plant* - plant having two cotyledon (Jackson, 1971)

*Exudates* - compounds of low molecular weight that leak from root cells into either intercellular spaces and then to the soil via cell junctions, or directly through epidermal cell walls into the soil (Gliński and Lipiec, 1990).

*Lysates* - compounds released from autolysis from older epidermal cells (Gliński and Lipiec, 1990).

*Medullar ray* - plates of parenchyma or cellular tissue radiating from the pith to the cortex (Jackson, 1971).

*Meristem* - is a tissue in which the cells are capable of repeated cell division (Berrie et al., 1987).

*Monocotyledonous plant* - plant having but one cotyledon (Jackson, 1971).

*Morphology* - is the study of the external features and their parts (Berrie et al., 1987).

*Mucigel* - This term is used for the gelatinous material at the surface of root grown in non-sterile soils. Mucigel includes original and modified plant mucilages, bacterial cells, etc. (Bowen and Rovira, 1991)

*Mucilages* - hydrophilic polyglucuronate and polygalacturonate polymers across which ions and uncharged solutes should be able to pass freely (Gliński and Lipiec, 1990).

*Parenchyma* - a tissue of undifferentiated cells, which are more or less spherical, frequently unspecialized, and with cellulose cell-walls. This tissue is often for storage (Usher, 1970).

*Pericycle* - a cylinder of vascular tissue, 3-6 cells thick, laying immediately inside the endodermis

of a root. It consists of parenchyma, and sometimes fibres (Usher, 1970).

*Phloem* - vascular tissue which conducts synthesized foods in vascular plants (Usher, 1970).

*Protoderm* - rudimentary dermal tissue derived from the primary meristem of the apical region (Jackson, 1971).

*Root growth pressure* - pressure available for a root to accomplish work against an external constraint has been termed root growth pressure (Taylor, 1974)

*Root primordium* - a group of meristematic cells originating below the surface of an existing root or shoot (Berrie et al., 1987).

*Secretions* - compounds of low and high molecular weights which are released as a result of metabolic processes (Gliński and Lipiec, 1990).

*Vacuolation* - is a process during which cells vacuoles increase in size and usually coalesce to form a single, large vacuole (Berrie et al., 1987)

*Vascular cambium* - meristematic tissue that is usually responsible for the radial growth of roots is called the vascular cambium. It has indeterminate growth with the possibility for propagating vegetatively for very long period of time. It is called the vascular cambium because it gives rise to vascular tissues, the phloem and the xylem (Woods, 1991).

*Xylem* - vascular tissue which conducts water and minerals salts throughout the plant and provides mechanical support (Usher, 1970).

## APPENDIX II

### SYMBOLS

$\alpha$	initial orientation angle of fibre with respect to shear surface
$\beta$	load spread angle
$\gamma$	unit of weight of soil
$\gamma_w$	weight per unit volume of water.
$\delta$	angle of friction on base of footing
$\theta$	angle of shear distortion
$\mu$	coefficient of soil friction
$\mu_e$	effective coefficient of friction
$\nu$	Poisson's ratio
$\sigma_c$	tensile stress of composite
$\sigma_f$	failure stress
$\sigma_{fb}$	tensile stress of fibre
$\sigma_{fs}$	tensile stress developed in the fibre at the shear plane
$\sigma_m$	tensile stress of matrix
$\sigma_{max}$	maximum, or ultimate tensile stress
$\sigma_n$	effective stress normal to the reinforcement
$\sigma_s$	tensile stress developed in fibre at the shear plane
$\sigma_z$	peak stress under a wheel at depth $z$
$\tau$	tangential stress
$\tau'$	maximum tangential stress
$\epsilon$	tensile strain
$\varphi$	friction angle of the soil
$\epsilon_c$	tensile strain experienced by composite
$\epsilon_{fb}$	tensile strain experienced by fibre
$\varphi_g$	soil-geosynthetic angle of friction

$\epsilon_m$	tensile strain experienced by matrix
$a_b$	cross sectional area of the reinforcement in bearing
$a_r$	fraction of shear cross-section filled by roots
$a, b, c, f$	root constants for barley and pine
$A$	cross-sectional area of soil sample
$A_o$	cross-sectional area of composite
$A_{fb}$	cross-sectional area of fibre
$A_m$	cross-sectional area of matrix
$A_r$	cross sectional area of reinforcement or root
$A_s$	soil shear surface
$B$	loaded width
$B_2$	half width of plane strain footing
BCR	bearing capacity ratio.
$c$	cohesion of the soil
$D$	root diameter
$D_0$	mean initial diameter of lateral root
$D_t$	Stem diameter
$E$	Young's modulus of elasticity
$E_F$	form modulus
$E_t$	tangent Young's modulus
$E_M$	material modulus
$E_{li}$	overall stiffness modulus on cycle loading i
$E_{11h}$	overall stiffness modulus for the first loading cycle in the hyperbolic curve
$E_{11s}$	overall stiffness modulus for the first loading cycle in the sigmoid curve
$E_{ui}$	overall stiffness modulus on unloading cycle i
$\Delta\epsilon_{ei}$	elastic part of incremental modulus on unloading cycle i
$\Delta\epsilon_{pi}$	plastic part of incremental strain in cycle i
$\Delta\epsilon_{1h}$	plastic strain increment for the first loading cycle in the hyperbolic curve
$\Delta\epsilon_{1s}$	plastic strain increment for the first loading cycle in the sigmoid curve
$E_r$	elastic modulus of reinforcement

$E_s$	Young's modulus of elasticity of solid
$F$	factor of safety
$f_b$	bond coefficient
$g$	acceleration due to gravity
$H$	vertical distance from failure plane to soil surface (slip height)
$h$	soil depth or mesh height
$k_1$	shear distortion ratio
$K_0$	coefficient of lateral earth pressure
$K_a$	active earth pressure coefficient
$K_p$	passive earth pressure coefficient
$K_l$	curve fitting parameter
$L$	length of loaded root
$L_{\text{bound}}$	length of reinforcement
$L_t$	total length of lateral root
$n$	number of traverse bearing members behind the failure surface
$N$	number of laterals formed on stem
$N_c, N_q, N_\gamma$	bearing capacity numbers
$N_b$	number of root branches
$P$	unit normal load
$P_F$	point load
$P_{\text{bond}}$	maximum bond force
$P_c$	load carried by composite
$P_T$	total pullout force ( $P_T = P_f + P_p$ )
$P_f$	pullout capacity
$P_a$	atmospheric pressure
$P_{fb}$	load carried by fibre
$P_N$	unit normal load
$P_m$	load carried by matrix
$P_p$	passive pullout capacity
$P_R$	reinforcement force

$P_x, P_z$	forces in x and z directions parallel and perpendicular to the sides of the shear box
$q$	stress at the contact area between wheel and soil
$q_u$	ultimate soil bearing capacity
$q_{ur}$	ultimate bearing capacity at failure of reinforced ground
$r$	radius vector
$R_p$	radius of plate
$R$	radius of failure surface
$R_{rs}$	root-soil resistance
$S$	shear stress
$S_{(fallow)}$	shear strength of root free soil
$S_{Fmax}$	maximum shearing force
$S_w$	suction in the soil water
$S_1$	shear stress of non-slipping roots
$S_2$	shear stress of slipping roots
$S_e$	equilibrium shear strength
$S_r$	shear strength of rooted soil
$S_s$	soil's shear strength
$S_L$	longitudinal stiffness
$\Delta S_f$	shear strength increase by fibre reinforcement
$\Delta S_a$	absolute increase in soil's shear strength by root
$T$	torque
$T_N$	tensile stress at point N
$v$	concentration factor
$v_a, v_b$	specific volumes at states a, and b respectively.
$v_c$	volume of composite
$v_{fb}$	volume of fibre
$v_m$	volume of matrix
$V_m$	volume fraction of matrix
$V_{fb}$	volume fraction of fibre

$W_r$	width of reinforcement
$X_1, X_2$	coordinate directions parallel and perpendicular to the direction of shear
$x$	horizontal component of shear displacement
$y, m, b$	sinkage, sinkage exponent, and sinkage modulus respectively.
$z$	depth
$Z$	thickness of shear zone
$\xi$	stiffness of root mat
$\xi_r$	stiffness of reinforcement
$k_2, k_3, K_i, n_i$	dimensionless parameters
$R_f$	failure ratio
$f_f$	Drucker-Prager failure function
$\chi$	degree of saturation
$\lambda_c^*, \kappa_c^*$	slopes of the Normal Consolidation Line and Swelling Line respectively, plotted on log-log scale
$\lambda_c, \kappa_c$	slopes of the Normal Consolidation Line and Swelling Line respectively, corrected for PLAXIS
$K_0$	coefficient of lateral earth pressure



## APPENDIX III

### SOIL PARAMETERS

Table 1. Soil parameters derived from Mawcook gravel-sandy loam and Ste-Rosalie clay.

Parameters		Mawcook gravel-sandy loam		Ste-Rosalie clay	
		depth <25 cm	>25 cm	depth <25 cm	>25 cm
<b>Hyperbolic model:</b>					
cohesion	c (kPa)	25.7	29.0	61.4	45.8
failure ratio	$R_f$	0.78	0.77	0.79	0.82
Internal friction	$\phi$ (°)	31.4	32.2	7.4	18.2
	K	83.3	105.6	26.6	39.0
	n	0.0	0.0	0.57	0.52
<b>Cam-clay model:</b>					
critical state line	M	1.59	1.47	0.86	1.16
NCL slope	$\lambda_c^*$ ( $\times 10^{-2}$ )	4.98	4.70	5.88	1.75
SL slope	$\kappa_c^*$ ( $\times 10^{-3}$ )	6.79	4.81	5.23	2.05
Shear modulus	(MPa)	6.34	6.53	3.88	5.45
Preconsolidation	(kPa)	60	100	15	30

Source: Chi et al. (1993)

## SAMENVATTING

Grondmechanica met betrekking tot plantengroei is ver ontwikkeld, zoals blijkt uit een reeks van handboeken (Gill en Van den Berg, 1967; Koolen en Kuipers, 1983; McKyes, 1985; Larson e.a., 1989; Soane and Van Ouwerkerk, 1994). Dit proefschrift handelt vooral over:

- (3) literatuuronderzoek over plantenwortels, basistechnieken voor grondwapening en mechanismen van grondwapening door wortels
- (4) metingen van mechanische eigenschappen van wortels
- (5) simulaties van het wapeningseffect van wortels met behulp van de Eindige Elementen Code PLAXIS 7.0.

Onderzoekingen naar de geschiktheid van boomwortels om te dienen als grondwapening toonden dat de potentie van wortels om grond te wapenen afhangt van een ingewikkelde combinatie van:

- (1) de morfologie en fysiologie van wortels
- (2) oppervlakte-structuren van wortels
- (3) mechanische eigenschappen van wortels
- (4) bodemeigenschappen.

Experimentele resultaten toonden aan dat de diameter van dikke wortels geen significant effect heeft op de bezwijkspanning en -rek. Voor de bezwijkspanning van dikke beukewortels werd gevonden: 20,0 MPa (standaard afwijking = 4,1 MPa). Proeven met cyclische belasting van wortels lieten zien dat het aantal belastingscycli om te komen tot bezwijken van de wortel afhangt van het opgelegde spanningsniveau. Plastische rek incrementen van individuele stukjes wortel bleken af te nemen met een toename van het aantal belastingscycli en toe te nemen met een toenemend percentage spanningsniveau. In afzonderlijke experimenten bleek dat de spanning-rek waarden van stukjes wortel die elkaars buien waren dicht bij elkaar lagen dan die van willekeurige stukjes uit een vergelijkbare diameter-wortelklasse. Ook werd gevonden dat de wortelsterkte toeneemt met ongeveer 8-20% als de reksnelheid toeneemt van 10 mm m<sup>-1</sup> tot 400 mm m<sup>-1</sup>.

Modellering van de effecten van wapening door wortels toonde aan dat de toename van de draagkracht van de bodem door boomwortels adequaat gemodelleerd kan worden met een eindige elementen code zoals PLAXIS. Deze simulaties betroffen de situatie waarin

nog geen significante slip optreedt tussen de wortelmat en de grond. De initiële stijfheid van de wortelmat,  $E_{\text{initial}}$ , was geschat uit de globale stijfheidsmodulus,  $E_{\text{overall}}$ , die gevonden was in voorgaande experimenten.  $E_{\text{initial}}$  was gelijk genomen aan ongeveer 5 maal  $E_{\text{overall}}$ . Simulatieresultaten lieten zien dat de aanwezigheid van een wortelmat in de bodem de draagkracht van de bodem sterk vergroot. Een verbetering van 10% was gevonden voor een worteldiepte van 0,1 m, bij waarden voor wieldruk, wielbreedte en wortelmatstijfheid van resp. 200 kNm<sup>-2</sup>, 0,5 m en 4500 kNm<sup>-1</sup>. PLAXIS berekende voor de referentiesituatie een grootste longitudinale spanning in de mat beukewortels van 6,54 MPa.

Laboratorium metingen van de longitudinale bezwijkspanning van beukewortels (Liu, 1994) gaven waarden van  $24 \pm 1,58$  MPa. Deze waarden zijn ongeveer 4 maal groter dan de waarde gevonden door PLAXIS. Dit rechtvaardigt het gebruik van een initiële elasticiteitsmodulus voor de gesimuleerde wortels. Simulatie van het effect van buiging van een wortel liet zien dat de dikte van de wortel een grote rol speelt bij de verhoging van de draagkracht van de bodem. Het bleek dat met toenemende dikte van een individuele wortel zowel de spoordiepte als het niveau van de spanningen onder de wortel afnamen. Toevoeging van interface elementen en het variëren van de breedte van de beschouwde bodemdoorsnede hadden weinig effect op de berekende last - verplaatsing curve.

De studie toonde ook nog dat:

- (1) wapeningseffecten toenemen met toenemende stijfheid van de wapening en afnemen met toenemende plaatsingsdiepte van de wapening
- (2) de spoordiepte toeneemt met toenemende hoogte van het raster (bodemdiepte). Voor de praktijk zou grond-wapening door wortels geanalyseerd moeten worden als een driedimensionaal probleem. Zulke driedimensionale modellerings-technieken zullen de simulatie resultaten verbeteren en behoren in toekomstige studies gebruikt te worden.

## **CURRICULUM VITAE**

Peter Cofie was born on the 9<sup>th</sup> of August, 1964 in Accra, Ghana. He obtained his G.C.E (General Certificate Examination) Ordinary and Advanced Level certificates at Ghana National College, Cape Coast - Ghana in 1984 and 1986 respectively.

In 1991, he graduated with B Sc. (Hons) Agricultural Engineering in the University of Science and Technology (U. S. T), Kumasi - Ghana. Thereafter he was posted to the University of Ghana, Accra - Ghana where he completed his National Service as a Research and Teaching Assistant.

He obtained his M Sc. degree in Agricultural Engineering at the Wageningen University, Wageningen - The Netherlands in 1995. In the same year (i.e., September 1995), he began his research work on "Mechanical properties of tree roots for soil reinforcement models" with the Wageningen University, Soil Technology Group, Wageningen, The Netherlands.